

NASA CONTRACTOR
REPORT



NASA CR-133

NASA CR-133

GPO PRICE \$ _____

OTS PRICE(S) \$ _____

Hard copy (HC) 1.50

Microfiche (MF) 1.50

FACILITY FORM 002

N65-12301

(ACCESSION NUMBER)

140

(PAGES)

CR-133

(NASA CR OR TMX OR AD NUMBER)

(TITLE)

1

(CODE)

21

(CATEGORY)

OPTICAL INERTIAL SPACE SEXTANT FOR AN ADVANCED SPACE NAVIGATION SYSTEM

*by W. D. Foley, W. D. Gates, R. M. Derby,
and J. J. Wilczynski*

Prepared under Contract No. NAS 2-1087 by

GENERAL ELECTRIC COMPANY

Johnson City, N. Y.

for

OPTICAL INERTIAL SPACE SEXTANT FOR AN
ADVANCED SPACE NAVIGATION SYSTEM

By W. D. Foley, W. D. Gates, R. M. Derby,
and J. J. Wilczynski

Distribution of this report is provided in the interest of
information exchange. Responsibility for the contents
resides in the author or organization that prepared it.

Prepared under Contract No. NAS 2-1087 by
GENERAL ELECTRIC COMPANY
Johnson City, New York

for

NATIONAL AERONAUTICS AND SPACE ADMINISTRATION

FOREWORD

This report summarizes the work performed by the General Electric Co., Light Military Electronics Department, Armament and Control Products Section, Johnson City, New York, to fulfill the requirements of the National Aeronautics and Space Administration Contract NAS2-1087, "Optical-Inertial Space Sextant for an Advanced Space Navigation System." This contract was initiated under Control No. 37974001, and administered under the cognizance of Mr. D. Hegarty of the Ames Research Center, Moffett Field, Palo Alto, California.

The work was performed by the Advance Engineering Component of the Armament and Control Products Section. It was initiated under Mr. J. D. Welch at Schenectady, N. Y., and completed under the direction of Mr. W. D. Foley as Project Engineer, in Johnson City, N. Y.

Principal contributors to the project were Messrs. W. D. Barber, B. Bezio, H. E. Brunelle, G. J. Colter, H. Demkowski, R. M. Derby, W. D. Foley, W. D. Gates, D. M. Merz, J. T. Pilkington, N. Rosenberg, J. D. Welch, J. Wilczynski.

The results of this study have been published within the Armament and Control Products Section of the Light Military Electronics Department of the General Electric Company under publication number LMEJ 6914.

ABSTRACT

12201

An operating tracker head subsystem consisting of dual-mode geometric optics, electrostatic vidicon, T.V. camera chain and data processor, was designed, built and successfully tested. This tracker head, which is capable of precise off-axis angularity measurement in a non-nulling mode, is a logical first step in a complete Space Sextant system incorporating bodybound, free rotor gyroscopes as angle transducers.

This report summarizes the work performed during the contract period of January 1963 to February 1964.

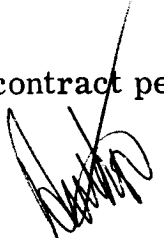


TABLE OF CONTENTS

	<u>Page</u>
1. INTRODUCTION	1
Summary of Results	6
2. OPTICS	9
Introduction	9
Description of Dual Field Optics	9
3. ELECTROSTATIC VIDICON AND T.V. CAMERA	17
Introduction	17
Electrostatic Vidicon	17
General Electric Vidicon	21
Vidicon Bias Circuit	22
Video Chain	22
Deflection System	28
Detection Circuitry	45
General Discussion	46
4. DATA PROCESSOR	53
Introduction	53
Modes of Operation	56
Star Mode	56
Sequencing	56
Data Handling	58
Noise Gating	61
Reticulization	61
Disc Edge Mode	63
Calibrate Mode	63
Readout	64
Detailed Mechanization	67
General	67
Sequential Logic	67
Data Processing	68
Horizontal Measurement	73
Vertical Measurement	74
Dump Logic	75
Some Further Observations	77
Summary of Significant Characteristics	77
Position Measurement and Noise Rejection	78
Data Averaging and Display	78
Total Power	78
Flip Flop Symbols or Glossary	79

TABLE OF CONTENTS (CONT'D)

	<u>Page</u>
5. ANALYSIS AND SYSTEM CONSIDERATIONS	85
Introduction	85
Optical Transfer Function of the Space Sextant Optics.	85
Study of Target and Image Characteristics for the	
Wide Angle Optics	90
Scan Techniques for Wide Angle Mode of Operation ..	92
Utilization of Space Sextant Data for Self-Contained	
Space Navigation Systems	95
6. SYSTEM TESTS AND RESULTS	99
Introduction	99
Facilities	99
Evaluation Tests-Vidicon Reticle Pattern	104
Calibration of Laboratory Star Light Source	107
Evaluation Tests Narrow Field Optics	109
Evaluation Tests Wide Field Optics	114
Photometric Tests at ATL Observatory	117
Off-Axis Tests Narrow Field	121
REFERENCES	137
APPENDIX I LOGIC ELEMENTS	139
APPENDIX II GEC 7522 VIDICON	143
APPENDIX III GEZ 7815 VIDICON	151

ILLUSTRATIONS

<u>Figure</u>		<u>Page</u>
1-1	Space Sextant Phase A System Diagram	3
1-2	Optics - Vidicon Tracker Assembly for Space Sextant in Cross Section	4
1-3	Space Sextant Gimballed Version Study Layout	5
1-4	Image Plane Relationships - Narrow Field	7
2-1	Optical Configuration	10
2-2	Sectional View of Dual Field Space Sextant	11
2-3	Typical Spot Diagram Narrow Field Optics	14
2-4	Calculated Angular Transfer Function in the Wide-Field System	15
3-1	Camera System Block Diagram	18
3-2	Camera Chain	19
3-2a	Electronic Control Unit	20
3-2b	Camera Head	20
3-3	Vidicon Bias Supply	23
3-4a	Video Chain Circuitry (Preamplifier and High Peaking Amplifier)	24
3-4b	Video Chain Circuitry (Variable Gain Video Amplifier) . . .	25
3-4c	Video Chain Circuitry (Aperture Correction Amplifier) . .	26
3-5a	Horizontal Sweep Circuit	29
3-5b	Vertical Sweep Circuit	30
3-6	Radial Scan Block Diagram	32
3-7	Radial Sweep Circuit Assembly	33
3-8	Radial Sweep Circuit Output (Oscilloscope Traces)	35
3-9	Space Sextant Radial Scan Logic Layout	36
3-10	Space Sextant Radial Scan Summing Amplifier	38
3-11	Space Sextant Radial Scan Sweep Generator	39
3-12	Space Sextant Radial Scan, Power Supply and Input - Output Wiring	40

ILLUSTRATIONS (CONT'D)

<u>Figure</u>		<u>Page</u>
3-13	Deflection Amplifier	41
3-14	Fail Safe Circuit	42
3-15	Synchronizer	44
3-16a	Video Processing	47
3-16b	Pulse Center Detection	48
3-17	Star Center Detection Illustration	49
4-1	Data Processor System Block Diagram	54
4-2	Front and Rear Views of the Data Processor	55
4-3	State Diagram - Star Sequence	57
4-4	State Diagram - Calibrate Sequence	65
4-5	Sequencing	82
4-6	State Diagram - Vertical Reticulization Sequence	83
4-7	Timing - Vertical Reticulization	84
5-1a	Optics Coordinate System	86
5-1b	Target Ray Geometry	87
5-1c	Vidicon Target Presentation Corresponding to Figure 5-1b .	88
5-2	"Off Vertical" Horizon Geometry	91
5-3	Image Plane Horizon	93
5-4	Image Plane Horizon	94
6-1	Angularity Test Setup (Narrow Mode)	100
6-2	Optics/vidicon Tracker Assembly on Optical Dividing Head	101
6-3	Angle Transfer and Image Quality Test Setup (Wide Mode) . .	102
6-4	Test Setup Off-Axis Angular Evaluation Tests	103
6-5	Optical Comparator Presentation of Reticle Pattern on Vidicon	105
6-6	Vidicon Reticle Measurements	107
6-7	Laboratory Star	108
6-8	Stellar Visual Magnitude	110

ILLUSTRATIONS (CONT'D)

<u>Figure</u>		<u>Page</u>
6-9	Test Results - Calibration of Laboratory Star	111
6-10	Image in Narrow Field System	112
6-11	Linearity Deviations in Narrow Angle System	113
6-12	Image in Wide Field System (Source Diameter 0.007 Inch). .	115
6-13	Off Axis Angle vs. Radial Position of Image - Wide Field . .	116
6-14	$(\theta - \theta_0)$ vs R - Wide Field (where $\theta_0 = 90.19 - 136.3r$ $-85.94r^2$)	116
6-15	Equatorial Mount ATL Observatory	118
6-16	Space Sextant on Equatorial Mount	118
6-17	Canis Minor β Signal (Oscilloscope Trace)	119
6-18	Ursa Major β Signal (Oscilloscope Trace)	119
6-19	Orion ϵ Signal (Oscilloscope Trace)	119
6-20	Orion α Signal (Oscilloscope Trace)	119
6-21	Photometric Test Results	120
6-22	Test Point Location X & Y Angular Accuracy Tests	122
6-23	X-Axis Angular Accuracy Test Results (Sheet 1 of 2)	124
6-23	X-Axis Angular Accuracy Test Results (Sheet 2 of 2)	125
6-24	Y-Axis Angular Accuracy Test Results	126
6-25	"Half-Moon" Wide Angle Test	128
6-26	Off-Axis Angle Relationships	128
6-27	Data Processor Input, Wide Mode Boresight Test (Oscilloscope Traces)	129
6-28	Disc Images Wide Mode Optics	130
6-29	Image Shift vs Offset Angle	132
6-30	Deviations from Circle - Boresight	133
6-31	Deviations from Circle - 5° Offset	133
6-32	Deviations from Circle - 10° Offset	133
6-33	Image Location vs Off-Axis Angle Edge Crossing "B"	134

ILLUSTRATIONS (CONT'D)

<u>Figure</u>		<u>Page</u>
6-34	Brightness Measurements Wide Angle Target	134
6-35a	Video Signals - Wide Mode Tests (Boresight- $Y \approx 800$)	136
6-35b	Video Signals - Wide Mode Tests (Boresight- $Y \approx 500$)	136

Section 1

INTRODUCTION

The National Aeronautics and Space Administration Contract NAS2-1087 covering an "Optical - Inertial Space Sextant for an Advanced Space Navigation System" was placed with the Armament and Control Products Section of the Light Military Electronics Department, General Electric Company, in January 1963.

This is the final report, summarizing the work accomplished on this contract and covering in detail the period from April 10, 1963 to February 29, 1964. The report divides the effort into the following major areas, each of which is reported in detail in a separate section.

- o Optics
- o T.V. Camera
- o Data Processing
- o Analysis
- o Test Results

An interim report, Reference No. 2, issued April 10, 1963 covered in detail the work accomplished during the first 12 weeks of the contract period.

CONCEPT

The complete Space Sextant concept, for which the work covered by this contract is a logical first step, combines a dual field optical system and a T.V. camera chain with two bodybound, free rotor, gyroscopes which form a unique celestial navigation instrument.

This overall concept is discussed in detail in Reference No. 20.

PHASE A DESCRIPTION

The contract work, which has been entitled Phase A of the overall concept, was largely hardware oriented and limited to the optics, T.V. camera and readout subsystems.

Figure 1-1 illustrates, in block diagram form the specific pieces of hardware which have been developed and fabricated.

Figure 1-2 is a schematic assembly of the optics/vidicon tracker head assembly, which forms the sensing element of this system.

Figure 1-3 is a preliminary study layout which projects the Phase A tracker head assembly into an integrated gimballed system with two body-bound E/S (Electrostatic) free rotor gyros. The overall size indicated is based upon the present state-of-the-art of component sizes with no attempts made at miniaturization. This type of an assembly is in keeping with one version of the original growth concept. In an assembly of this type the gimbals are employed for acquisition only, the gyros forming the basic angular readout transducers.

The overall concept of the Space Sextant was begun with General Electric Company funded development work, which by the end of 1962, had established the basic feasibility and had resulted in working laboratory models of preliminary optics and T. V. camera systems.

Based upon test results obtained with these components the following design goals were established for the contract hardware:¹

Optical Fields	:	Narrow Mode	1° to 1.5°
		Wide Mode	$80 \pm 10^{\circ}$ to $160 \pm 5^{\circ}$
Sensitivity	:	Narrow Mode	+2.0 M _V Stars with S/N ≥ 10
		Wide Mode	Track Earth, Moon, Mars and Venus with S/N ≥ 10
Angular Accuracy	:	Narrow Mode	
		On Boresight	± 3 arc-seconds
		Off Boresight	$\pm (3 \text{ arc-seconds} + 0.3\% \text{ of off-axis angle})$
		Wide Mode	± 5 arc minutes on boresight
Size	:	Optics/Vidicon Assembly 5 inches O.D. by 16 inches long	

¹These goals are covered in greater detail in Reference No. 2, pp. 47-51.

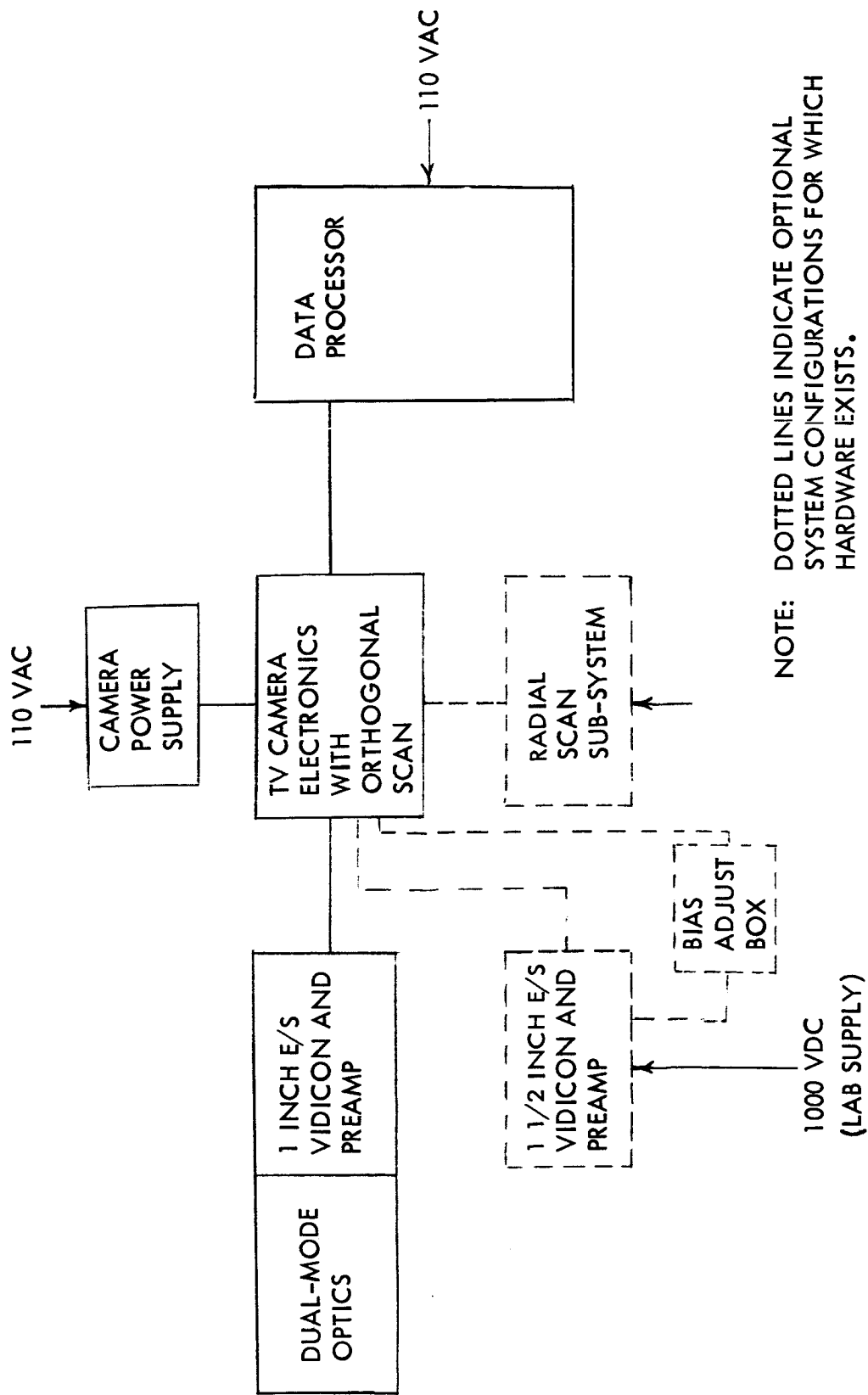


Figure 1-1. Space Sextant Phase A System Diagram

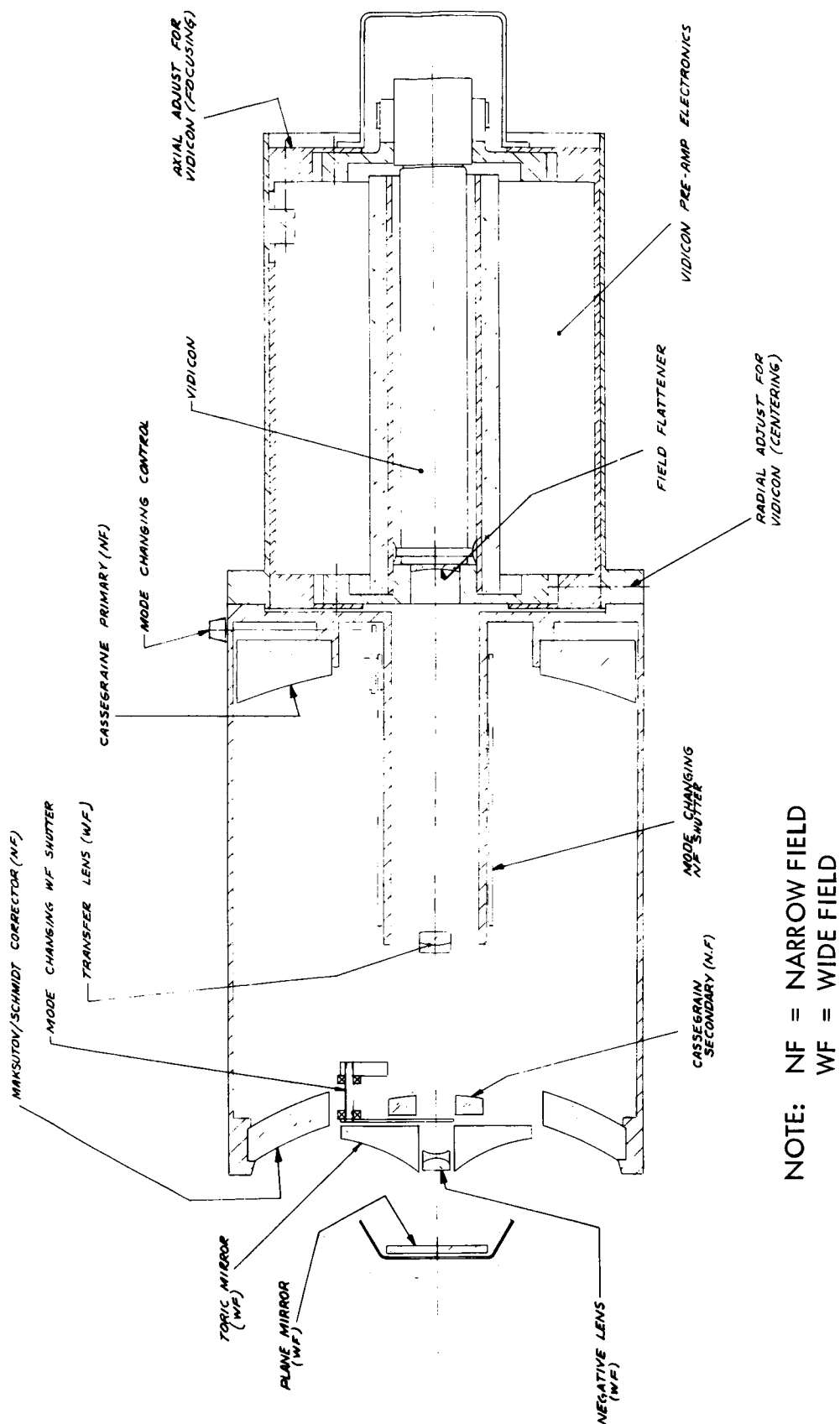


Figure 1-2. Optics-Vidicon Tracker Assembly for Space Sextant in Cross Section

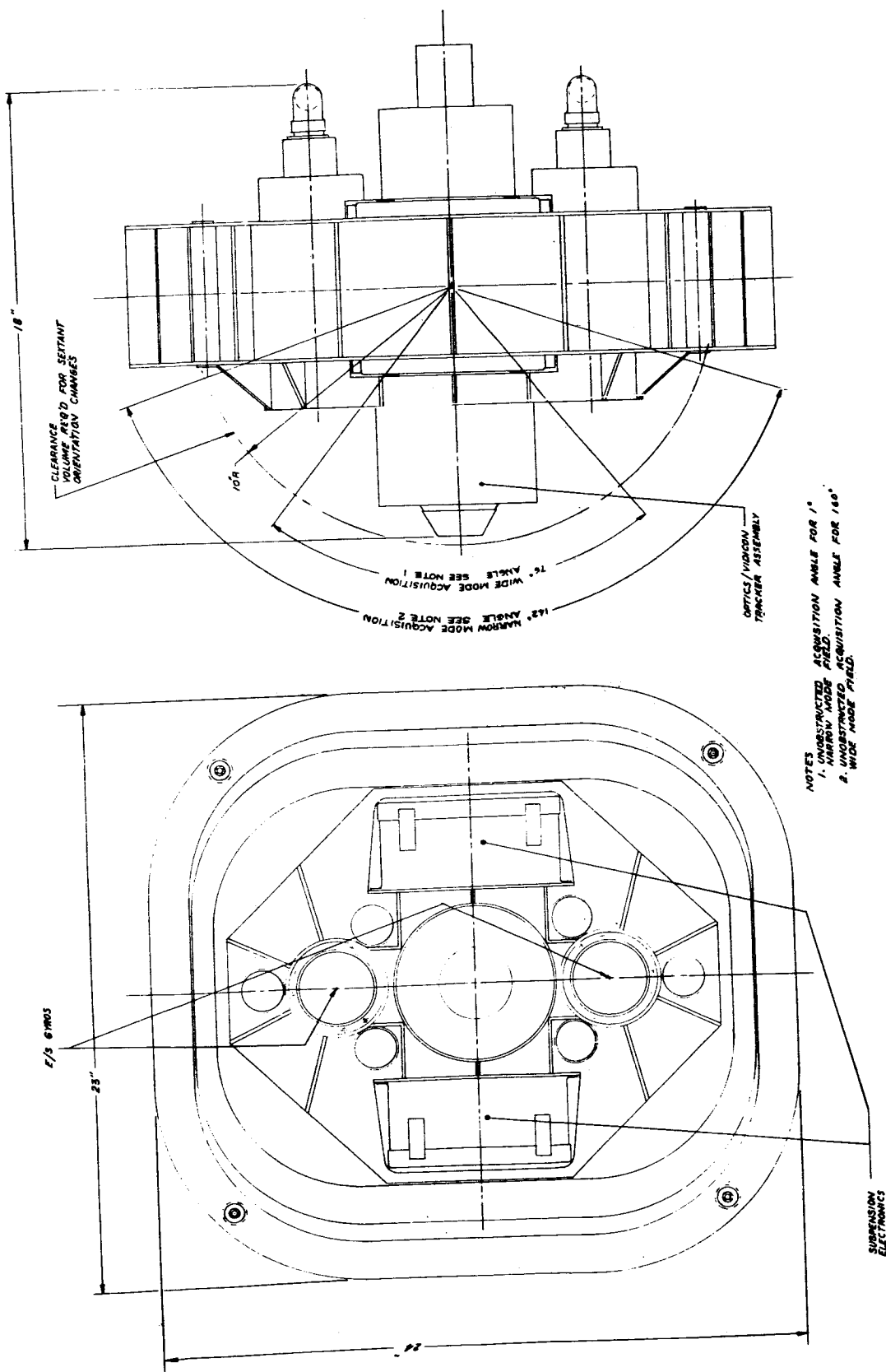


Figure 1-3. Space Sextant Gimballed Version Study Layout

SUMMARY OF RESULTS

The results achieved on the Phase A project are as follows:

o Optical Fields

The narrow mode optics have a field of view of 1° - $9'$. The vidicon target has a square reticulized area within this field of view corresponding to a field of 0.741° by 0.741° (1.048° diagonal). (Ref. Figure 1-4)

The wide mode optics have a field of view of 86° to 164° .

o Sensitivity

The narrow mode system was tested on actual stars at the General Electric Company's Observatory in Schenectady, N. Y. A S/N ratio of $10/1$ (1) was achieved on a +2.4 Mv star. This makes no allowances for viewing conditions or residual coherent noise.

The wide mode system, tested on the laboratory extended disc target produced a $S/N = 8/1$ for a target brightness of 1.0 candles/square foot. The minimum brightness of the celestial targets covered in the goals is 37 candles/square foot (Moon at 135° phase angle) so the demonstrated sensitivity is more than adequate.

o Angular Accuracy

In the narrow mode, system tests were conducted of the off-axis angularity accuracy in two orthogonal directions corresponding to the X and Y coordinate on the Vidicon target.

Difficulties arose in completely eliminating the dark-current warping which is common in vidicon tubes. This residual warping made detection of some of the darker-than-dark reticle pattern on the vidicon sporadic.

As an interim expedient, a second vidicon with unusually low dark-current was employed and the dark-current built up to a suitable level by back lighting the target face. This allowed the majority of the reticle patterns to be detected consistently. However, slight non-uniformities in this illumination combined with the residual non-uniformities in the dark-current still prevented detecting the D reticles (those used for vertical correction) consistently.

- (1) S/N is defined as the ratio between peak signal and the rms value of the random noise. Ref. Figure 6-21.

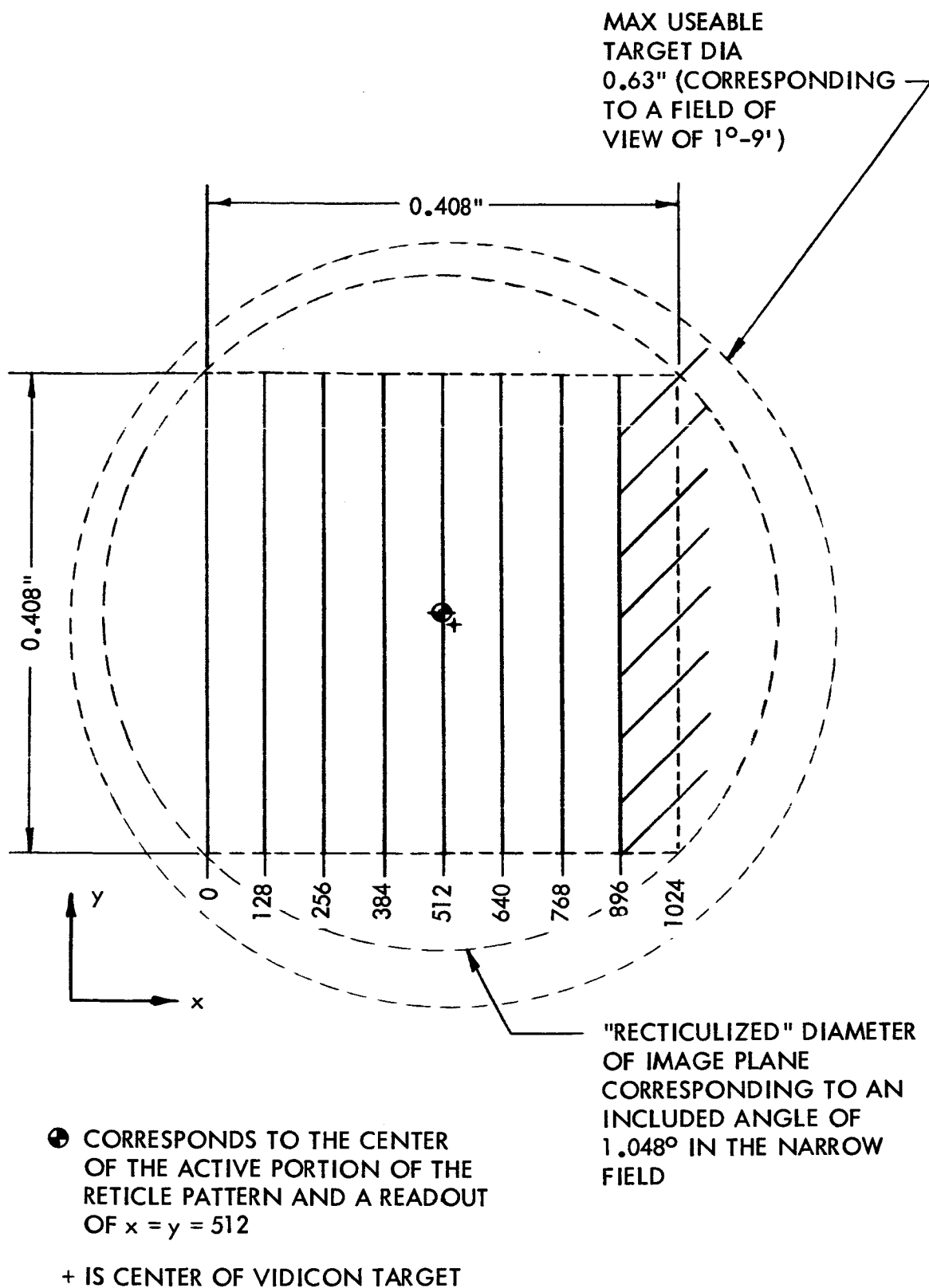


Figure 1-4. Image Plane Relationships - Narrow Field

This problem of the dark-current will be solved in the next phase of the program by one, or all of the following:

1. Addition of beam landing correction to the camera electronics
2. Improved filtering to remove the dark level working effect.
3. Alteration in the width and/or location of the reticle lines.

Using the equipment at hand it was possible to run off-axis angularity accuracy tests in the X coordinate direction with the reticles in operation.

The results indicate a normal distribution of error with a standard deviation of 4.2 arc-seconds. This is based upon 73 test points located in a semi-random fashion throughout the field of view.

Tests on the Y-axis accuracy, without reticle correction resulted in maximum errors of 28 arc-seconds with 70% of the test points falling under 16 arc-seconds error.

In the wide mode system, the tests were conducted without reticle correction of either coordinate. The tests were not extensive enough to establish a firm angular accuracy. However an off-axis shift of 5° produced a image center shift of 93 decimal counts. Since the data processor readout is quantized in unit counts a resolution of 5 arc-minutes appears to be within the capability of the system, since this corresponds to $1/60$ of the 5° motion.

o Size

The optics/vidicon tracker assembly developed on this contract has a maximum O.D. of 6 inches and an overall length of $18 \frac{1}{4}$ inches. This latter dimension includes the amphenol connector on the rear of the capsule. (Reference Figure 1-2).

Based upon the results of the sensitivity tests it appears well within the state-of-the-art to reduce these dimensions further on future models.

Section II

OPTICS

INTRODUCTION

The design studies and prototype hardware tests leading up to the selection of the final Optics configuration have been covered in detail in a previous report.¹

The detailed design and fabrication of the final optics was done by R. R. Willey, Jr., of the Instrument Corp. of Florida. The description of the optics which follows is taken from his report.

The configuration chosen for the optics is shown in Figure 2-1.

DESCRIPTION OF DUAL FIELD OPTICS

The Dual Field Optical Tracker consists of two optical systems which come to a focus on the same plane. This plane is the photo sensitive surface of the Vidicon tube. One of the optical systems is a compact Cassegrain-type telescope of 36.1 inches focal length which allows the Vidicon to receive a 1° field of view. The second optical system is a wide field optical system which presents a 160° field of view to the Vidicon. The 160° field is turned optically "inside-out" so that the extreme angles of the field appear toward the center of the Vidicon, and the more central regions of the field appear toward the edge of the Vidicon. The two optical systems are co-axial and confocal so that the change from viewing one field to viewing the other is accomplished by obscuring the light from one system while allowing light to pass through the other. There are no moving optical parts in the field changeover process. Figure 2-2 shows, sectionally, the assembly of the instrument.

The present instrument was designed to satisfy specifications which were partially evolved from experience gained from an earlier model Dual Field Optical Tracker. The previous instrument was of similar configuration, but had significantly different apertures and focal lengths.

One of the objectives of the design was to obtain as compact an instrument as was compatible with the image quality at the edge of the telescope's field of view, yet tempered by the feasibility of fabricating any system designed. The resulting design is what we choose to call the Maksutov Schmidt-Cassegrain (MSC) telescope. The corrector has the general shape of a

¹ Ref # 2 Sections II and IV.

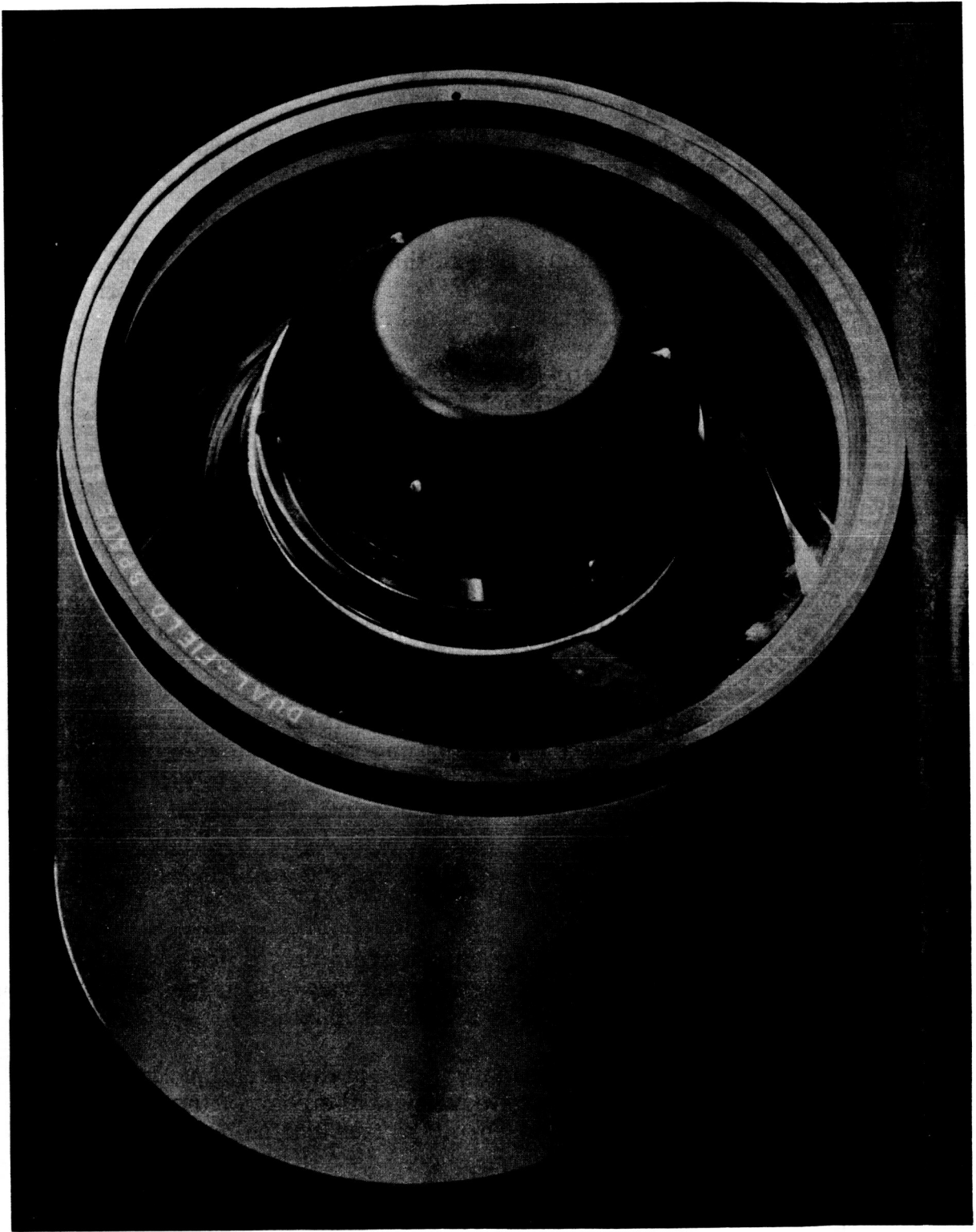


Figure 2-1. Optical Configuration

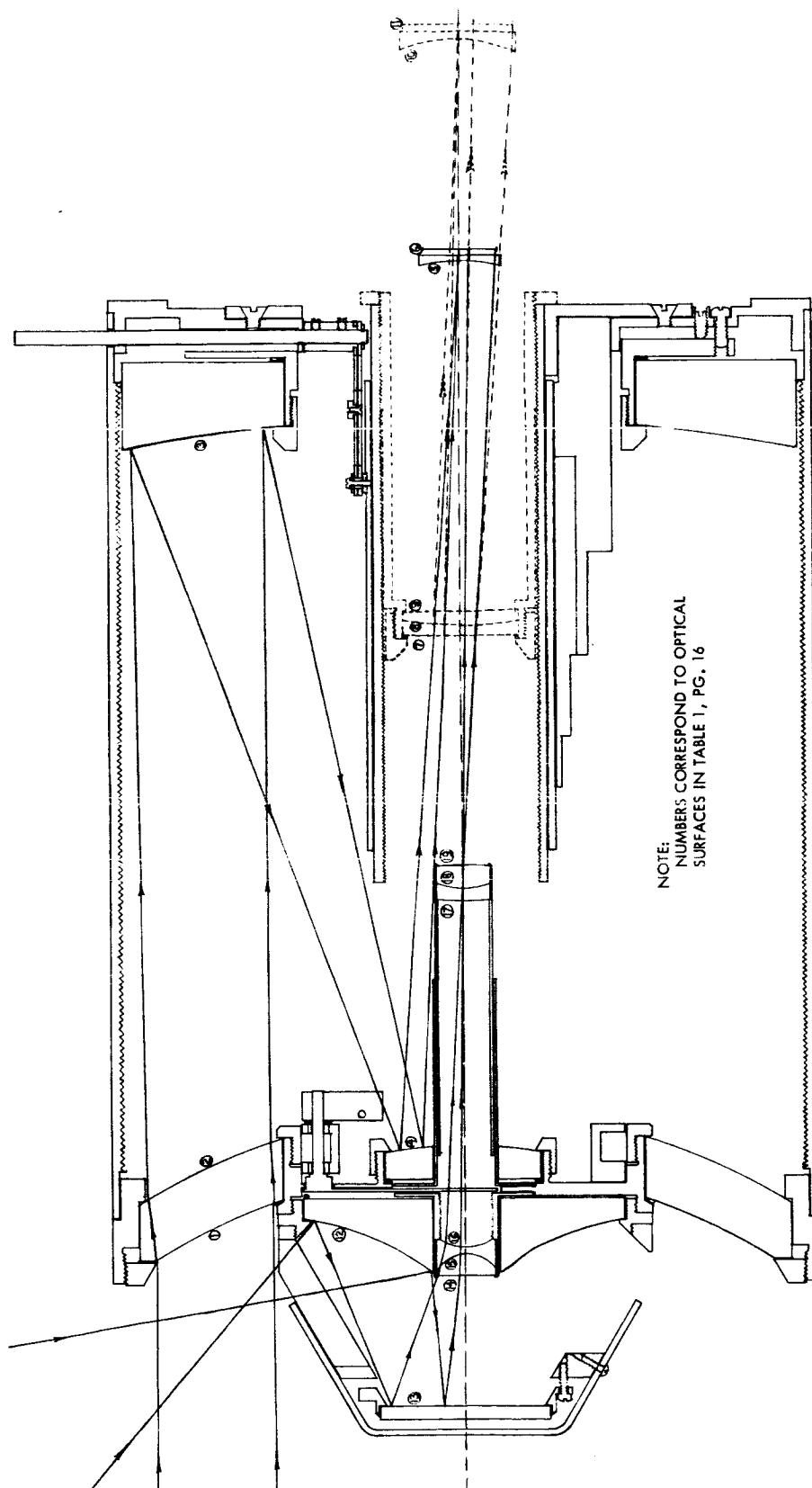


Figure 2-2. Sectional View of Dual Field Space Sextant

Maksutov corrector shell, but has a significant amount of aspheric figuring on the corrector, as does a Schmidt corrector. The primary and secondary mirrors are spherical; a minimal number of degrees of freedom are required in the adjustments; and a minimal amount of auxiliary test equipment is required in fabrication. A further advantage is that the corrector shell utilizes the features of the simple Maksutov and Schmidt correctors which have spherochromatism of opposite signs and therefore tend to negate each other. Therefore, the color correction is quite good.

In the present instrument, a transfer lens is required that can be introduced to expand the 0.63 inch format for a 1 inch Vidicon to a 0.95 inch format for a 1 1/2 inch Vidicon. The transfer lens assembly is designed so that it can be removed and replaced as desired, without disturbing the adjustment.

The wide field system has a relative aperture of $f/11$ and the central obscured cone is 80° in angular diameter. The present model also has a small "dead" area in the center of the image on the tube.

The co-axial combination of the wide field system (WFS) and the narrow field system (NFS) posed slightly different problems in the present design from those of the earlier model. It is specified that: the WFS shall have a relative aperture of $f/11$, and the NFS shall have a focal length of 36.1 inches and effective aperture should be 4.1 inches. This figure indicates that the area of the collecting aperture should be $(4.1/2)^2(\pi) = 13.20$ square inches. Since the $f/11$ cone of the WFS is to occupy the central obstruction cone of the NFS, we can project the $f/11$ cone 36.1 inches to find the diameter of the central obstruction at the entrance pupil; this we find to be 3.28 inches, an area of 8.45 square inches. The area of the effective aperture (13.20 square inches) must, therefore, be contained in an annulus about this central obstruction, giving a total area of the aperture with obstruction of 21.65 square inches. This area, then, has a diameter of 5.25 inches, and essentially fixes the diameter of the telescope, which (with 3/8 inch thickness for mounting) brings the outside diameter of the instrument to 6 inches.

Some degree of sophistication has been included in the mechanical design. Wherever thermal expansion effects could be troublesome, steel is used, since it has a lower coefficient than aluminum and a high Young's modulus.

The mechanical changeover from narrow to wide field of view is accomplished by turning a single shaft, located on the rear of the instrument, approximately 1/4 turn. This causes a tube to slide forward over the light baffle tube (see Figure 2-2) until it obstructs the NFS light converging from the primary mirror to the secondary mirror. As this outer tube approaches

the end of its travel, it engages a lever and causes a shutter in the WFS to open and admit WFS light to the Vidicon. The process is reversed to change from WFS to NFS viewing.

The baffling of stray light is accomplished very easily in both the WFS and NFS, due to the present configuration. With reasonable tolerances on fabrication of the component parts, only the primary mirror of the NFS and the flat mirror and positive lens of the WFS need adjustments. The system, once adjusted, should maintain alignment and performance under conditions of the specified environment.

The instrument is somewhat heavier than absolutely necessary due to the use of steel. However, it seems impractical at the moment to attempt a bimetallic thermal compensation in the space available.

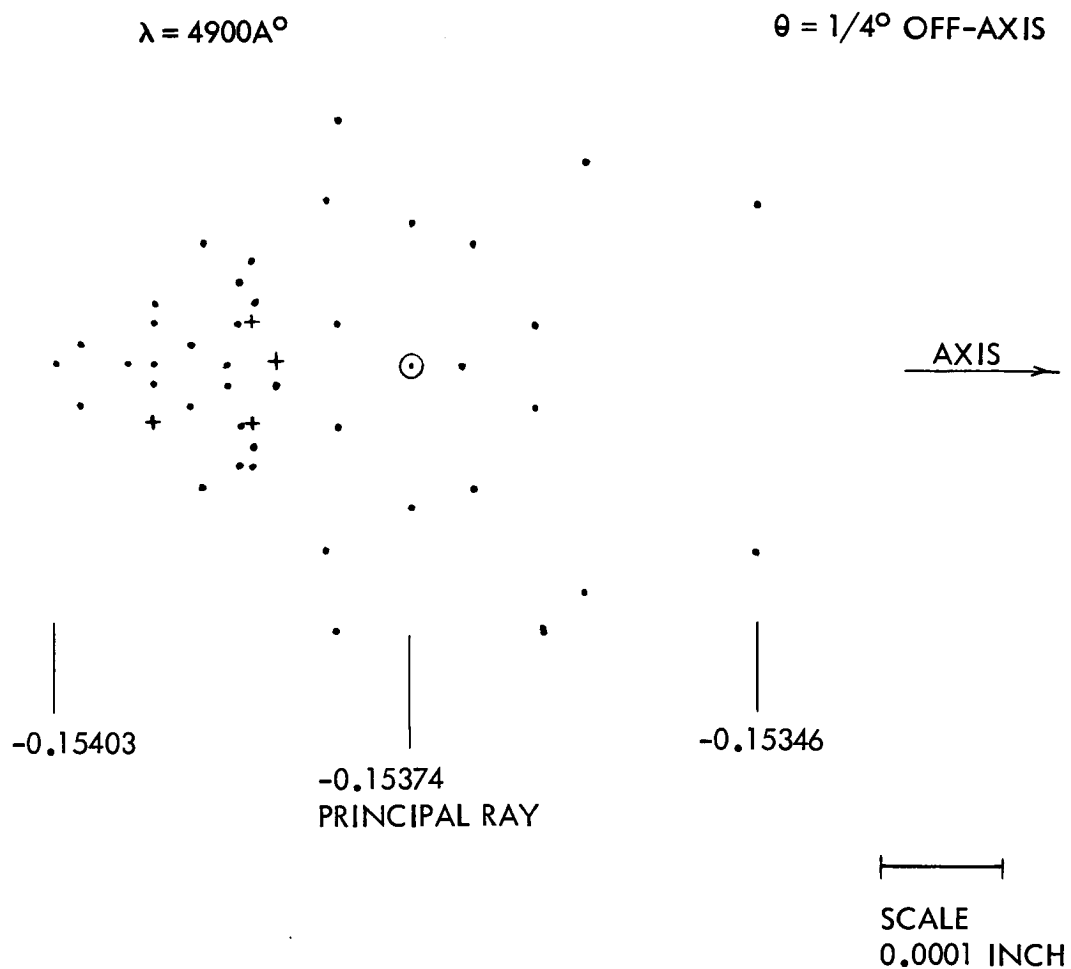
COMPUTED OPTICAL PERFORMANCE

The optical performance of the telescope was predicted using a ray tracing computer program developed by R.R. Willey, Jr. The extent that the image of a star departs from an ideal geometric point (neglecting diffraction) is shown by the distribution of dots in the spot diagram produced by the program. Each dot represents an equal amount of energy. Therefore, the distribution of spots shows the distribution of energy in the image of a star on the focal plane. The obscuring effects of the WFS and secondary mirror core are included in the spot diagrams. Figure 2-3 illustrates a typical spot diagram. Other diagrams were run for different off axis conditions and different light sources ($\lambda = 4861\text{\AA}$) with similar satisfactory results.

It was seen that at least 80% of the energy is contained within a 0.001 inch circle even at the extreme field angles of $1/2^\circ$ off-axis.

To locate horizons as precisely as possible, the images in the wide field system have been optimized to give minimal spread in a radial direction. The angular Transfer Function of the WFS is shown in Figure 2-4. In the present model, the unused area in the center of the image field is approximately 27% of the field diameter or 7% of the field area. This is a considerable improvement over the earlier model. The plot shows this system to have very little non-linearity in the angular transfer function. The general slope of the angle versus distance off axis plot indicates that the system is performing as though it had a focal length of approximately 0.315 inches.

Mounting holes for the image tube unit and clearance holes for its adjustments have been provided in the mechanical parts. The field flattener lenses, if used, are most appropriately mounted on their respective image tubes. However, the transfer lens, when used, is mounted within the optical assembly. The external tube of the instrument is sufficiently rigid so that moderate clamping stresses can be supported at any position along its length.



- NOTES:
- a) THE PRINCIPAL RAY IS INDICATED BY A CIRCLE, \odot
 - b) THE + SYMBOLS ARE EQUIVALENT TO TWO • SYMBOLS AND ARE USED WHEN TWO RAYS FALL TOGETHER.
 - c) λ = WAVELENGTH OF MONOCHROMATIC LIGHT (IN THIS CASE 4900 ANGSTROMS)

Figure 2-3. Typical Spot Diagram Narrow Field Optics

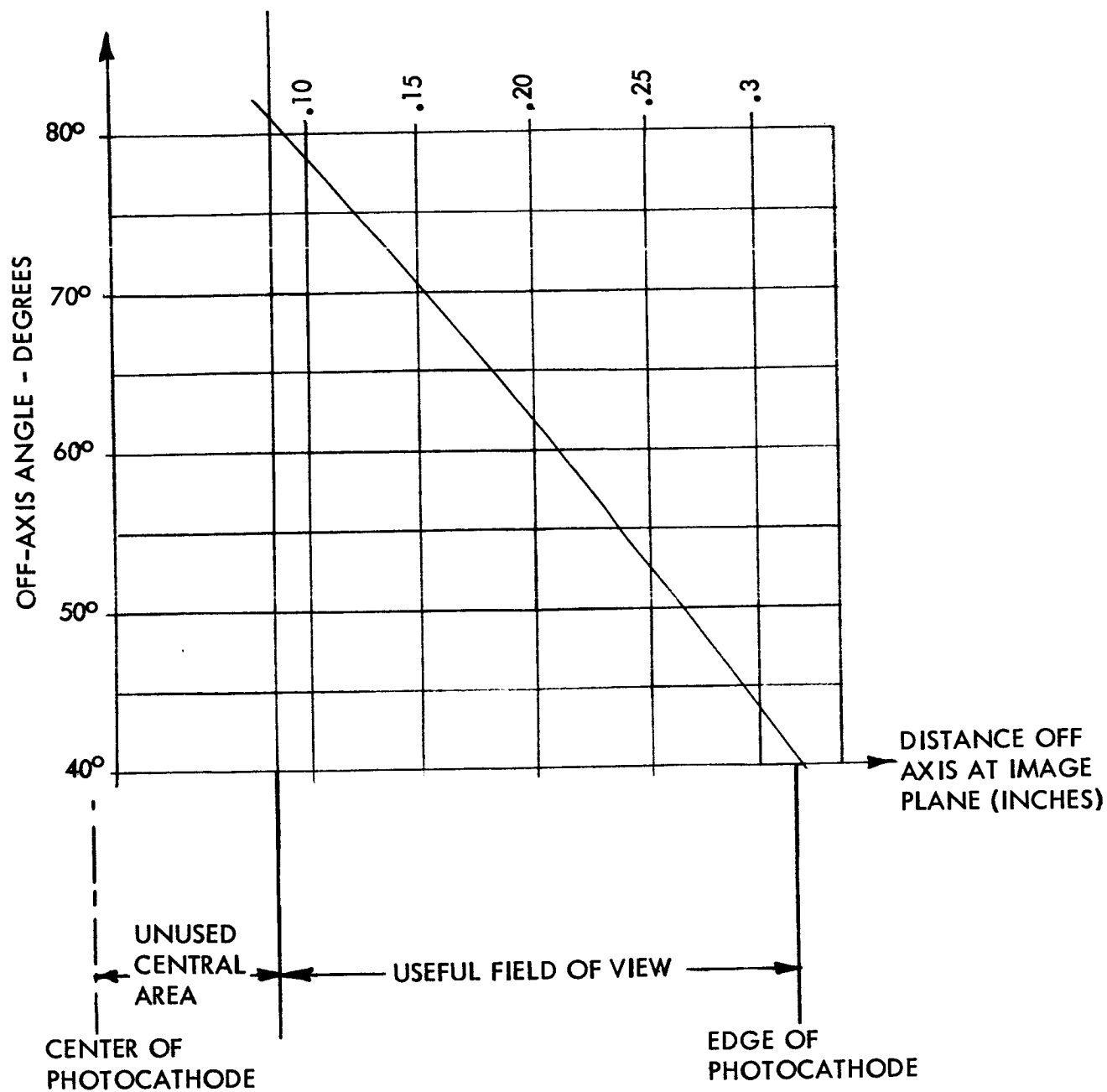


Figure 2-4. Calculated Angular Transfer Function In The Wide Field System

The secondary mirror, wide field system, and parts of the shutter mechanism are supported in the perforation of the MSC corrector so that no support vanes are seen through the NFS. However, WFS flat mirror is supported on vanes which will be seen in the WFS field of view. A light baffling cover fits over the WFS assembly and gives it some protection.

The exterior design of the instrument is simple and free from complications that would make its integration into an overall system difficult.

TABLE I
FINAL DESIGN PARAMETERS OF THE SYSTEM

RADIUS	VERTEX SEPARATION ⁽¹⁾	MATERIAL
	<u>Narrow Field System</u>	
1. -4.880 ± 0.005	0.506 ± 0.010	BSC-2
*2. -5.200 ± 0.005	5.790 (adj.)	Air
3. -15.150 ± 0.050	-6.085 (adj.)	Air, Pyrex, Al-Sio
4. -4.060 ± 0.050	7.540 (adj.)	Air, Pyrex, Al-Sio
5. -1.450 ± 0.025	0.050 ± 0.010	BSC-2
6. 0.000	(approx. 0.050)	(Face Plate)
	<u>Transfer System</u>	
7. -11.02 ± 0.100	0.075 ± 0.005	DBC-1
8. 2.83 ± 0.030	0.125 ± 0.005	DF-1
9. 11.02 ± 0.100	4.90 (adj.)	Air
10. -1.308 ± 0.025	0.050 ± 0.010	BSC-2
11. 0.000	(approx. 0.050)	(Face Plate)
	<u>Wide Field System</u>	
12. 1.700 ± 0.020 Major		
2.320 ± 0.010 Minor	1.625 (adj.)	Air, Pyrex, Al-Sio
13. 0.000	1.125 (adj.)	Air, Pyrex, Al-Sio
14. 0.000	0.200 ± 0.005	DF-1
15. -0.304 ± 0.005	0.050 ± 0.005	DBC-1
16. 0.406 ± 0.005	2.900 (adj.)	Air
17. 2.345 ± 0.020	0.100 ± 0.005	DF-1
18. 0.689 ± 0.005	0.200 ± 0.005	DBC-1
19. -2.345 ± 0.020	5.16 (adj.)	Air

(plus transfer system, when used, and appropriate field flattener)

*This surface is aspherically figured to eliminate residual spherical aberration at assembly.

(1) Vertex separation refers to the axial spacing of the surfaces of the optical elements.

Section 3

ELECTROSTATIC VIDICON AND T. V. CAMERA

INTRODUCTION

The image tube detector consists of a precision vidicon television camera chain. Its purpose is to provide accurate position information of objects within the field of view of the optical system. The camera system is shown in block diagram in Figure 3-1. The system consists of the following: (1) the vidicon tube which transduces the light image into a corresponding electron image and its associated bias circuitry (2) the deflection system which provides a precision scan of the vidicon target for accurate positional information relative to the tube face plate (3) the video amplifier chain which amplifies the electron image or signal for processing (4) the video processing and center detection circuitry which provides a digital output of analog signal information.

The camera chain is shown in Figure 3-2, and individual pictures of the electronic control unit and the camera head are shown in Figures 3-2a and 3-2b.

GENERAL ELECTRODYNAMICS 1 INCH ELECTROSTATIC VIDICON

The vidicon used in the camera is the General Electrodynamics Corporation 1351-50 electrostatic focus and deflection vidicon with an deposited reticle pattern on the conductive coating of the target which produces a blacker than black indication. (Blacker than black is defined as signals with opposite polarity to a white signal with respect to the zero target current level or dark level.) Two tubes were purchased but with different photo conductors on the face plates. One possesses a low leakage dark level which has to be back illuminated to see the reticle pattern and the other a normal higher-leakage dark level which allows the reticle pattern to be seen with no back illumination required. These tubes are essentially the GEC 7522 with the above mentioned modifications. The specification sheets for the GEC 7522 are included in this report as Appendix 2.

The reticle (see Section 6) was introduced on the tube in order to provide a mechanical fixed reference for the scanning electron beam. Therefore, an indication on the target then becomes accurately fixed in position by knowing the relative location from a mechanical reference thus eliminating many electronic drift errors.

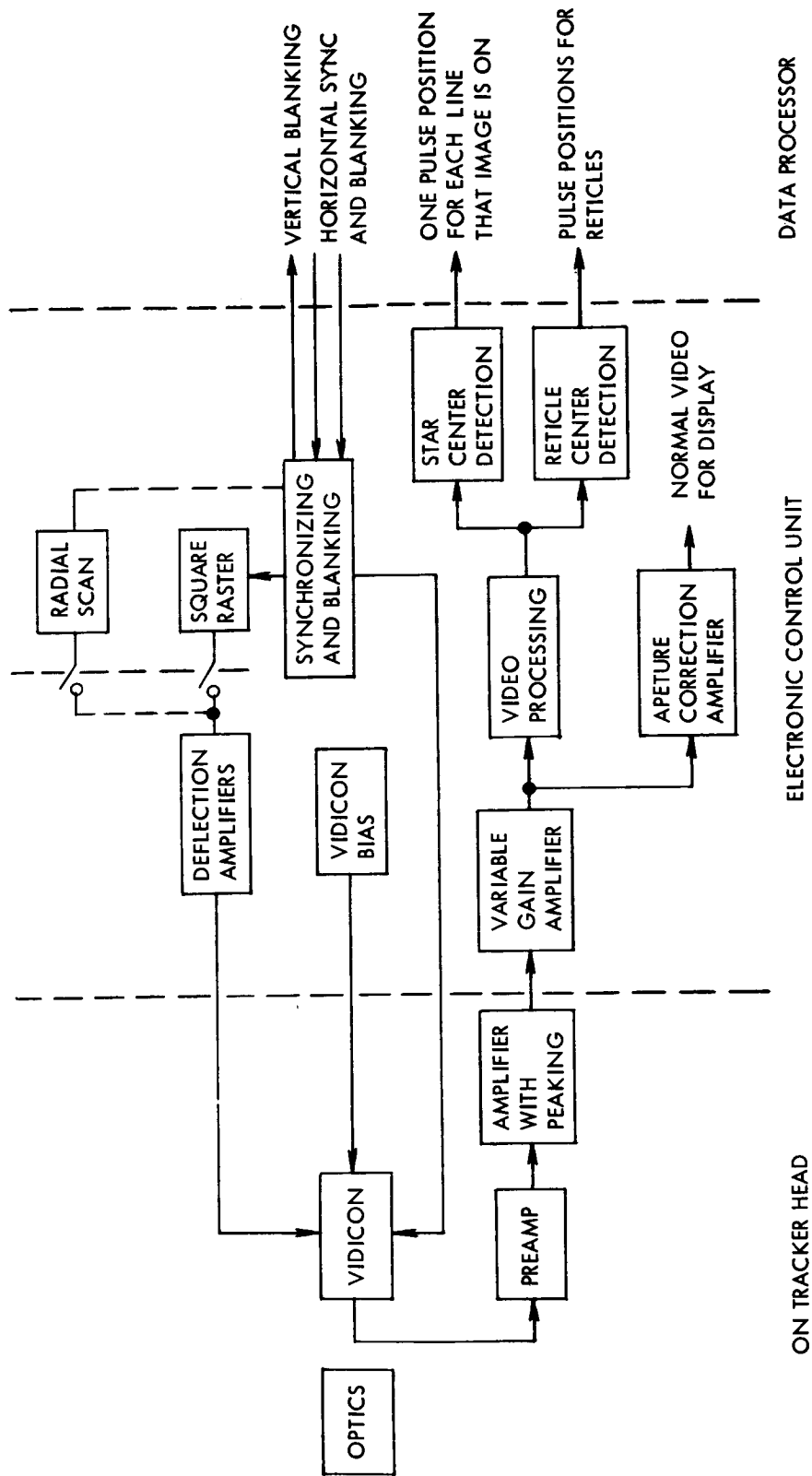


Figure 3-1. Camera System Block Diagram

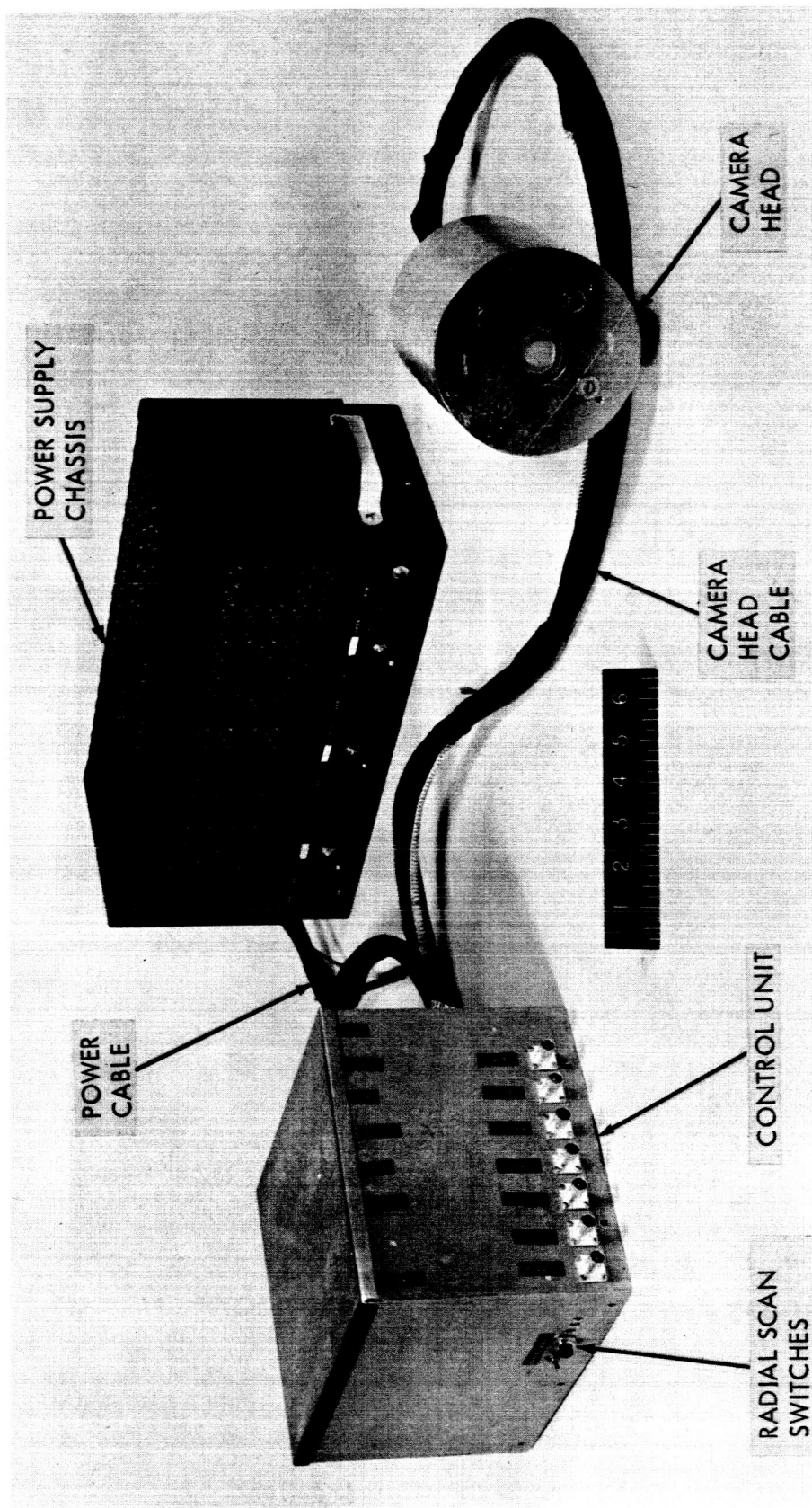


Figure 3-2. Camera Chain

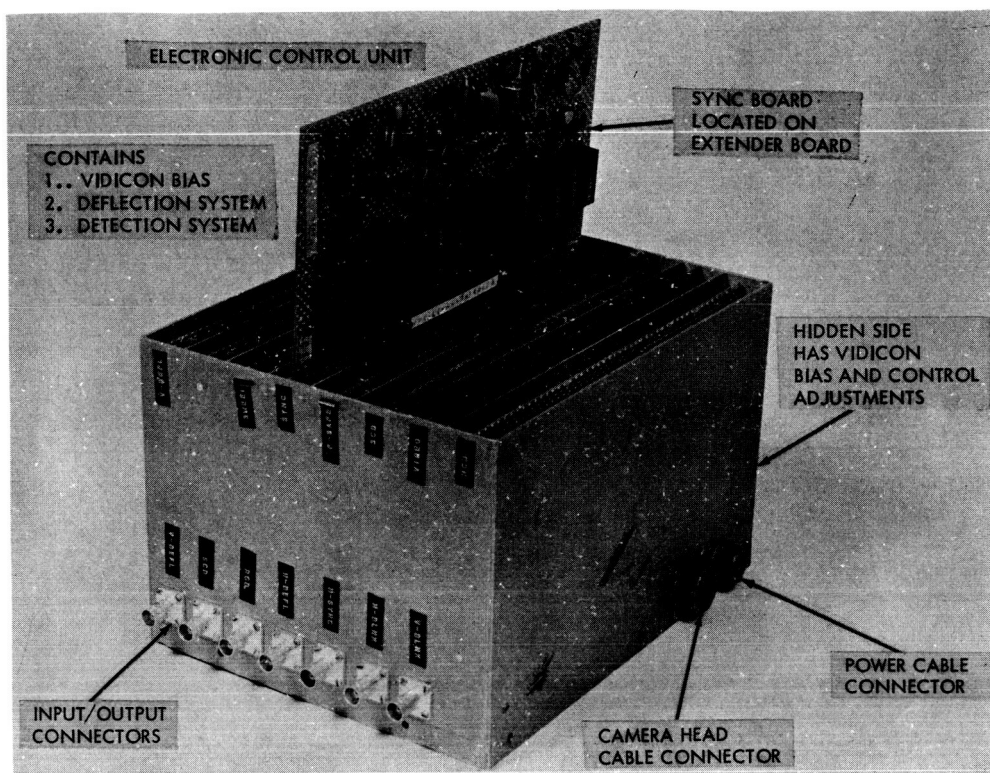


Figure 3-2a. Electronic Control Unit

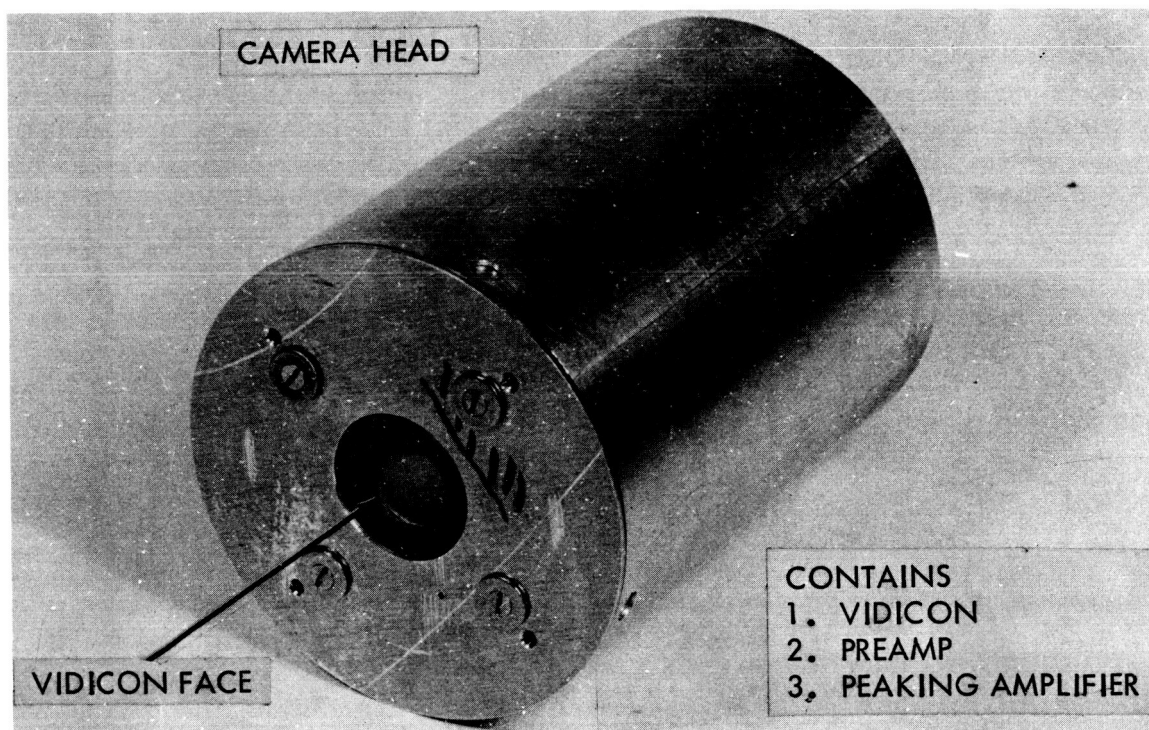


Figure 3-2b. Camera Head

The width of the reticles and the depth of deposit as well as the material used determines the degree of modulation produced by the reticle. A minimum width is set by the modulation required to indicate a detectable blacker than black reticle pulse.

GENERAL ELECTRIC 1 1/2 INCH ELECTROSTATIC VIDICON

Early in the project it was decided to design the optics/vidicon assembly to take advantage of the two sizes of electrostatic vidicons available, the 1 inch and the 1 1/2 inch. (The 1/2 inch size was ruled out, at that time, due to its lower resolution limits.)

Later developments, particularly in the area of reticulization, concentrated the major efforts on the GEC 1 inch vidicon, previously described.

However, due to its superior resolution (in excess of 800 T.V. lines) a G.E. Z7815 vidocon was procured and a housing and preamplifier built up to accommodate it. The housing is interchangeable with that of the 1 inch vidicon and bolts to the rear of the optics in the same manner.

The availability of this alternate vidicon makes the Phase A hardware of the Space Sextant a more versatile development tool as the program proceeds.

While no tests were run on the complete system with this vidicon, vidicon performance was witnessed at the Cathode Ray Tube Department in Syracuse. A resolution of 800 T.V. lines was easily obtained.

Except for relatively minor alterations involving the gun and the overall envelope dimensions the 1 1/2 inch vidicon is described in the specification sheets included in Appendix III.

VIDICON BIAS CIRCUIT

The sensitivity of the vidicon to slight changes in the DC bias settings (beam position, raster scan, etc.) requires that these points be held to within 0.1% accuracies. Regulated commercial supplies of $\pm 2\%$ are used to supply two, series regulator circuits. One regulator supplies voltage for the focusing electrodes and the other for the field mesh. Resistance divider networks from these voltages are used to supply focus control, target and deflection common. Beam current control being not as critical, is supplied by an individual negative 2% commercial supply.

The regulators are of the feedback type with a differential amplifiers inserted between the resistance divider and the control transistor to increase sensitivity to slight variations. The differential amplifiers are high frequency compensated to prevent any high frequency oscillations. For a $\pm 5\%$ change in input voltage the regulator output will vary $\pm .05\%$.

The vidicon bias supply circuitry is shown in Figure 3-3.

VIDEO CHAIN

The video chain consists of a preamplifier and peaking amplifier situated in the camera head along with a variable gain amplifier and an aperture correction amplifier in the electronics chassis (See Figure 3-2) The video chain circuitry is shown in Figures 3-4a, b, and c.

The video preamplifier acts both as a buffer between the high impedance vidicon and the video electronics, and as a low noise source of gain. The preamplifier uses a "Nuvistor" vacuum tube in the cascode connection since this connection is predicted to have the lowest noise of any vacuum tube arrangement. However, to minimize the number of tubes required, the stage was modified by replacing the normal output tube in the common grid connection with a common base transistor stage. This gave no degrading effect either on output noise or gain. The video preamp has a bandwidth of approximately 6Mc (1kc-6Mc) at a gain of 20db with a noise figure of approximately 6 db.

Since the vidicon is essentially a current source, the output signal must be transformed into a voltage signal for the vacuum tube preamplifier (a voltage amplifier). This necessitates a 100K resistor from target to ground. Any shunt capacity (such as stray, wire, input, etc.) will introduce a lag in the frequency response. To compensate, a peaking amplifier puts in a corresponding lead at the required position in the response.

The peaking amplifier is a single stage transistor amplifier with an emitter follower output. Peaking is added in the feedback circuit from the emitter of the emitter follower to the base of the transistor amplifier.

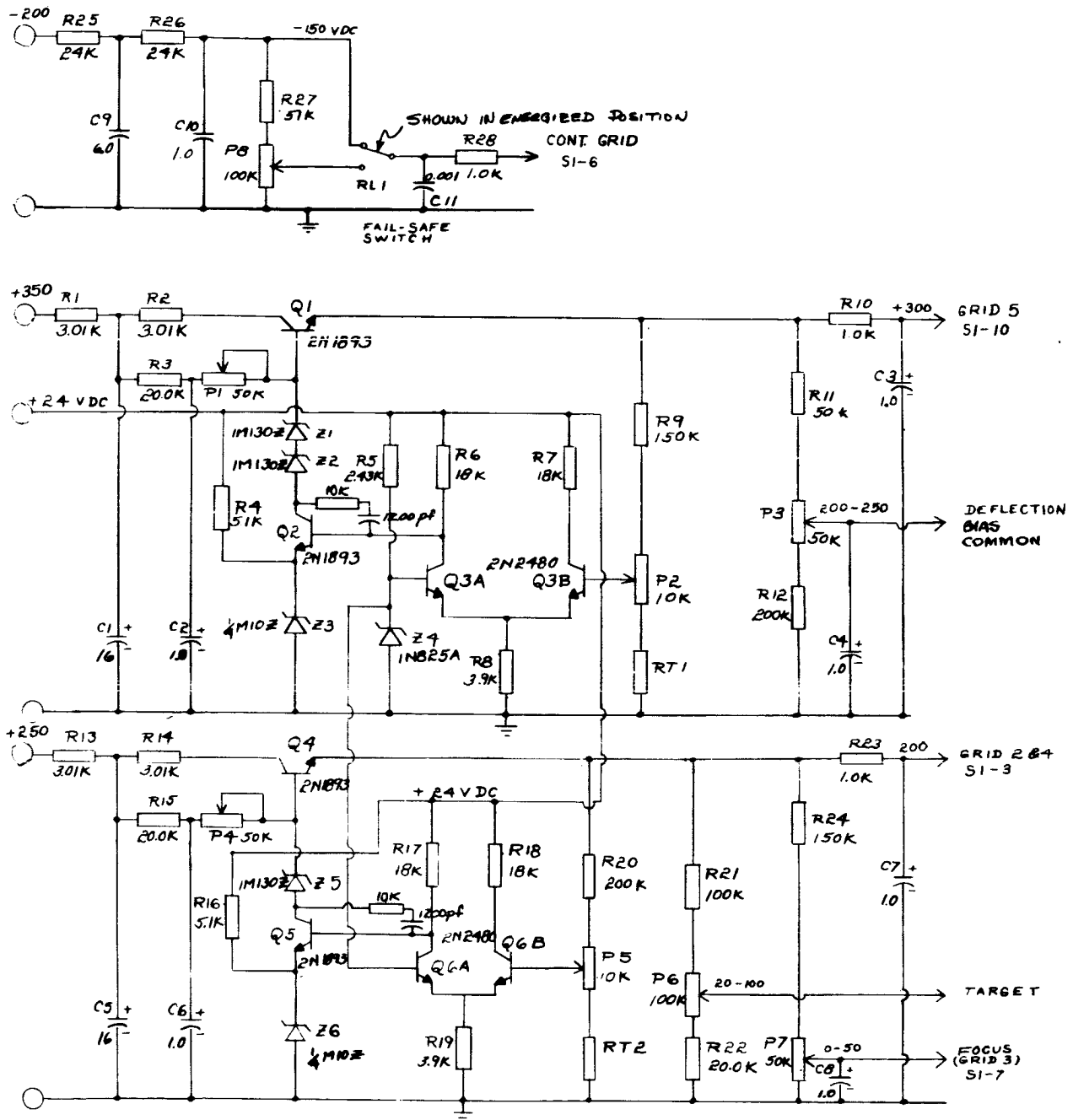


Figure 3-3. Vidicon Bias Supply

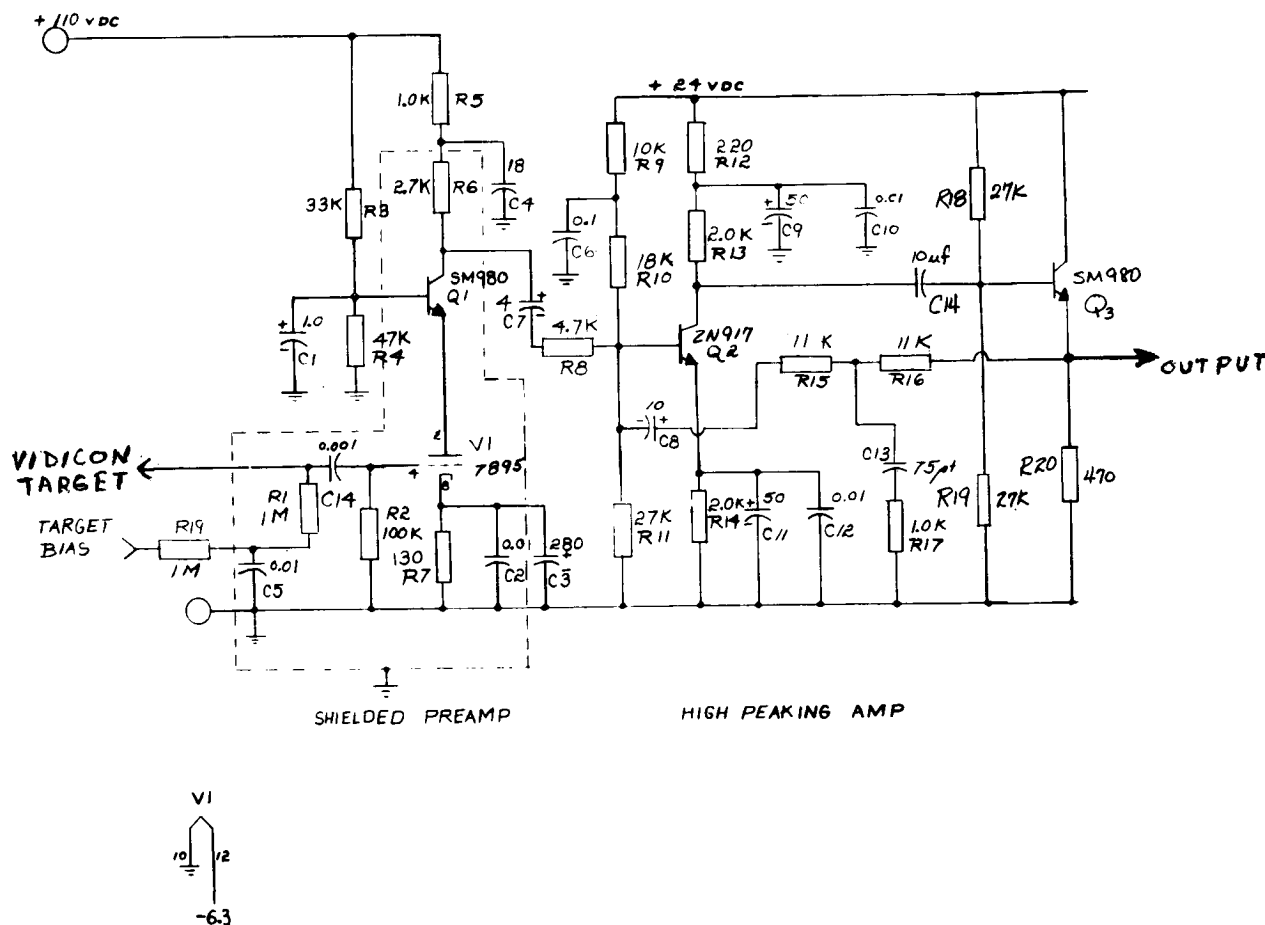


Figure 3-4a. Video Chain Circuitry
(Preamplifier and High Peaking Amplifier)

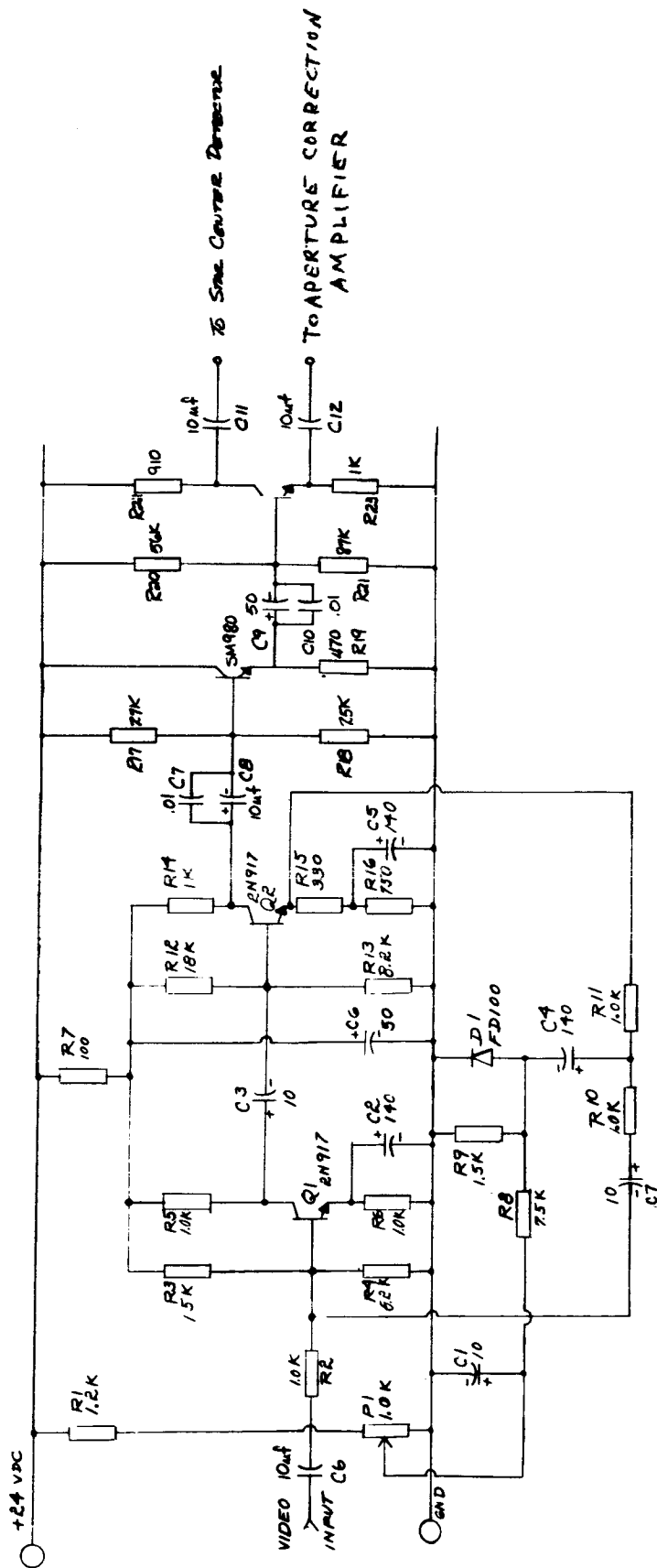


Figure 3-4b. Video Chain Circuitry (Variable Gain Video Amplifier)

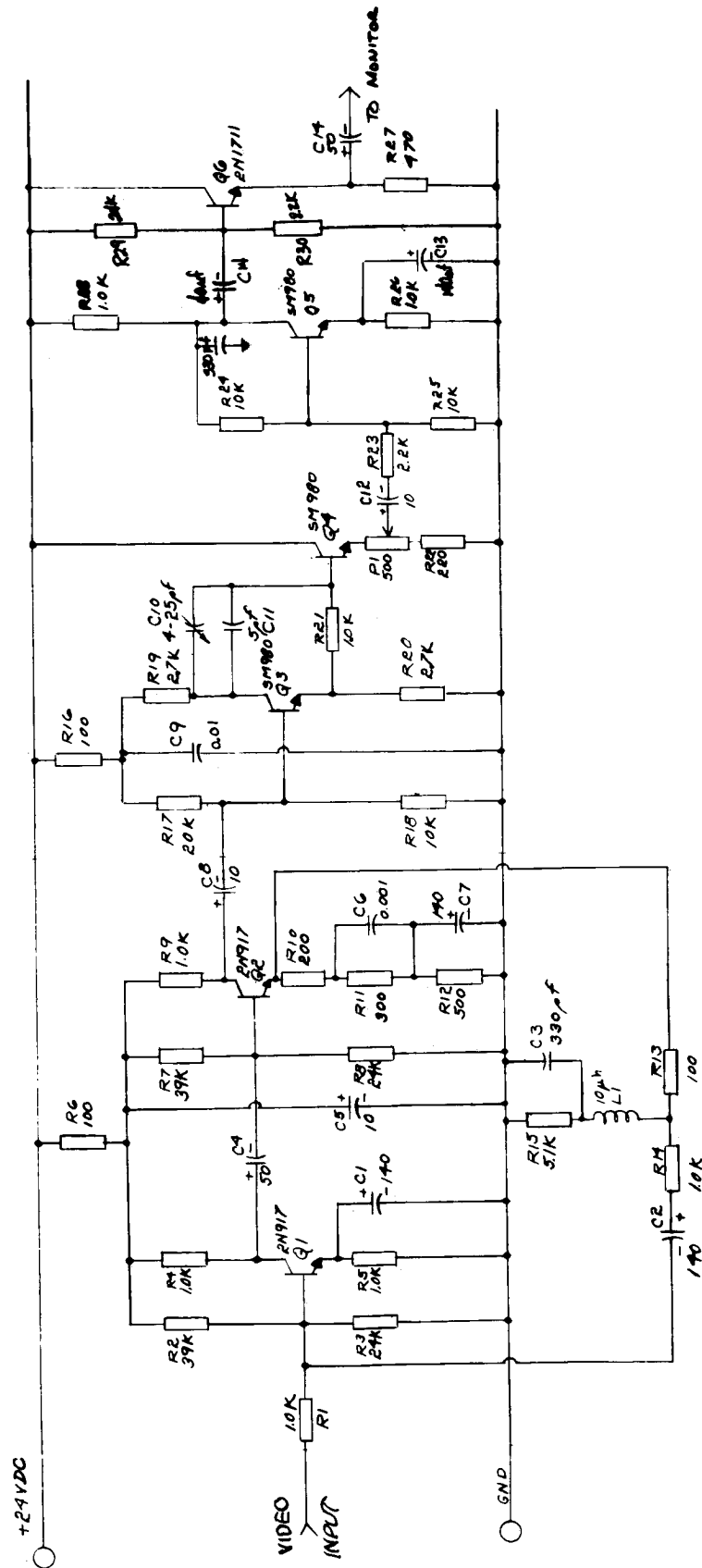


Figure 3-4c . Video Chain Circuitry (Aperture Correction Amplifier)

Peaking is adjusted by varying the capacity to ground in the feedback network. This is adjusted with the preamp in operation looking at a star pulse indication. Too much peaking will result in excessive undershoot on the trailing edge of the star indication. The amplifier has a bandwidth of 100 cps to 3 Mc with a 10 db gain at mid frequency. The lead occurs at approximately 100 Kc and flattens off at 1.5Mc at 20 db.

The overall response of the combined camera head amplifiers is 1 kc to 3 Mc with a 30 db gain at mid frequency, peaking to 40 db at about 1.5 Mc. Signal input levels are in the order of 1 millivolt or lower and output levels in tens of millivolts.

VARIABLE GAIN VIDEO AMPLIFIER

The first video amplifier in the chassis is used to increase the signal level for star and reticle center detection. It consists of a two transistor feedback amplifier with variable gain, emitter follower coupled to a phase-splitter. The gain control is achieved by splitting the feedback resistor and AC-coupling a diode to ground at this point. The dynamic resistance to ground of the diode is then varied by an external DC bias current. Increasing the current lowers the dynamic resistance of the diode and increases the overall loop gain. The emitter follower acts as a constant load to the amplifier. The phase-splitter provides output of a normal and inverted signal. The inverted signal is sent to the video processor. The normal signal is sent to the aperture correction amplifier. The gain is variable from 18 db to 22 db over a bandwidth of 1kc to 3Mc. Signal output levels are in the order of hundreds of millivolts.

APERTURE CORRECTION AMPLIFIER

The aperture correction amplifier is required to electronically reduce the apparent size of the scanning beam of the vidicon. Since the scanning spot is a certain minimum finite size, any sharp transition from black to white will take the beam a finite length of time to traverse. The effect of this is as though the video amplifier has a double lag break in the high frequency response. However, since the scanning beam is symmetrical the loss in response is not accompanied by a phase-shift.

The aperture correction amplifier is a two transistor feedback amplifier with the lag correction introduced by a combined RC and LC peaking network in the feedback. The phase shift introduced by this correction is compensated for with a unity gain phase-splitter so that the overall signal has the high frequency response correction with no accompanying phase shift. The compensating phase shift is realized by using in-phase and out-of-phase components of the phase-splitter. By properly combining the in-phase component through a resistor and the out-of-phase component

through a capacitor and summing, the desired phase-shift correction is produced with unity gain. The output is then amplified and emitter follower coupled to the monitor presentation.

Although this increases the high-frequency components of the signal response and apparent resolution of the camera to fine detail, it also amplifies the high frequency noise component which produces a large degradation in the signal-to-noise-ratio. For this reason, the aperture corrected signal is not used in the detection circuitry but is supplied for the eventuality of manned manual viewing.

DEFLECTION SYSTEM

LINEAR RAMP GENERATION FOR SQUARE RASTER SCAN

The linear ramps are generated by operational amplifiers used as integrators and fed with constant current sources. The integrators are reset by switching the output to a reset reference level insuring that the ramp always starts from the same point. By using this method, linear charging is not dependent on the amplifier gain but only on the requirement that the amplifier have a large negative gain.

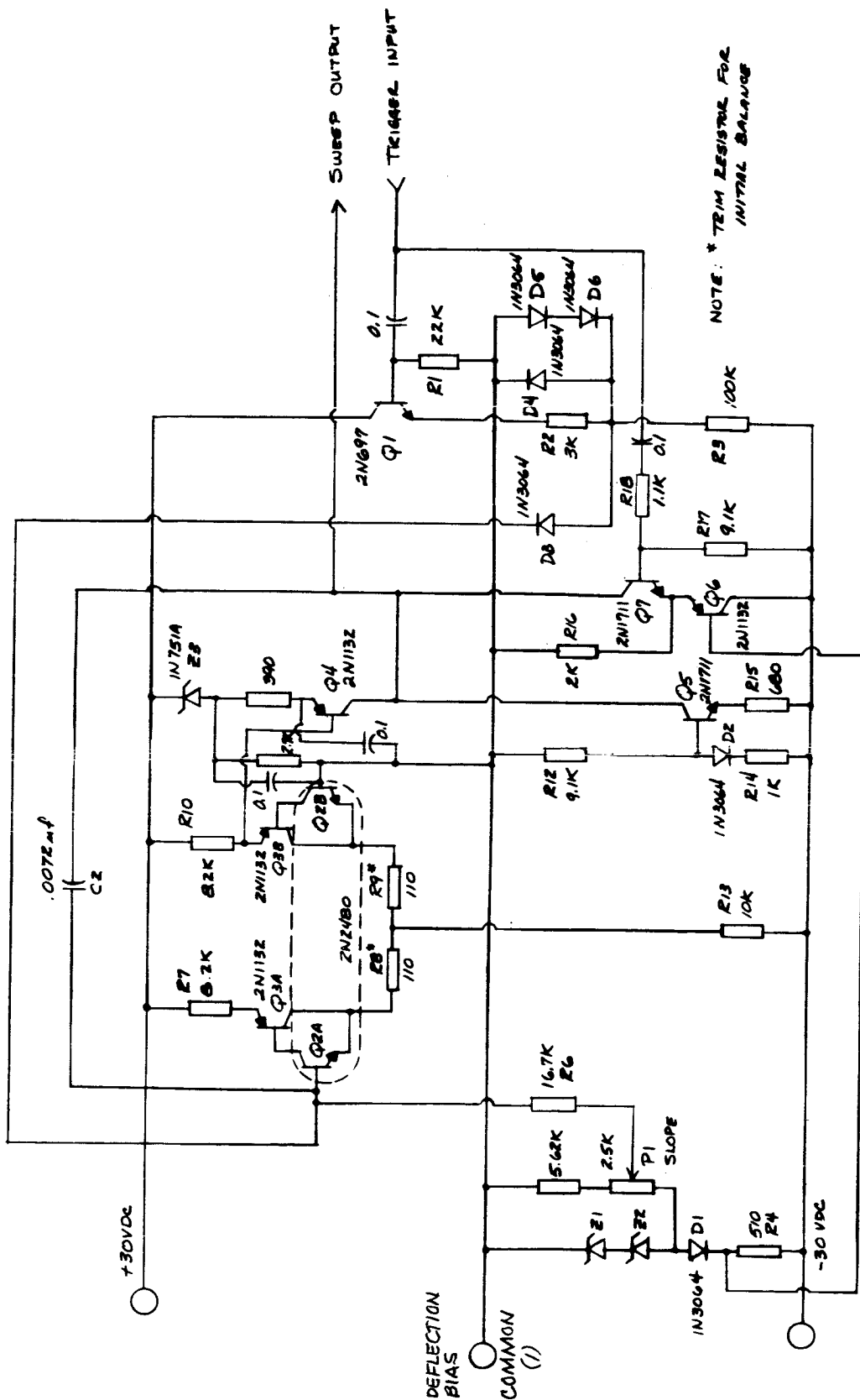
Temperature compensated Zener diodes provide the reset reference level. The current source is provided by two precision resistors and a variable potentiometer and the reference level. Adjustment of the pot P1 will vary the integration rate of the integrator in conjunction with a fixed precision feedback capacitor. Reset is accomplished by the sync pulse from the synchronizer. A matching of integration rate and period of reset will determine the deflection voltage swing. The present ramps swing 30 volts from a -17 volt reference. This circuitry is shown in Figure 3-5a.

The vertical sweep generator differs from that of the horizontal in that it has a pulse regenerator at its trigger input to square up any droop in the 34 msec reset pulse. It also has a switch to pull the input of the integrator to ground preventing any tendency to drift during this comparatively long reset period. The circuitry is shown in Figure 3-5b.

RADIAL SCAN

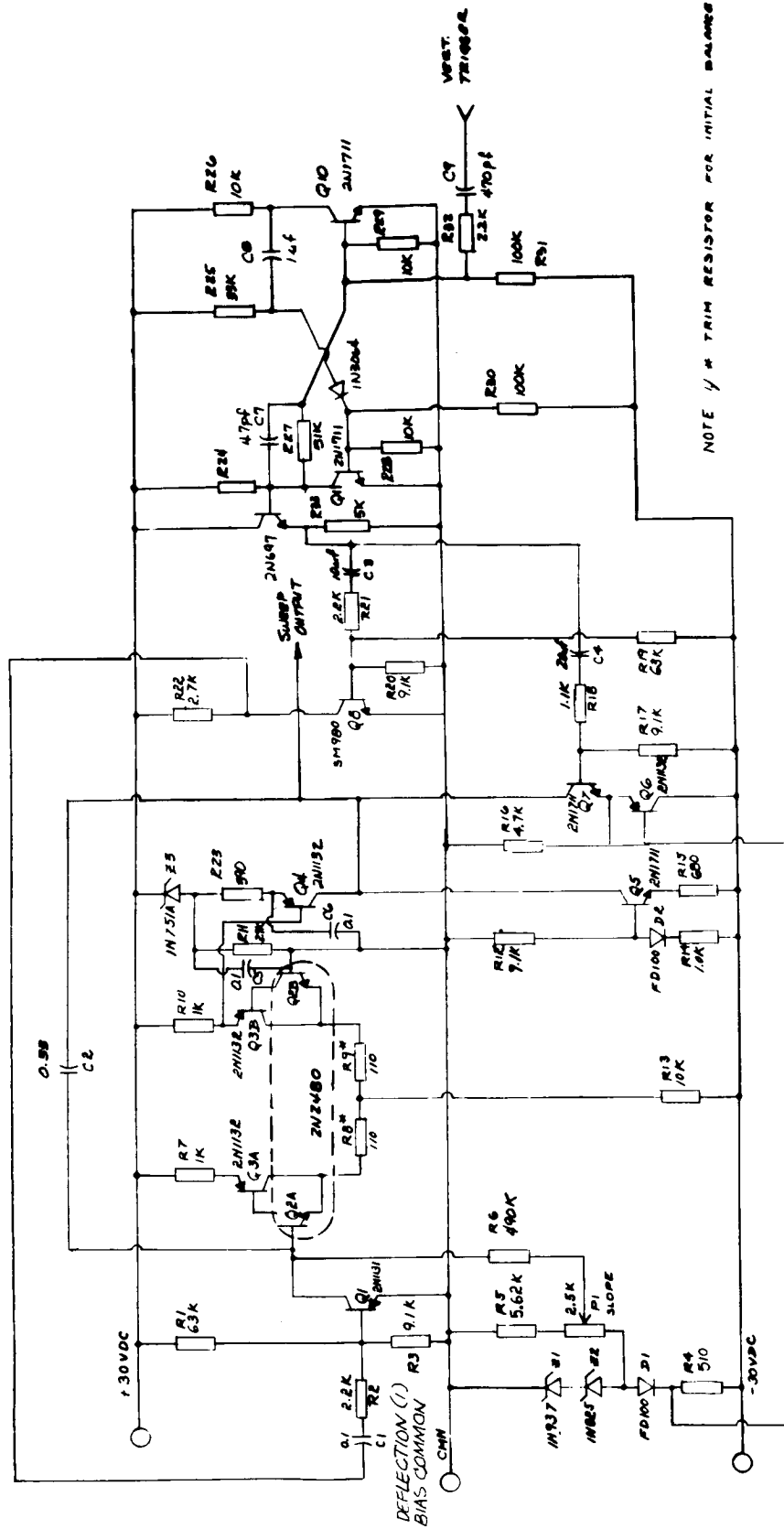
Introduction

The primary vidicon scanning technique employed in Phase A was an orthogonal raster of equal X and Y dimensions. This raster is ideally suited for point source tracking, provides uniform scan and integration



(1) THIS POINT NORMALLY IS BIASED 250 V DC ABOVE GROUND. THE +30 & -30 V INPUTS ARE WITH RESPECT TO THIS COMMON POINT.

Figure 3-5a. Horizontal Sweep Circuit



(1) SEE COMMENT ON FIG 3-7a

Figure 3-5b. Vertical Sweep Circuit

times and with a suitable analytical method can be applied to extended body tracking as well.¹

However, in applications when the Space Sextant would be used in a nulling mode, to track an extended target, the use of a radial scan has certain distinct advantages.

- A. Reduced computational complexity. By comparing all radial lengths, to target crossings to a common normalized value, nulling signals can be generated efficiently.
- B. Terminator elimination. By employing a priori knowledge of the sun's direction it is possible to devise a system which interrogates only the proper radii and thus eliminate the terminator crossings.
- C. The radial scan being circular in nature is more easily applied to the circular "inside out" images formed by extended celestial bodies in the wide mode system.

This is not to say that the radial scan is without undesirable features. The principal one being the non-uniform discharge of the vidicon target, possibly necessitating periodic returns to the orthogonal scan for "erasure".

In the light of the advantage however, it was decided, in Phase A, that the basic radial sweep circuits would be built up. The integration of these circuits with the T. V. camera and mechanization of the data handling technique would be carried out in the follow-on phases.

General Description

The radial scan system chosen produces 32 radii each starting at the target center and proceeding outward to the edge. The radii were designed to be equally spaced angularly. (The choice of number of radii is arbitrary and 32 was used for logic convenience and because this is a sufficient number for laboratory disc tracking.)

The radial scan system is shown in simplified block diagram form in Figure 3-6. The completed assembly is shown in Figure 3-7. For flexibility this prototype system was built up with its own integral power supplies. These supplies account for a good deal of the size shown in Figure 3-7.

¹Reference No. 12.

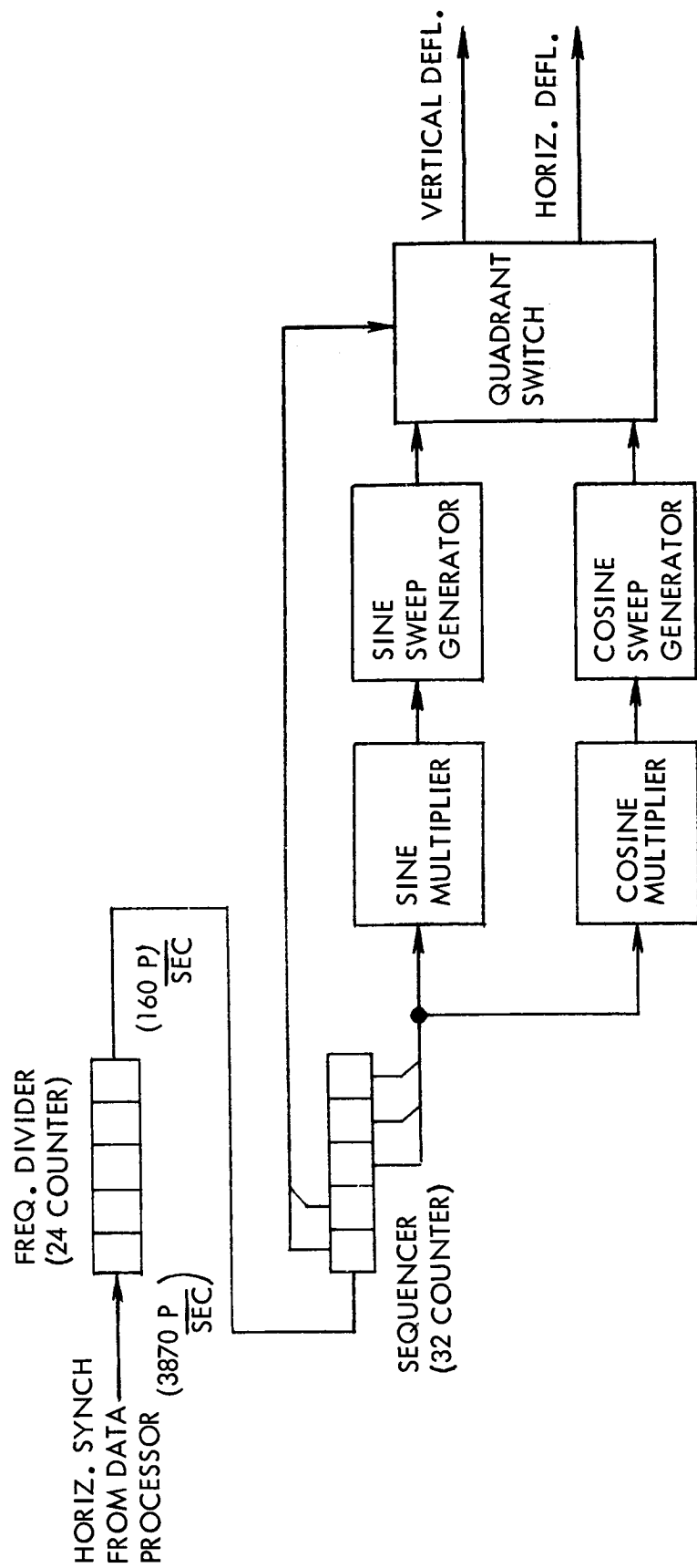


Figure 3-6. Radial Scan Block Diagram

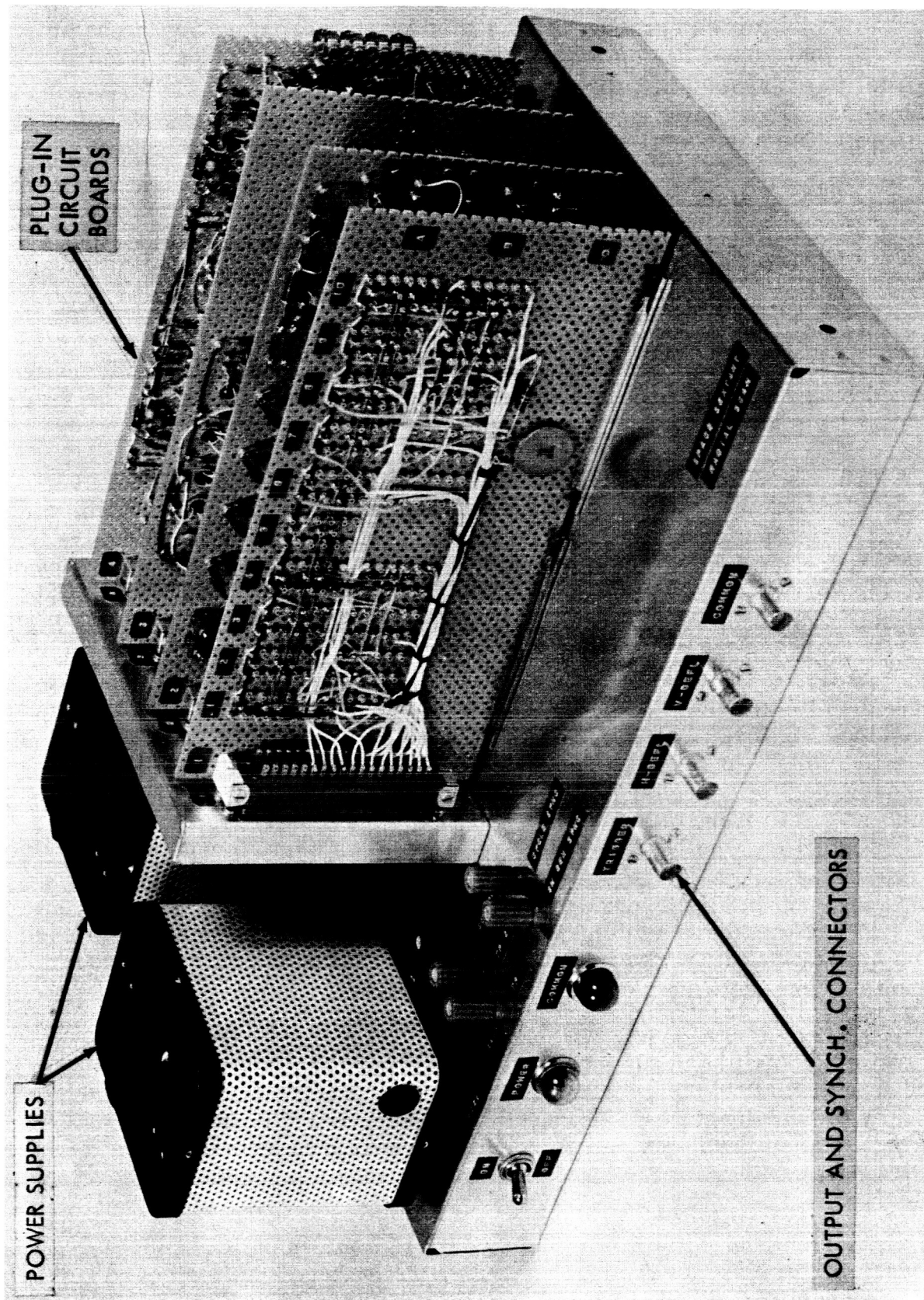


Figure 3-7. Radial Sweep Circuit Assembly

To keep the integration time of the target approximately the same as for the orthogonal scan a frame rate of 5/seconds was used. Each quadrant is expressed in 8 discrete steps, so a full scanning cycle consists of 32 steps. To achieve 5 frames per second, 160 steps per second are required. The horizontal synchronizer pulses from the data processor rate of $\frac{1}{258} \frac{p}{\mu\text{sec}} = 3870 \frac{p}{\text{sec}}$. The reduction in pulse rate from $3870 \frac{p}{\text{sec}}$ to $160 \frac{p}{\text{sec}}$ is accomplished by the frequency divider (24 - counter).

The sequence (32 counter) provides the 32 discrete steps for a full scanning cycle. The three lower stages of this counter are simultaneously decoded by a sin and a cos multiplier. The two upper stages, provide the quadrant switching.

The scanning operation is started in the first quadrant: then all stages of the 32 counter are zero, and a maximum horizontal and a minimum vertical deflection are supplied. While the first quadrant is scanned the horizontal deflection has to be decreased according to a positive cos function, while the vertical deflection has to be increased according to a positive sin-function.

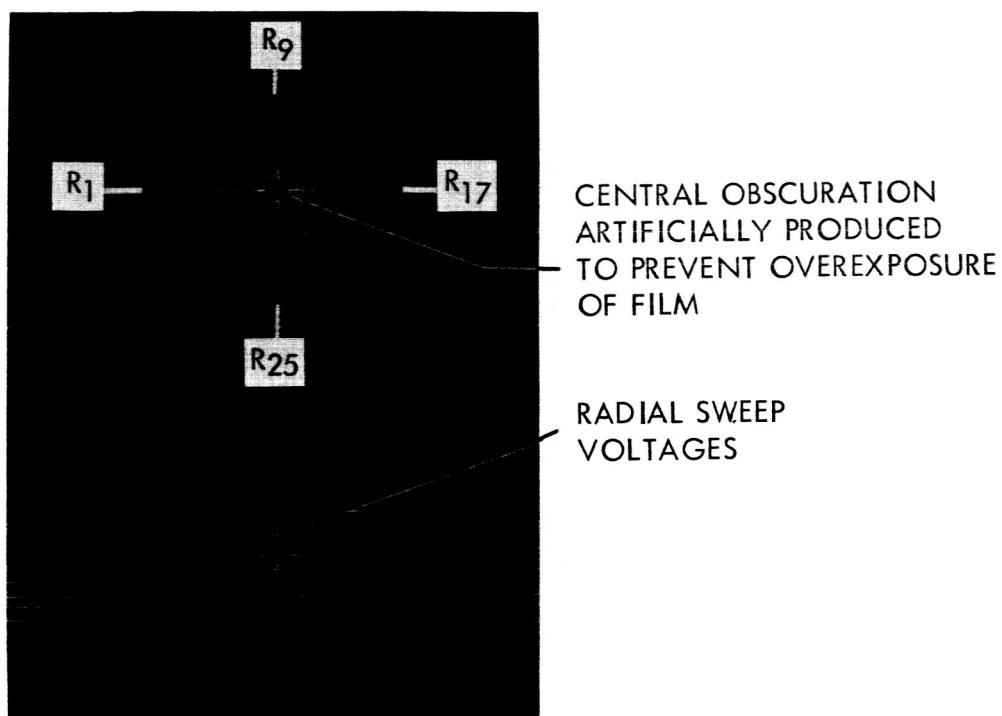
Entering the second quadrant the vertical deflection voltage has to correspond to a positive cos-function, the horizontal deflection voltage must correspond to a negative sin-function. In the third quadrant the vertical deflection voltage must correspond to a negative sin-function, while the horizontal deflection voltage corresponds to a negative cos-function. Finally, in the fourth quadrant the vertical deflection voltage corresponds to a negative cos-function, the horizontal deflection voltage corresponds to a positive sin-function.

All of the above switching, both functions and signs is accomplished by the quadrant switch network which is controlled by the two most significant bits of the sequencer count.

Figure 3-8 is a photograph of an oscilloscope trace of the output of the system. The use of unmatched dividing resistors in the breadboard model's sine and cosine generators, as well as a slight level change introduced by the quadrant switch, caused the observed deviation from equal spacing. These problems can be readily corrected in a final model.

Detail Design

As shown in Figure 3-7 the system is built up on four plug-in boards. Figure 3-9 is the logic layout of the system with the board limits shown in phantom.



NOTE: R_1 , R_9 , R_{17} , & R_{25} ARE THE INITIAL RADII IN THE RESPECTIVE QUADRANTS.

Figure 3-8. Radial Sweep Circuit Output (Oscilloscope Trace)

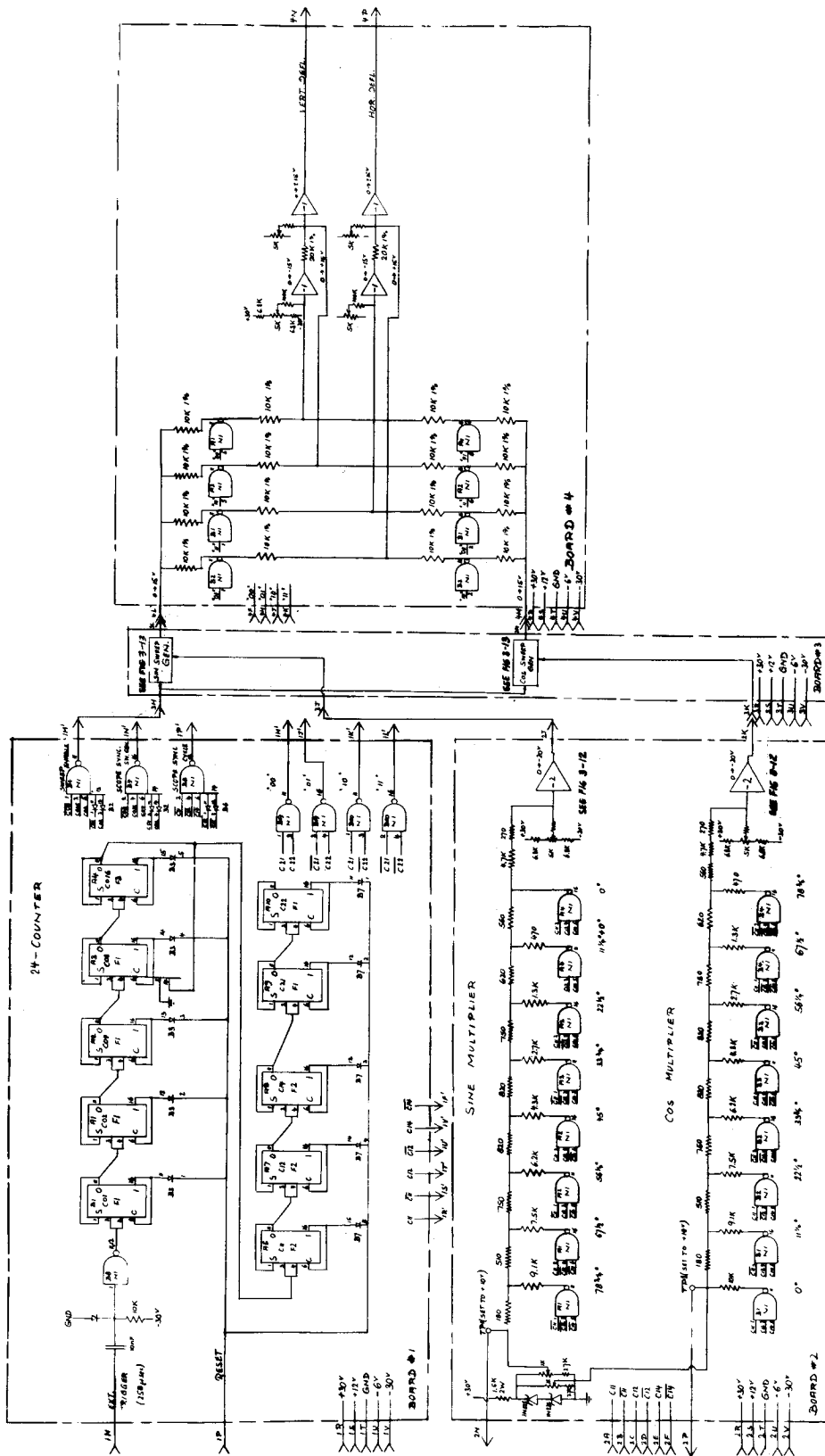


Figure 3-9. Space Sextant Radial Scan Logic Layout

Figures 3-10, 3-11 and 3-12 are the schematics of the summing amplifier, the sweep generator and the chassis wiring (including power supply) respectively.

DEFLECTION AMPLIFIERS

A pair of amplifiers are required for each set of deflection plates (horizontal and vertical). They are used in push-pull operation so that the axial field is zero during deflection, thereby minimizing the lens action of the deflection field. The first amplifier provides load isolation from the sweep generator and drives one plate with the inverted ramp signal. It also serves to drive the other amplifier providing the other plate with a non-inverted ramp. Potentiometers, P2 and P3, are used to adjust the DC centering of the raster. The required gain is determined by the signal level from the sweep generators (set now at approximately 30 volts). The gains are now set at approximately unity but may be adjusted by varying designated trimming resistors. The bandwidth required is approximately 2Mc for the horizontal amplifier and 2Kc for the vertical. However, both amplifiers are identical for compatible use with the radial scan option. The deflection amplifier circuitry is shown in Figure 3-13.

Because the raster may not be in rotational alignment with the recticle on the vidicon within the desired accuracy, a "skewing" system has been added. This provides a method of electronically rotating the raster into alignment with the reticles. This is accomplished by feedback from the horizontal to the vertical and vice versa. Skewing can be performed in either direction depending on which set of amplifiers is used in the feedback connections.

The amplifiers themselves are differential input operational amplifiers. The requirement for DC gain stability of 0.1% is met by having an open-loop gain of greater than 1000 at midband and degenerating the output stage to a gain of unity.

FAIL-SAFE CIRCUIT

The fail-safe circuit shown in Figure 3-14 is incorporated to protect the vidicon target from being damaged if the deflection circuits should fail. The circuit detects the presence of the deflection signals and clamps the vidicon control grid in cutoff in the event either signal should be absent.

It is desirable but not necessary to incorporate this circuit into the camera. The circuit is used as a precautionary measure to prevent damage to the tube during the testing phase.

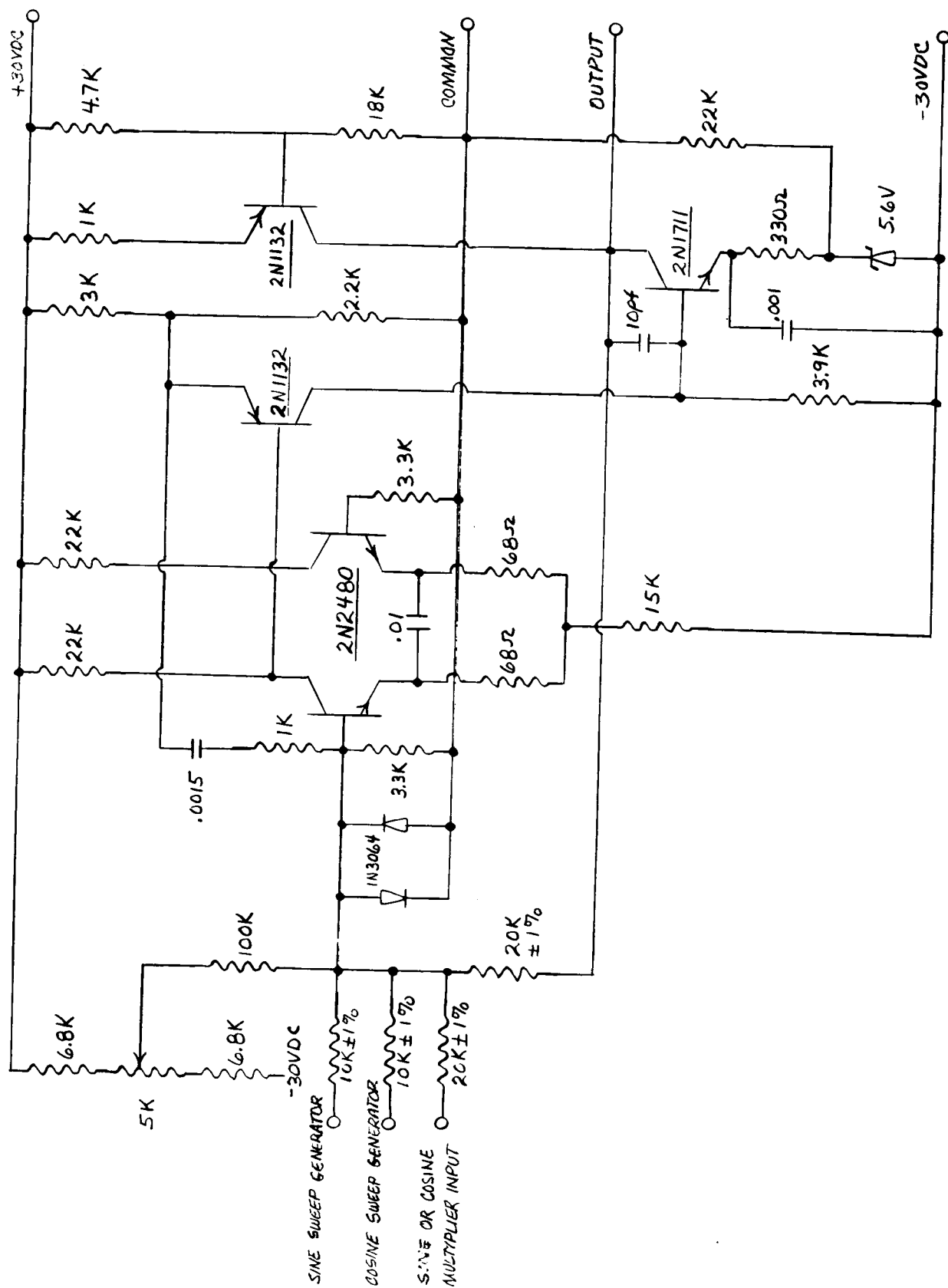


Figure 3-10. Space Sextant Radial Scan Summing Amplifier

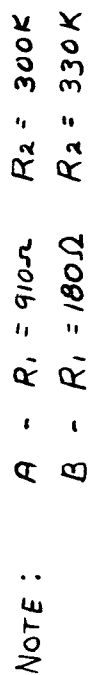


Figure 3-11. Space Sextant Radial Scan Sweep Generator

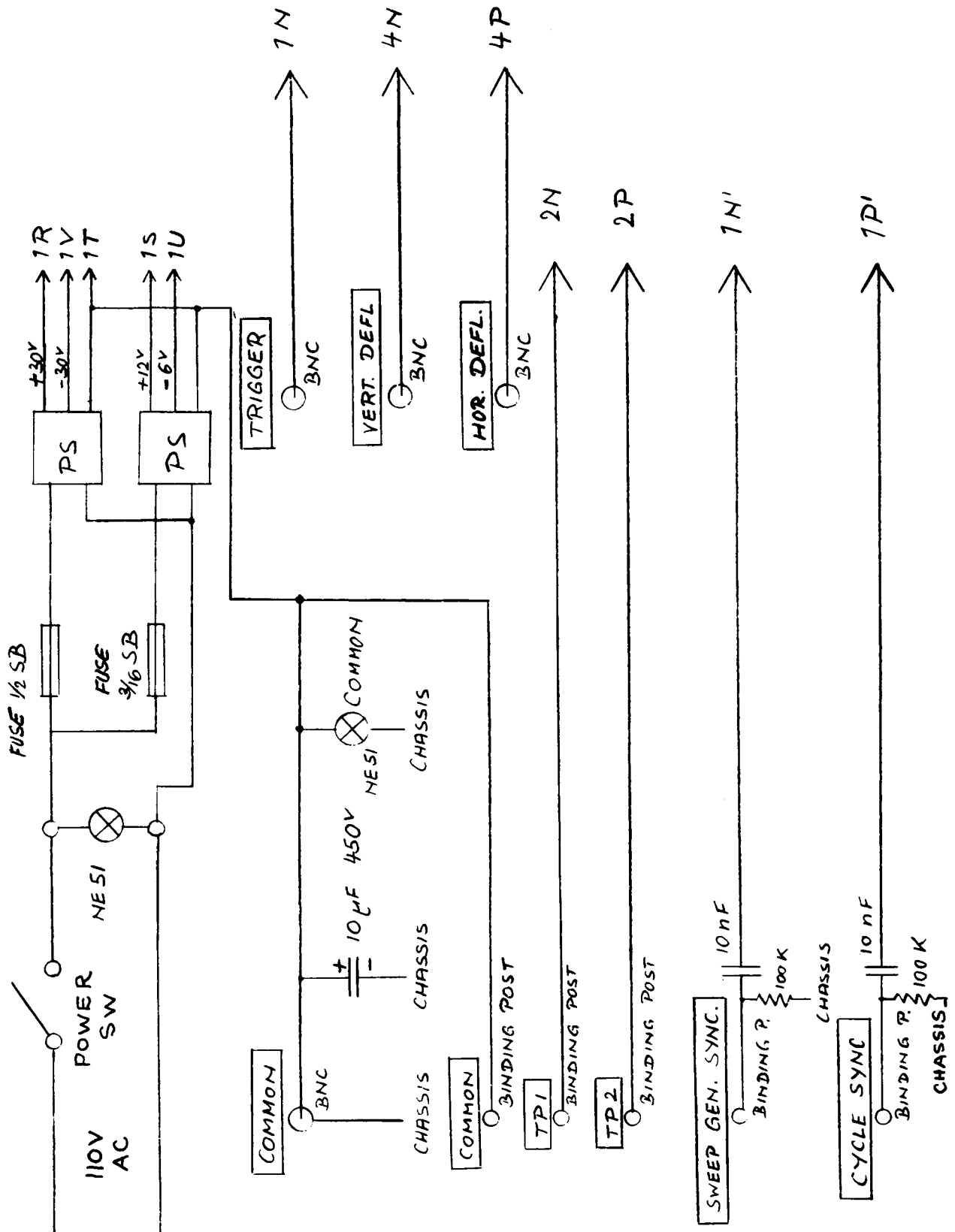


Figure 3-12. Space Sextant Radial Scan, Power Supply and Input-Output Wiring

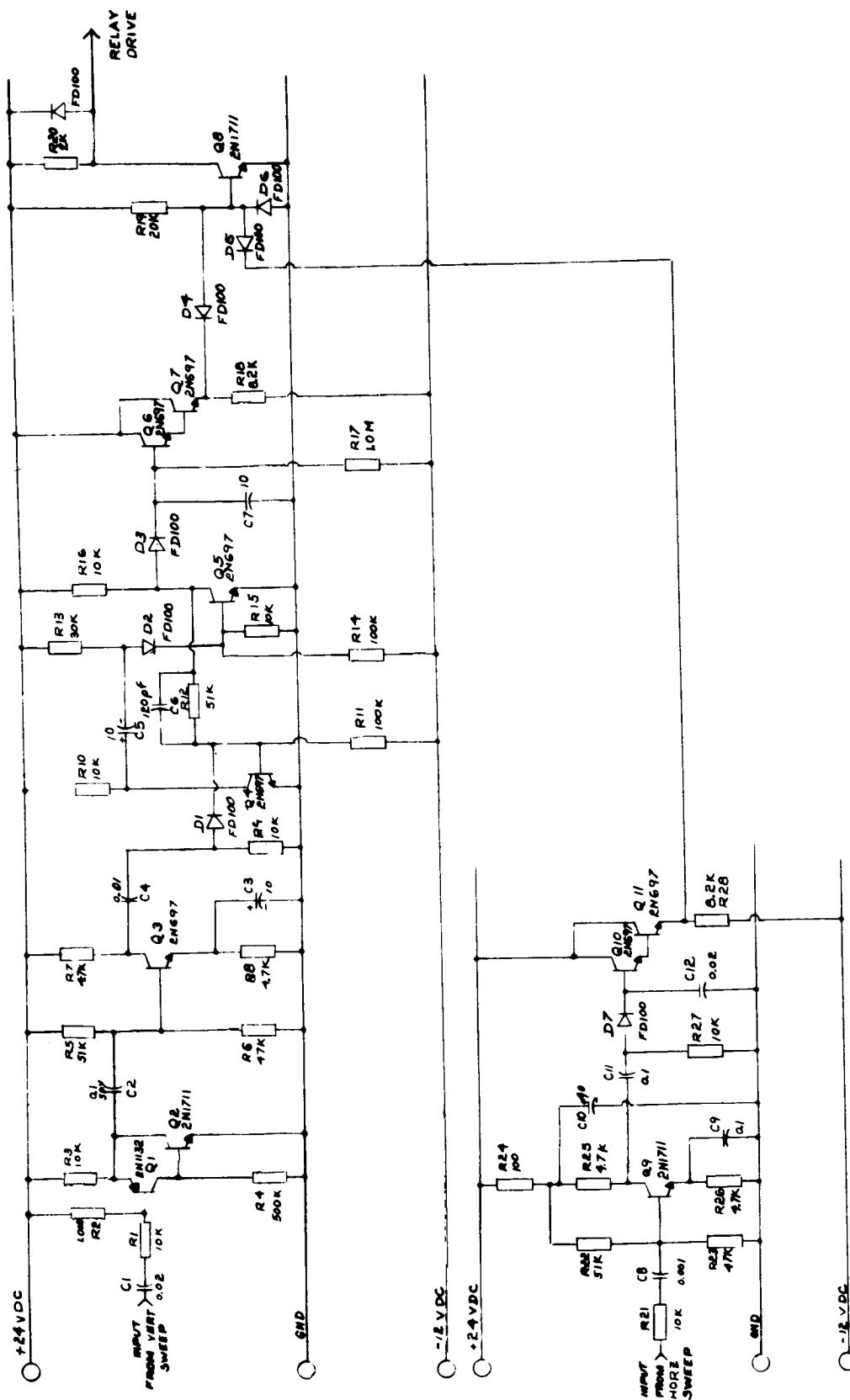


Figure 3-14. Fail Safe Circuit

The fail-safe circuit basically consists of a pulse inverter, a peak detector, and ANDgate and a relay drive circuit. The vertical channel has an added pulse shaper and a single shot to stretch the low repetition rate pulse. This was needed to allow the peak detector to hold during the longer period of the vertical.

The outputs of the deflection amplifier are capacitively coupled to the fail-safe circuits. During the sync period an inverted pulse is fed to a peak detector which holds the peak between sync pulses. These outputs are ANDed to the relay drive. As long as both are present the relay drive is shunted to ground. Failure of any one, will cause the relay to be energized, thus cutting off the beam.

SYNCHRONIZATION

The synchronizing circuitry shown in Figure 3-15 provides timing pulses to the sweep generators which determine the horizontal line frequency and vertical frame rate. In normal operation, the horizontal line frequency is determined by accurately timed sync pulses from the data processor. These pulses are used to reset the horizontal sweep and blank the electron beam of the vidicon during the retrace period. The vertical sweep is reset by counting horizontal sync pulses in an eleven stage binary ripple counter. ⁽¹⁾ Logic circuitry then determines the vertical sync drive rate from the horizontal rate thereby locking in time the horizontal and vertical sweeps.

For video blanking, during horizontal retrace, the data processor generates a pulse which overlaps the retrace blanking. The overlap eliminates the possibility of ringing and spikes, caused by blanking the vidicon electron beam, appearing in the video.

A similar overlapping video blanking signal is generated in the camera electronics for vertical retrace. This blanking generator has as an input the vertical counter. At the end of the blanking period, count 1280 in the table below, a pulse is generated which resets both the cameras' and the data processor's vertical counter. This synchronizes the two systems.

The logic is done using NOR circuits in conjunction with the counter and illustrated in the following tabulation.

	<u>Count</u>	<u>NOR Logic</u>
Video blanking start	1024	F-11, $\overline{F-9}$
Video sweep reset start	1088	F-11, $\overline{F-7}$, $\overline{F-8}$
Video sweep reset end	1216	F-11, $\overline{F-7}$, F-8
Video blanking end	1280	F-11, F-9
Counter reset	1280	F-11, F-9

(1) A ripple counter is a non-synchronous pulse counter. In general, a pulse entering stage No. 1 not only changes this stage but propagates a carry to the next stage. In the extreme case, this action must "ripple" the full length of the counter before the number in the counter is correct. This is opposed to a synchronous counter where all stages change to the correct new value at the same time.

The particular timing periods used are selected for convenient logic design after providing at least a 1000 line count. The counter is reset by the pull-chain process where all the flip flops are set to the zero state by diode clamps. The diode clamps are controlled by a single-shot triggered by count 1280. A self-operation feature is provided by the addition of two voltage comparators and two single-shot multivibrators. This allows operation independent of the data processor. A manual toggle switch connects the horizontal sweep to the voltage comparators whose reference levels (set by P1 and P2) are preset to correspond to the horizontal blanking start count (1088 count in data processor) and the horizontal sync start count (1150 count in data processor). Each in turn triggers a single-shot corresponding to horizontal video blanking ($51.2 \mu \text{ sec}$) and the horizontal sync or retrace period ($25.8 \mu \text{ sec}$). The input to the counter is provided with a diode AND gate so that it will accept inputs from either the data processor or the self-run mode.

Outputs of the synchronizer are four NOR's used as OR gates so that again either input, data processor or self-run will be accepted. The outputs provided are vertical and horizontal sweep reset, video blank and vidicon beam blank. The NOR's were chosen to furnish the higher voltages needed for the blanking and sweep resets and, thus, are different from the logic circuitry NOR's. The -6 volts needed for the counter flip flops and logic NOR's is supplied by -12 volts with a Zener reference drop.

DETECTION CIRCUITRY

VIDEO PROCESSING

The video signal has variations in sensitivity over the scanned target area because of non-uniformity of the photo conductive area and beam landing error. Beam landing error results in lower signal from the edges of the scanned area than from the center. This causes a humped warping in the dark-current level. It appears as a low frequency component in the AC signal from the target. Ideally a constant dark-level is desirable so that a uniform bias level at the detection circuitry may be used. To accomplish this the video is processed through a high pass filter which attenuates all frequencies below 5 kc, thus reducing the warp in the dark level. The output of the filter is then blanked by the wider video blank to eliminate any ringing and spiking of the beam blank pulse. (1)

An amplification of approximately 10 brings the signal level up to the detection level (order of 1-2 volts). A phase-splitter provides an inverted signal to the star center detector and a normal signal to both the reticle center detector and noise follower circuit.

(1) Other versions of this circuit employed a notch filter which failed to demonstrate any significant improvement over the simpler high pass filter and were temporarily discarded.

A peak detector follows the positive noise peaks thus establishing a noise reference level. This in turn is used to vary the bias output of a level changer which provides the detection bias level for both the detectors.

The video processing circuitry is shown in Figure 3-16a.

STAR AND RETICLE PULSE CENTER DETECTION

Pulse center detection is accomplished in the same manner in both the star and reticle detectors. In the case of a star, an integrator is started when the video signal produced by the star exceeds a set bias level. The integration continues until the signal falls below this level, indicating the end of the star signal. The integrator output is provided to both inputs of a voltage comparator. However, one input is delayed by a fixed delay τ (a delay line) and the other is fed directly with no delay but is attenuated to $1/2$ its original amplitude. The input receiving the halved signal is the off side of the comparator and the signal is in the direction of aiding turning ON. The delayed signal is directed to the ON side of the comparator but is in the direction aiding turn OFF. The mid point of the delayed signal corresponds in amplitude to the end point of the halved signal; therefore, when this point is reached the off side of the comparator turns ON and the on side OFF. (See Figure 3-16b.)

The OFF side output (a negative going pulse) is used to trigger a single-shot multivibrator which in turn drives a line driver sending a positive pulse to the data processor indicating the star pulse center delayed by τ . The ON side output (a positive going pulse) is used to reset the integrator which has been holding its integrated level.

Actual star observations indicate that star pulse widths will not exceed 4μ sec. The pulse width limitation on the center detector is twice the delay time τ of the delay line. Therefore, a 2μ sec. line was employed.

Disc edge tracking is accomplished by using the same pulse center detector circuitry as for the star. Edge detection is limited to black to white transitions only. Refer to Figure 3-17.

GENERAL DISCUSSION

The original camera concept called for a 1000 line raster with each line having a resolution capability of 1000 parts. For purposes of low bandwidth requirements, a slow scan system was decided upon. Readily available 5 mc clocks and logic components indicated the desirability of an approximate 5 frame/sec system and this became the original goal. For convenience, the 1000 line and 1000 part resolution per line were upped to 1024 (a binary multiple). A 20% allowance for blanking and retrace was then specified for each

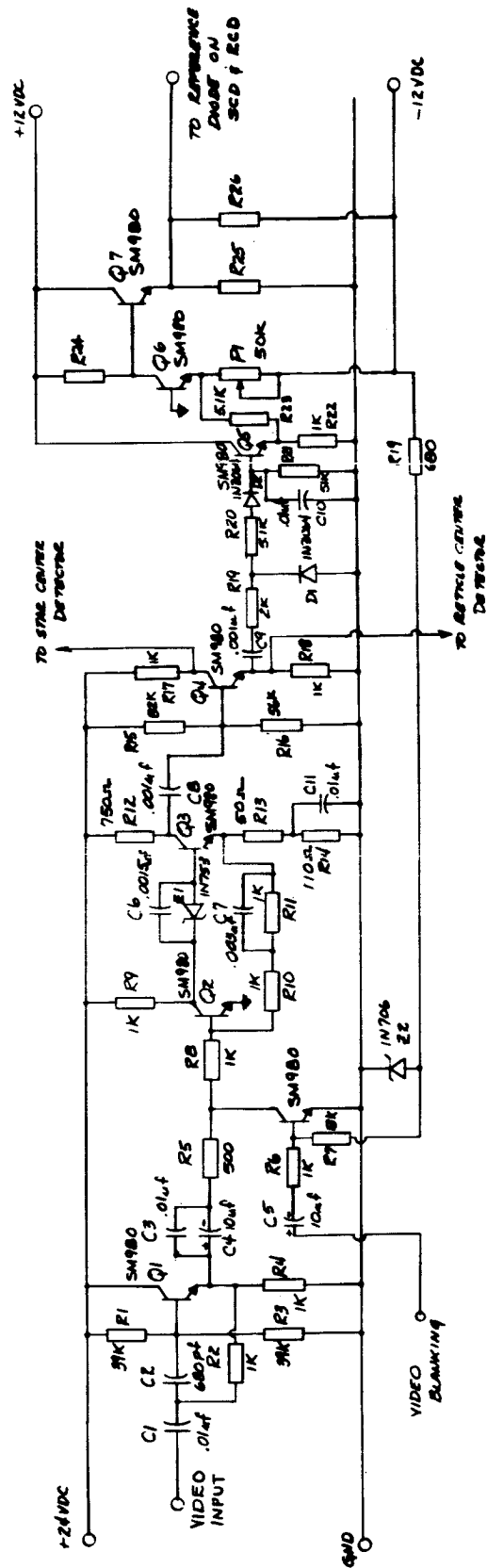


Figure 3-16a. Video Processing

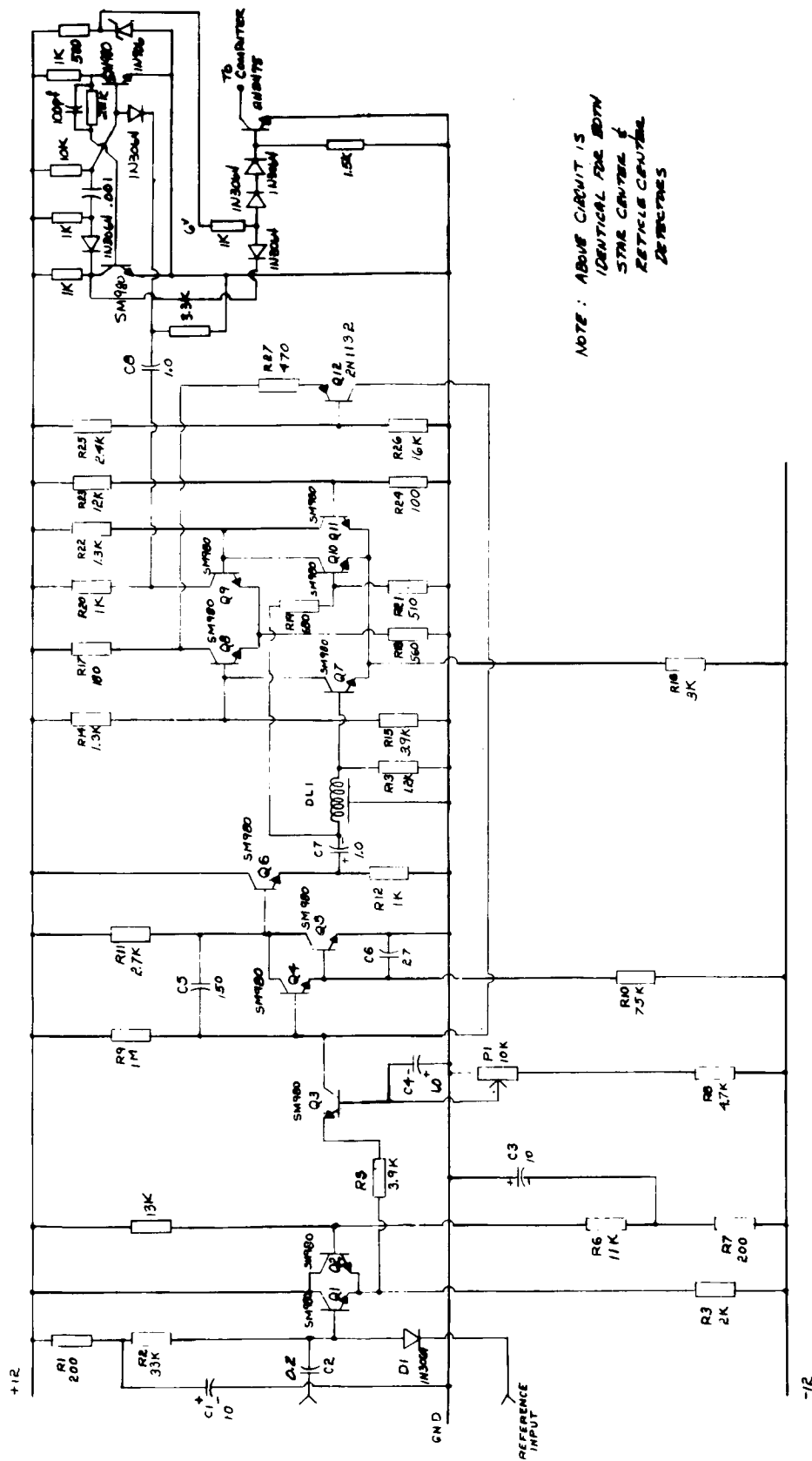


Figure 3-16b. Pulse Center Detection

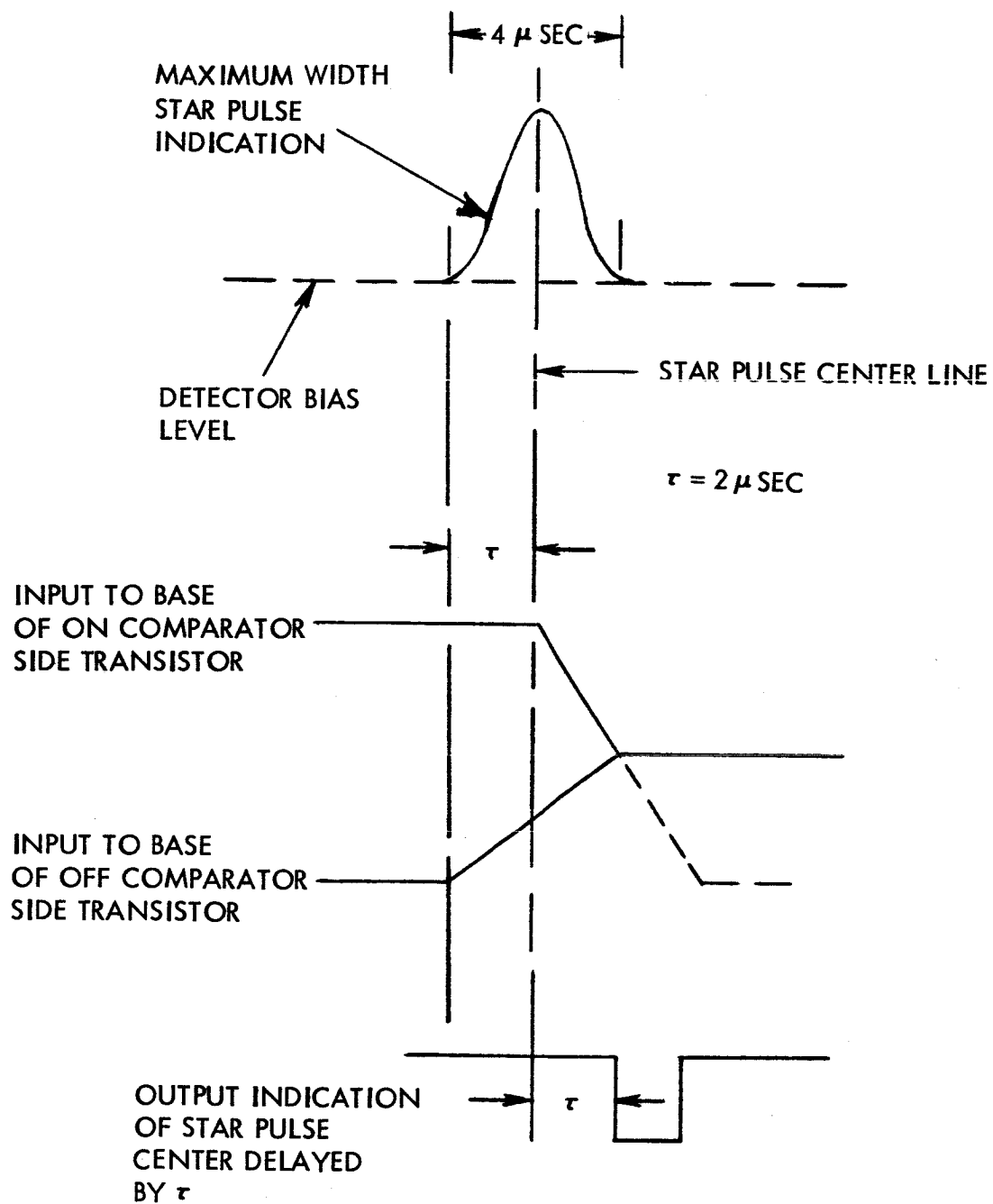


Figure 3-17. Star Center Detection Illustration

line and each frame. This resulted in a requirement for 1228 lines with 1228 part resolution per line.

To further simplify the logic manipulations, these numbers were finally increased and rounded off to 1280 lines and 1359 ± 15 part resolution/line. The horizontal rate then became:

$$f_H = \frac{5 \times 10^6}{1359} = 3.68 \text{ kc}$$

The vertical rate (frame rate) then became:

$$f_V = \frac{3.68 \text{ kc}}{1280} = 2.87 \text{ cps}$$

Without changing components, some of the slack in these allowances can be removed to increase the frame rate to 3.9 cps.

By replacing the 5 mc clock and making appropriate circuit adjustments, within component state-of-the-art limitations, the system can be operated at any desired frame rate between 3.9 cps and 15.0 cps.

The most challenging camera problem was the warping of the dark-level current due to beam landing error. This low frequency component as stated in the video processing section was to be removed by a high pass filter. The high pass filter does eliminate this low frequency component but also is essentially a differentiator. This means any star indication is differentiated and the undershoot appears as false reticle. Conversely, the reticle's undershoot appears as false stars. The first problem was taken care of in the data processor which was made to ignore the false reticle. Increasing the bias level at the star center detector eliminated the false star indications.

The beam landing error also lowers the sensitivity of the edges of the scanned area thus the first reticle (V_0) and the diagonal reticles were weaker signals than the center reticles. This meant the bias level of the reticle center detector had to be lowered to accommodate these lower signal levels making the detection circuitry susceptible to noise disturbances at various positions on the tube face.

Reticle modulation of the high leakage vidicon was particularly poor in the edge regions and required high beam-currents. For the above reasons a sporadic reticle pattern occurred. The switch to the low leakage tube with background illumination proved more successful but added the complexity of

a method for background illuminating. The method used illuminated the target from the edges which greatly helped the edge presentation but added non uniformities in illumination across the target face. The high pass filter was unable to cope with the above and good reticle presentation was obtained only through tedious bias level and illumination adjustments. The diagonal reticles were erratic and could not be used effectively by the data processor.

Conferences held with the vidicon manufacturer and tests run at his plant have shown that the dark level warpage can be significantly reduced by operating at higher mesh voltages and to keep the raster the same size, higher deflection voltages. These changes will be incorporated into the system during the follow-on Phase B effort.

Section 4

DATA PROCESSOR

INTRODUCTION

The data processor for the Space Sextant system performs four functions for the system. These are:

- A. Data averaging - Since the star image covers several horizontal lines, there is redundant data present. By averaging the several readings a more accurate measurement is effected.
- B. Reticulization - The data processor measures the image position relative to the reticle deposited on the face of the vidicon. Thus the system accuracy is unaffected by minor drifts and nonlinearities in the vidicon electronics.
- C. Noise gating - At least two star center pulses must occur on successive sweeps and within the horizontal confines of the noise gate in order for the system to classify the signal as a star. Thus random noise will not give rise to erroneous data.
- D. Calibration - Alignment of the vidicon deflection circuits is expedited by the data processor in the calibrate mode.

These functions are performed by three hundred and fifteen logic cubes organized into the following sections.

- 1. Horizontal - measures the X coordinate of the star or disc edge relative to the reticle.
- 2. Vertical - measures the Y coordinate relative to the reticle.
- 3. Data Processing and Display - averages the several readings and presents the data.
- 4. Sequencing - controls the other sections to reject noise and process the data.
- 5. Timing - insures orderly progress.

The block diagram of the data processor system is shown in Figure 4-1 while Figure 4-2 shows the appearance of the assembled unit. (The relay-rack construction, shown in Figure 4-2, was chosen for ease of setup and adjustment, and significant reductions in size are possible for a final model. This is discussed later in this section.)

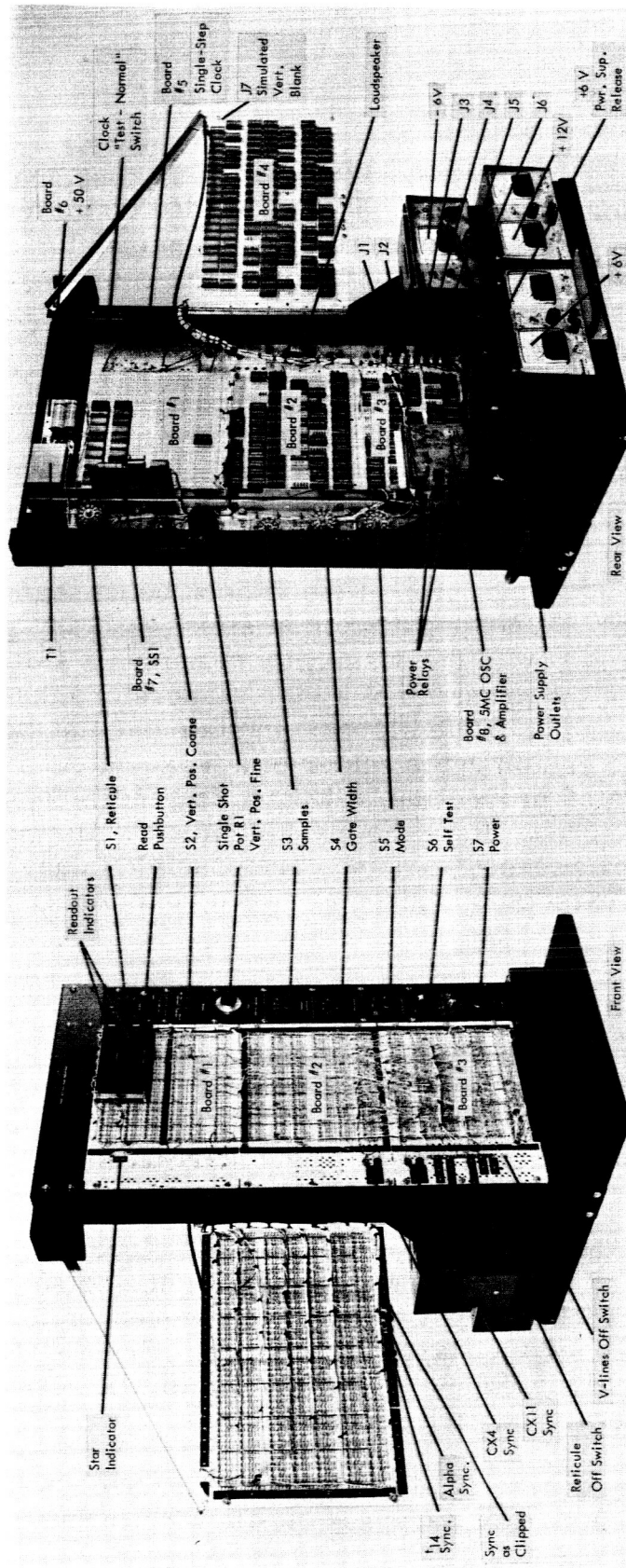


Figure 4-2. Front and Rear Views of Data Processor

MODES OF OPERATION

STAR MODE

Sequencing

The data processor was optimized to obtain star coordinates, the other modes being modifications to this one. It was decided that effective noise rejection could be obtained by requiring star center pulses to occur on at least two successive horizontal lines, with horizontal coordinates differing by less than some constant, δ . Similarly, it was required that one star center pulse could be missed without causing a lost star indication.

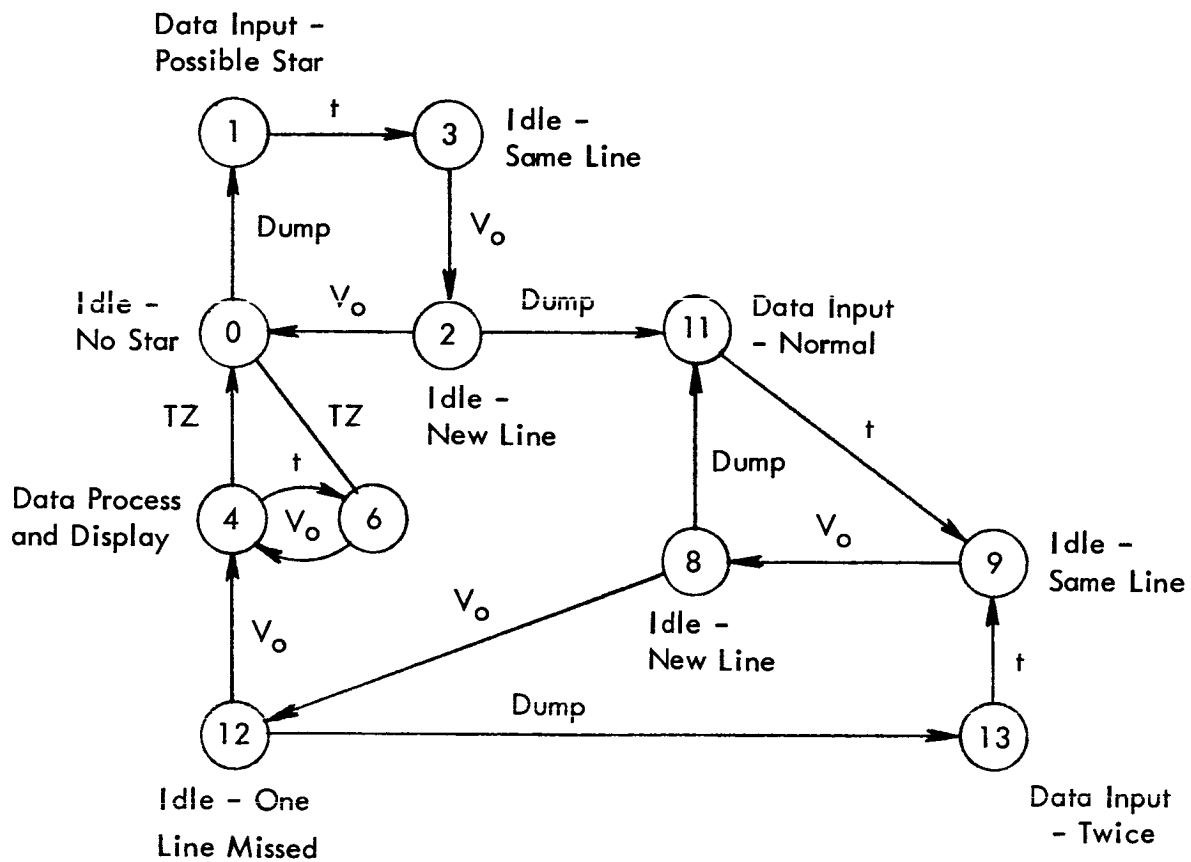
Operation of the star mode is best understood by referring to the state diagram in Figure 4-3. The state numbers refer to flip flop combinations in the sequencing logic and are discussed in the subsection covering mechanization. Transitions between states occur in one bit-time (200 nanoseconds) or less.

If no star is present in that area of the vidicon being scanned, the sequencer is in state zero. No noise gating is in effect, and any star center pulse will cause a dump. Due to the possibility of noise, a single dump is not interpreted as indicating the presence of a star. Therefore the sequencer moves to state one rather than state eleven. In state one the star's horizontal coordinate is used to establish the center of a noise gate. Following completion of this "First Data" processing, a t pulse is generated and the sequencer moves to state three. Here the machine idles while waiting for the start of a new horizontal sweep. No dumps are possible in any odd state, therefore, if two stars exist on a horizontal sweep, only the first will be recognized.

At the start of the next horizontal sweep a " τ " pulse moves the sequencer to state two where it waits to determine whether the previous star center pulse was noise or a star. If it is a star, a star center pulse will occur within the noise gate and will cause a dump. If it is noise, it is unlikely this will occur and the sweep will be completed without a dump. The lack of a dump leaves the sequencer in state two at the start of the next sweep and the τ generated then causes a transfer back to state zero.

If a dump occurs the sequencer moves to state eleven. Here the star's coordinates are input and a new center computed for the noise gate. With the completion of this processing a t pulse moves the sequencer to state nine where the machine waits for the start of a new line. From state eight a dump will cause the transfer to state eleven, and this cycle will recur as long as the star center pulse occurs on each successive line.

* " τ " is a one bit pulse generated at the end of the horizontal blanking and precedes V_0 by 16 counts. For purposes of following through Figure 4-3, V_0 and τ are interchangeable.



$t = 1 \Rightarrow$ Data from dump has been processed
 $V_o = 1 \Rightarrow$ Start of new horizontal sweep (τ)
 $TZ = 1 \Rightarrow$ Data processing and display period complete
 $Dump = 1 \Rightarrow$ Star center pulse within gate NOW

Figure 4-3. State Diagram--Star Sequence

If a line is swept without the star center pulse, the second tau will cause transfer to state twelve. This may occur either because of noise or because scanning of the star's image is complete.

If the miss were due to noise, the dump on the second sweep will cause transfer to state thirteen. Here "twice" normal data processing will be performed and the sequencer will return to the normal cycle.

If the miss were caused by the end of the star's image, a third tau will transfer the sequencer to state four. States four and six have identical functions, state six existing only to simplify mechanization. In these states the data is averaged to obtain the star's center which is then displayed. When the display is complete a TZ pulse is generated which returns the sequencer to state zero.

Data Handling

Introduction

During the data processing and display states two functions are formed, Y_{average} and X_{average} . The X_{average} is formed in the classic manner, dividing the summation of the X readings by the number of readings. The Y_{average} however is considerably simplified, being formed by subtracting one half of the number of lines from the last vertical reading. A further discussion of these processes will follow the discussion of the data input.

Three types of data input may occur. These are First, Normal and Twice. First and Twice are more easily understood following a discussion of Normal.

Normal Data Input

When the sequencer enters state eleven the following operations are initiated:

- x_1 , the horizontal coordinate just dumped, is added to $N(C)$, the contents of the C-register;
- one is added to $N(B)$, the contents of the B-register which indicate the number of sweeps through the star so far; and
- the difference $x_1 - \Delta$ is generated and placed in the X-register. Δ is a switch-selected number corresponding to one half the gate width. This difference determines where the gate will open on the next sweep.

This processing requires thirty microseconds which corresponds to two word times of fifteen bits each. In addition there is a waiting period of up to fifteen microseconds which allows the B- and C-registers to get into position. These operations are controlled by the bit and word time counters.

During the first of the two word times the data in the X-register is circulated once unchanged, thus being made available for addition to the data in the C-register. $N(X)$ is the x_i transferred from the x-counter by the last dump. Thus if this were the third sweep through the star,

$$N(C) = x_1 + x_2 + x_3$$

following the addition.

During each word time the data in the B-register circulates three times due to its length of five bits. During the last third of the first word time a one is added in the Normal data input state.

During the second word time x_i is again input to the adder/subtractor. This time a subtraction takes place and the difference between x_i and Δ is generated. This difference is shifted into the X-register, replacing x_i .

The vertical coordinate, y_i , is not involved in the input processing. Each dump merely replaces the previous contents of the A-register with the latest vertical coordinate.

At the end of the second word time the t pulse is generated.

First Data Input

The First data input operations differ from the normal only in two respects. During the addition of x_i to $N(C)$ the old contents of the C-register are prevented from entering the adder/subtractor, thus $N(C)$ becomes $x_i + 0 = x_i$; and the contents of the B-register are cleared to zero during the first third of the first word time.

Twice Data Input

The Twice data input operations result from having missed one reading in the midst of a sequence. Due to the manner in which Y_{average} is formed some cognizance must be taken of the missing line. This is done by adding two to $N(B)$ instead of the usual one. This in turn causes difficulty in forming X_{average} . To compensate for this $2 \cdot x_i$ is added to $N(C)$. In effect the reading following a missing pulse is given double weight. If evaluation shows this to be undesirable several alternatives are available. These include adding an additional register to record the number of lines separately from the number of readings, and adding two additional registers such that Y_{average} is formed in the same manner as is X_{average} . The cost of the first alternative is six flip flop and six NOR cubes. The cost of the second is twenty-five flip flops and fifteen NOR cubes. The second alternative also adds one hundred and seventy microseconds to the data processing period.

Data Processing and Display

In the data processing and display states two arithmetic operations take place. These are:

$N(V)$ becomes equal to $N(A) - 1/2 N(B)$, forming Y_{average} , and $N(H)$ becomes equal to $N(C) \div N(B)$, forming X_{average} .

$N(V)$ is the data in the vertical display register and $N(H)$ is the data in the horizontal display register.

Y_{average} is formed during the first complete word time of the state following the waiting period of up to fifteen microseconds. The factor of one half is generated by subtracting the next to the least significant bit of $N(B)$ from the least significant bit of $N(A)$. This in effect shifts the binary point of $N(B)$. This operation is completely analagous to shifting the decimal point to divide by ten in a decimal number. The difference formed is shifted directly out of the adder into RV, the vertical display register. Zeros are shifted into RA.

Since the summation of the x_i was formed during the data input, it only remains to divide by the number of readings. This division is simplified by the fact that only positive numbers are present. Like most division processes, the quotient is formed most significant bit first. As the quotient bits are formed they are shifted into the horizontal display register RH, one shift occurring every fifteen microseconds. Ten shifts of one bit each suffice to form the quotient in RH where it remains until the next data processing and display period.

When the division is complete a TZ pulse is formed, the entire process having taken from 183 to 197 microseconds.

Summary

In summary, during First data input

$$N(A)_1 = y_1$$

$$N(B)_1 = 1$$

$$N(C)_1 = x_1$$

during Normal data input

$$N(A)_i = y_i$$

$$N(B)_i = N(B)_{i-1} + 1$$

$$N(C)_i = N(C)_{i-1} + x_i$$

during Twice normal data input

$$N(A)_i = y_i$$

$$N(B)_i = N(B)_{i-1} + 2$$

$$N(C)_i = N(C)_{i-1} + 2 \cdot x_i$$

and during Data Processing and Display

$$N(V) = N(A) - N(B)/2$$

$$N(H) = N(C)/N(B)$$

Noise Gating

Following any data input state the X-register contains the difference $x_i - \Delta$, where Δ is a switch-selected positive number representing one half of the desired gate width. The same switch which selected Δ controls the output logic of the noise gate counter. This counter, CD, has a maximum of 31 states. When the X-counter, CX, reaches the count equal to the contents of the X-register, RX, the noise gate is opened and CD is released. When CD has counted 2Δ counts, its output logic closes the gate and changes CD to zero again. The gate will then remain closed until $N(CX)$ again equals $N(RX)$. In the event that the last star lay so close to $x = 0$ that $N(RX)$ is negative, the gate will open when $N(CX) = 0$ and 2Δ will be counted from there. The noise gate is not effective during state zero. In addition to the noise gating, star center pulses are blocked during odd states of the sequencer, during data processing, during horizontal and vertical retrace, and following the horizontal retrace but prior to count zero.

Reticulization

Introduction

Reticulization refers to the process of making the horizontal and vertical counters agree with the reticle deposited on the face of the vidicon. This procedure allows errors in the spot positioning circuits to be corrected by the data processor. Horizontal and vertical position may be off by 3%, and the horizontal sweep may be off 0.5%. The vertical sweep may also err by 3% without impairing the 0.1% accuracy of the result. The tolerance on the vertical sweep could be relaxed still further if the vertical average were computed in the same manner as the horizontal.

Horizontal Reticulization

The horizontal counter is corrected by referencing it to the eight, vertical, V-lines of the reticle. These lines are numbered V_0 through V_7 and are so spaced that exactly 128 counts should occur between line crossings. The count is started by V_0 . When the next reticle center pulse is received the least significant seven bits of CX are examined to see whether the count is above or below 128. If they are all zero the count is exactly 128 and no correction is made. If the most significant of the seven is one, the count is below 128 and a partial reset occurs pulling the least significant bits up to zero and propagating a carry to the most significant bits of CX. Since the most significant of the seven bits toggles every 64 counts, the count may be up to

64 counts slow and the correction will still be made correctly. Due to the necessity for reading a star correctly at coordinate 127, the tolerance on the sweep can't be the -50% this might indicate.

In the present mechanization the count can be corrected only one bit per reticle crossing if the count is high. This is easily made more tolerant, but time prevented modifying the hardware on this phase of the program. This one-bit correction was based on the need for sweeps linear to 0.5% which would therefore eliminate the need for any greater correction. The correction is made by inhibiting one count input if either of the two least significant bits are one. This in effect subtracts one from $N(CX)$.

The action at the remaining V-lines is identical to that at V_1 , the count differing only in the most significant three bits of CX which are not considered anyway. In other words the least significant seven bits count modulo 128^* and are therefore the same at each V-line.

Vertical Reticulization

The vertical corrections are made by assuming the horizontal count is correct and comparing the two counts when the sweep crosses a diagonal line drawn at 45° to the X-Y coordinate system. Analysis of the trigonometric functions involved shows that a tilt of $\pm 3^\circ$ will not affect this operation. Since some difficulty might occur if the diagonal line were drawn across the vertical lines, the diagonal line was broken up into nine segments and placed at the extreme right of the vidicon; i.e., at the high count end. The only effect of this segmentation is that the most significant digits of the counters will no longer agree; but, since errors are expected to be small (less than 64 counts), this is immaterial. Care was taken in the segmentation so that the distance between diagonals measured horizontally was exactly 128 counts.

If the vertical sweep is correct, one count enters the vertical counter at the start of each horizontal sweep. If the vertical count is high, this count is inhibited. If the count is low an additional count is entered during the comparison period. No equivalent to V_0 exists, the vertical counter being reset by the end of the vertical blanking period. Since this period is gated by the same mechanism that resets the vertical sweep circuits, this reset will be within a few percent. With one count correction per horizontal sweep, this same percentage of 1024 represents the number of horizontal lines required to bring the vertical count into agreement with the vertical position. Thus if the starting position were off by 1%, the first ten or eleven sweeps would have erroneous vertical coordinates.

Since the vertical correction logic has 100% authority, relative to the normal vertical rate, ** the limitations on the vertical sweep accuracy arise from considerations such as the method of calculating Y_{average} and the maximum number of data inputs possible before the B-and C-registers overflow.

*For a discussion of modulo numbers refer to page 69.

**The correction logic can vary the normal count rate by 100%, i.e. from zero to twice normal.

DISC EDGE MODE

In this mode the aim is to obtain several points on the edge of a disc. In the noise free case one sample would be enough to define a point, but in a real system it is necessary to take several in order to assure that the sample is indeed on the disc edge. Note that the number should be limited so that the curvature of the disc does not draw the average in towards the center.

The location of the several points along the edge is not well defined at this stage of the development, therefore a manual control is provided for the selection of the vertical coordinate of the sample.

With the exception of these two items, Disc Edge operation is identical with Star mode operation. No change is made in the sequencer, the transition to the data processing state being effected by simulating a continuous string of tau's when the number of samples reaches that selected by setting a switch. Thus the transition from state nine to state four requires three tau's or 0.6 microseconds. Possible switch positions select either four, eight, or sixteen, samples.

The vertical position selection is effected by a highly stable single-shot triggered at one of four points in the vertical cycle. Thus the Vertical Position setting features a coarse, switch, selection and a fine, ten-turn, potentiometer, setting. The possible range is from line one to line 1024. This circuitry controls, blanks off, only the bottom of the vertical sweep, so in effect the setting defines the minimum vertical position. The actual vertical position is measured as it was in the Star Mode.

Following the data processing and display state, the sequencer returns to state zero. Subsequent dumps move it through states one and three, but the tau's continue, returning it to state zero each time. The string of tau's ends with the occurrence of the pulse which resets the vertical counter, thus releasing the sequencer for the next frame.

Selection of the desired number of samples is accomplished by examining a particular bit of $N(B)$. Which bit is determined by the switch setting.

Reticulization is identical with that of the Star Mode.

CALIBRATE MODE

In calibrate the object is to adjust the electron optics and sweeps so as to minimize any differences between theory and practice. This in turn minimizes the need for reticulization in the other modes. The data processor expedites this adjustment by measuring the position at which various reticles are crossed and displaying this information. Two sub-modes may be defined;

calibration of V_0 and calibration of any other reticle line. Calibration of V_0 is relative to the horizontal blanking; i.e., to the actual gate which resets the sweep. Calibration of the other reticles is relative to V_0 .

Sequencing is shown in Figure 4-4, a single sample being taken on any vertical sweep. In contrast with the other modes, the dump which moves the sequencer out of state zero is gated. This gate is a combination of the minimum vertical position selected by the VERTICAL POSITION controls, and a minimum horizontal position selected by the RETICLE switch. No high end is provided for either gate other than that provided by the horizontal and vertical blanking signals which cover the retraces.

In the calibrate V_0 operation the horizontal counter is reset by tau, the one-bit pulse which immediately follows the end of the horizontal blanking. The only gating is that of the Vertical Position circuit and the standard horizontal and vertical blanking. The horizontal position of the deflection circuits should be set so that V_0 is encountered sixteen counts after the end of the blanking. This is indicated by a reading of 0020_8^* on the indicators. The READ pushbutton must be depressed for each reading. Readings taken at several vertical positions will disclose any "bending" of the raster.

With the RETICLE switch in positions V_1 through V_7 it is possible to adjust the horizontal sweep rate and linearity. When these are adjusted correctly the horizontal readout will be an integral multiple of 0200_8 at any point on the raster. One-count deviations, 0177 or 0201 , are acceptable.

In the D-line position of the RETICLE switch it is possible to adjust the vertical deflection circuits by monitoring the diagonal reticle lines. This should not be done until after the horizontal is correct. Vertical position is adjusted by setting the VERTICAL POSITION controls for a vertical readout of 0001 or 0002 . The deflection circuits are then adjusted to give a horizontal readout equal to the vertical. Vertical rate and linearity are adjusted by varying the VERTICAL POSITION controls and adjusting for equal horizontal and vertical readout from bottom to top on the raster. All horizontal adjustments must be completed prior to this step.

READOUT

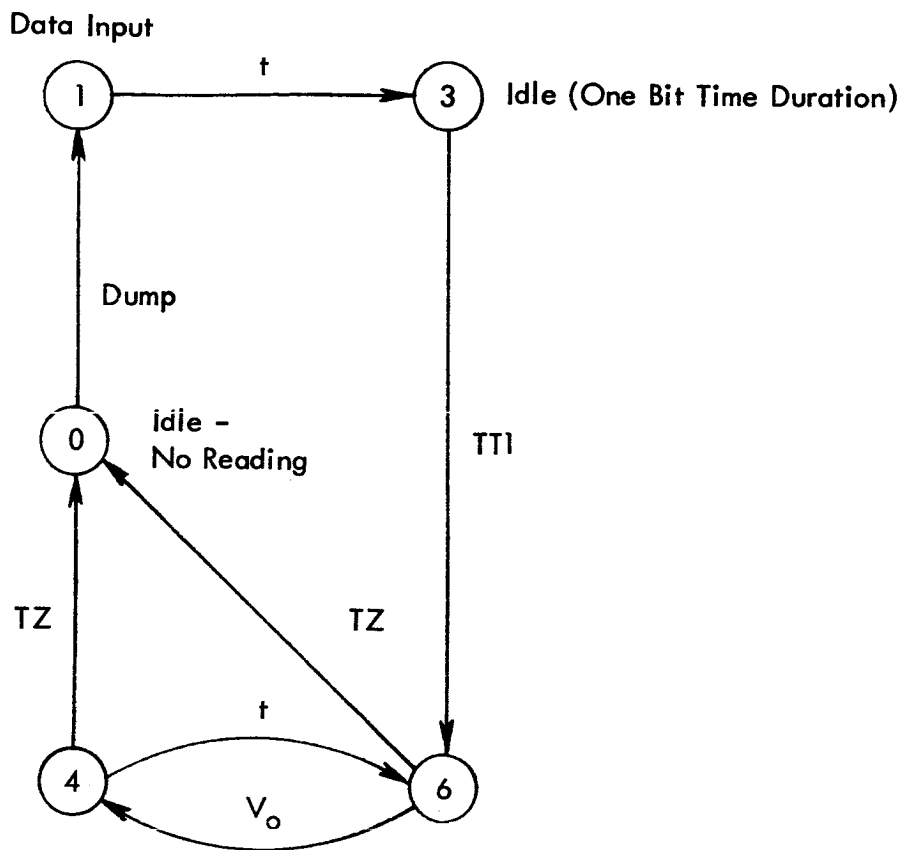
Octal Representation

The indicators provided for reading out the average X and Y coordinates are basically a binary indication. By grouping these indicators in groups of three a pseudo conversion to octal** is accomplished. This conversion considerably decreases the amount of writing needed to record data. If a one indicates a lighted tube and a zero indicates an unlighted tube, the following tabulation shows the conversion from binary to octal.

*The subscript 8 implies that the number is represented in octal notations.

For a further discussion see the following section.

**The output is still binary, the conversion to octal being made by the observer aided by the grouping of the indicators.



- Dump = 1 \Rightarrow Reticule center pulse within gate NOW. Vertical position greater than or equal to setting. Read PB depressed.
- t = 1 \Rightarrow Data dumped has been processed
- TT1 = 1 \Rightarrow One bit time since entering state three
- V_o = 1 \Rightarrow Start of new horizontal sweep
- TZ = 1 \Rightarrow Data Processing and display complete

Figure 4-4. State Diagram - Calibrate Sequence

lts. -digit	lts. -digit
000 - 0	100 - 4
001 - 1	101 - 5
010 - 2	110 - 6
011 - 3	111 - 7

Thus an indication of

0 110 010 101 - Vertical
1 011 100 111 - Horizontal

would correspond to an octal reading of

0625 - Vertical
1347 -- Horizontal

To convert these to decimal it is convenient to use the formula

$$N_{10} = 512 \times A_3 + 64 \times A_2 + 8 \times A_1 + A_0$$

where A_0 is the least significant digit, A_1 the next more significant, and A_3 the most significant. In the above example the vertical reading converts to

$$0 \times 512 + 6 \times 64 + 2 \times 8 + 5 = 405 \text{ decimal}$$

while the horizontal converts to

$$512 + 3 \times 64 + 4 \times 8 + 7 = 743 \text{ decimal}$$

An alternate method of conversion is to sum the digits from the following table.

lts.	A_3	A_2	A_1	A_0
000	0	0	0	0
001	512	64	8	1
010	---	128	16	2
011	---	192	24	3
100	---	256	32	4
101	---	320	40	5
110	---	384	48	6
111	---	448	56	7

Modulo Defined

When reading the D-lines in calibrate, readings will progress (in Octal) 1776, 1777, 0000, 0001, etc. This does not mean that D-lines are being found at the beginning of the sweep, but rather represents the modulo 1024 nature of the readout, Modulo being a fancy method for stating that with a finite length number one cannot represent larger numbers. In angular measurement, angles are usually stated modulo 360°. Thus 5°, 365°, 725°, and 2525° are all represented as 5°. The American representation for time is modulo 12 hours, and a typical automobile odometer is modulo 100,000 miles. In general, with an N digit number (integral), one can only represent quantities modulo b^N where b is the base of the number system involved. Thus our ten bit readout can only represent numbers modulo $2^{10} = 1024$. The general formula is:

$$A \bmod B = A \pm n \times B$$

where n is any integer including zero.

DETAILED MECHANIZATION

SEQUENTIAL LOGIC

The sequencer is the decision making portion of the data processor. The detailed logic diagram is shown in Figure 4-5. The four flip flops KK1 through KK4 determine the state of the sequencer and their output is decoded to direct the action of the data handling logic. By the definition used in this logic system a one indicates that the output marked one on the symbol is grounded and a zero indicates that the output marked zero is grounded. The state number may be related to the particular flip flops by the following table.

KK 1234	state	KK 1234	state	KK 1234	state	KK 1234	state
0000	0	0100	4	1000	8	1100	12
0001	1	0101	5*	1001	9	1101	13
0010	2	0110	6	1010	10*	1110	14*
0011	3	0111	7*	1011	11	1111	15*

* unused but possible

If one studies the sequence diagram, Figure 4-3, together with the above table, one will discover that only three of the sixteen state changes require more than one flip flop to change. Thus the possibility of noise generated by passing through unwanted states is reduced to a minimum. In the three cases where two flip flops are required to change, care was taken to insure that the intervening states had the same action as the terminating states.

NOR logic is used to decode the states into the signals f, no, tw, dp, gamma, and alpha. These correspond to First data input, Normal data input, Twice normal data input, Data Processing and Display, not data input, and idle, respectively.

Inputs to the Sequential Logic include dump, t, TZ, SC1 (Samples Complete), CAL (Calibrate Mode), and KR2 and KR3 which decode to yield tau. The small f to the left of each flip flop indicates the source of its 5MC clock input and is not related to the f which denotes First data input.

DATA PROCESSING

Introduction

On command from the sequencer, the data processing section performs the various arithmetic functions described previously. Within each state, this section's actions are controlled by the timing circuits. These include the bit and word time counters, the 1 Mc clock counter, WT1, DV1*, and other miscellaneous logic. The basic source of all timing including the input to the horizontal counter is a crystal controlled oscillator which provides a 5 Mc clock signal accurate to $\pm 0.0001\%$. This clock signal is used for the sequential logic and other circuitry involved with the horizontal measurement, but the data handling section has no need for this speed. The 5 Mc is therefore counted down by a recursive counter to provide a 1 Mc, square wave, clock having a 60-40 duty cycle.

For troubleshooting a manual clock is also available. This consists of a pulse generator which provides one clock pulse for each push of the button. This allows leisurely examination of data which would normally be rapidly changing, and also permits the simulation of inputs with clip leads.

Timing

Data in the B- and C-registers is continuously circulating. In order to keep track of the location of the least significant bit, the bit time counter is also allowed to run continuously. This counter is divided into two sections, a five bit shift register (counts modulo five)** and a three state counter. Thus the total count is modulo fifteen. The normal length of the C-register is fifteen bits, that of the B-register, five. Therefore the least significant bit of N(C) is in RC2 at count one each time, and the least significant bit of N(B) is in RB2 at counts 1, 6, and 11.

*Refer to Flip-Flop Biography Section

**The counter counts by shifting a "one" to one of five positions.

The word time counter is a ripple counter which is locked in state zero during all sequencer states marked idle. When unlocked for data processing (including data input) its count is incremented one each time CB reaches a count of fifteen. No attempt is made to have the sequencer states changed in synchronization with the bit time counter; therefore a transfer into a data handling state may be such that the word time counter goes to one on the next bit, or it may be such that up to fifteen bit times (microseconds) elapse before that count. Whatever the delay, the word count will become one at the instant that $N(C)$ is first available for input to the adder.

Data Input

The generation of a dump pulse by the dump logic causes a parallel transfer of data from the X- and Y-counters to their respective buffer registers. This transfer requires 0.2 microsecond. Generation to this pulse will be discussed later. Following the transfer of data, the sequencer moves to a data input state. The operation of the Normal data input will be discussed first.

When the sequencer moves to state eleven, the "no", (normal), signal is grounded. This releases the word time counter which in turn moves to word time one following the next count of fifteen from the bit time counter. During the first ten bits of word one, the X-register's RX1 supplies its output as the augend input to the adder/subtractor. During the last five bit times the augend input is zero. At the end of each of the first eleven bit times a shift pulse is sent to the X-register. The X-register's input during word one is RX1. Therefore $N(X)$ is circulated unchanged while being made available to the adder. The addend input for the entire word one is $RC2$, * and sigma, the adder's output, is taken as the input to the C-register for this word time. Thus at the end of word one, $N(X)$ is unchanged, and $N(C)_i = N(C)_{i-1} + N(X)$.

At all times the data in the B-register is circulating through the increment adder which forms part of the input to RB5. As long as the increment input to the adder is not grounded, this has no effect on its contents ($B + 0 = B$). During the eleventh bit time of word one, the increment input is grounded, thus causing one to be added to $N(B)$.

During word one the add flip flop AD1 was set to add. At the end of word one, AD1 is reset to subtract, and the carry flip flop CC1 is reset to prevent a carry propagating into word two.

The action during word two is identical for all input operations. A shift pulse is sent to the X-register at the end of each of the first eleven bit times, the minuend input to the adder is taken from RX1, the subtrahend input is taken from the GATE WIDTH switch (Δ), the adder/subtractor output sigma is taken as the input to the X-register, and during the fifteenth bit time a "t" pulse is generated. Therefore $N(X)_i = x_i - \Delta$ at the end of word two.

*RC2 is used to shorten the register. Its normal length of 16 is used to effect precision during division.

The action during First data input is the same except that the addend input to the adder during word one is zero, and the clear input to the B-register is grounded for the first five bit times of word one. Therefore $N(C)_1 = 0 + N(X)$ and $N(B)_1 = 1$.

During Twice normal data input the action is the same as that during normal except that the augend is taken from RX11 during the first eleven bits of word one. This has the effect of shifting the binary point of $N(X)$ to the right, thereby multiplying it by two. The other exception is that the increment input to the B-register is ground during the twelfth bit of word one. Thus the one is added to the two's position and is equivalent to adding two.

Data Processing and Display

The data processing and display state is divided into two sections by the action of WT1 and DV1. WT1 is in the one state or "on" during word time one, and DV1 is on during word times two through twelve. DV1 controls the division and is turned off by TZ during bit two of word thirteen.

Calculate Y Average (WT1 = 1)

During word time one the vertical data is processed. The output of the A-register, RA1, is taken as the minuend during the last ten bits of word one. RB2 is taken as the subtrahend during bits six through ten of the word, the subtrahend being zero for the remainder of the word. Following each of the last ten bits a shift pulse is sent to both the A- and V-registers. The input to the V-register is sigma. The use of RB2 as the subtrahend effectively divides $N(B)$ by two. Thus at the end of word one, $N(V) = N(A) - N(B)/2$. Zeros are shifted into the A-register.

The A-register was originally intended as an accumulator for the quotient formed in calculating X_{average} , the present configuration being a fix for a timing problem which arose rather late during the Phase A program. The original configuration is recommended if the output is to be taken for other than visual display since it would permit shifting out the quotient least significant digit first.

Calculate X Average (Divide) (DV1 = 1)

As was mentioned above, the division is simplified by the fact that both the dividend and the divisor are positive quantities. As is typical of most division processes, the quotient is formed most significant digit first. At odds with the paper and pencil method is the fact that a nonrestoring scheme is used. As the quotient bits are generated they are sent to the input of the H-register. At the end of each is sent a shift pulse. Thus at the end of the tenth shift the first bit is in RH10 and the display is complete.

While DV1 is on, the augend/minuend is taken from RC2, and the addend/subtrahend from RB1. The addend/subtrahend is zero during the least significant ten bits of each word, and equals N(B) during the most significant five. DV1 also results in the C-register being extended to sixteen bits by the inclusion of RC1. The inclusion of this flip flop causes the C-register to precess relative to the bit time counter. Since the addition or subtraction always takes place during the most significant five bit times of the counter's word, this precession causes N(B) to be divided by two each word time relative to the remainder held in the C-register.

Since the maximum number in the C-register is 31,744 which is considerably less than its maximum capacity of 65,535*, the result of the first subtraction will always yield a quotient bit of zero. This bit is therefore discarded.

In the paper and pencil division process familiar to most of us, repeated subtractions are made until the difference becomes negative. An addition is then made which restores the difference to the positive realm, following which the divisor is shifted (divided by ten) and the process repeated. (In practice most of us attempt to guess the number of subtractions necessary and then multiply our guess by the divisor to verify it. This is cheating.) Each subtraction which results in a positive remainder causes the quotient digit to be incremented by one. When this form of division is performed properly, the first subtraction is made with the divisor far enough to the left to insure that each quotient digit is less than the radix (number system base). Thus no carries are propagated in the quotient. With this precaution it will be noted that the total number of subtractions is equal to the radix, and that the total number of effective subtractions is one less than the radix. In the binary number system then (radix = 2), the total effective subtractions will be one! This scheme is called restoring division thanks to the final addition.

If one considers the final addition, the shift, and the next subtraction, taken together in the binary number system, one finds that they simplify to a shift followed by an addition.

$$+X - X/2 = +X/2$$

This means that following the initial subtraction one can shift immediately without waiting to discover whether it did or didn't "go". If it didn't the correction is made by adding instead of subtracting the next time. Not "going" is signified by the remainder being negative, therefore, if the remainder is negative the quotient bit is zero and the next operation is an addition. Conversely if it did go, the remainder is positive, the next operation is another subtraction, and the quotient bit is a one.

* $2^N - 1$ since one of the states is zero.

As an example consider a star with a last vertical coordinate of 1621_8 (913 decimal), a summation x_i of $67,764_8$ (28,660 dec.), and a total number of samples equal to 35_8 (29 dec.). This implies that:

$$\begin{aligned} N(A) &= 1 \ 110 \ 010 \ 001 \\ N(B) &= 11 \ 101 \\ N(C) &= 110 \ 111 \ 111 \ 110 \ 100 \end{aligned}$$

During WT1 the processor performs:

$$\begin{array}{r} 1 \ 110 \ 010 \ 001 \\ - \quad 1 \ 110 \\ \hline 1 \ 110 \ 000 \ 011 \end{array} = 1603_8 = 899_{10} \text{ goes to RV}$$

During DV1 the processor performs:

$$\begin{array}{ll} (0) & 110 \ 111 \ 111 \ 110 \ 100 \\ \text{sub.} & \underline{111 \ 01} \\ & 1 \ 111 \ 101 \ 111 \ 110 \ 100 \text{ negative -- 0 (unused)} \\ \text{add.} & \underline{11 \ 101} \\ & 0 \ 011 \ 010 \ 111 \ 110 \ 100 \text{ positive -- 1 MSD of display} \\ \text{sub.} & \underline{1 \ 110 \ 1} \\ & 0 \ 001 \ 100 \ 011 \ 110 \ 100 \text{ positive -- 1} \\ \text{sub.} & \underline{111 \ 01} \\ & 0 \ 000 \ 101 \ 001 \ 110 \ 100 \text{ positive -- 1} \\ \text{sub.} & \underline{11 \ 101} \\ & 0 \ 000 \ 001 \ 100 \ 110 \ 100 \text{ positive -- 1} \\ \text{sub.} & \underline{1 \ 110 \ 1} \\ & 1 \ 111 \ 111 \ 110 \ 010 \ 100 \text{ negative -- 0} \\ \text{add} & \underline{111 \ 01} \\ & 0 \ 000 \ 000 \ 101 \ 100 \ 100 \text{ positive -- 1} \\ \text{sub.} & \underline{11 \ 101} \\ & 0 \ 000 \ 000 \ 001 \ 111 \ 100 \text{ positive -- 1} \\ \text{sub.} & \underline{1 \ 110 \ 1} \\ & 0 \ 000 \ 000 \ 000 \ 001 \ 000 \text{ positive -- 1} \\ \text{sub.} & \underline{111 \ 01} \\ & 1 \ 111 \ 111 \ 111 \ 001 \ 110 \text{ negative -- 0} \\ \text{add} & \underline{11 \ 101} \\ & 1 \ 111 \ 111 \ 111 \ 101 \ 011 \text{ negative -- 0 LSD of display} \end{array}$$

Therefore when DV1 is reset, $N(H) = 1 \ 111 \ 011 \ 100 = 1734_8 = 988 \text{ dec.}$

HORIZONTAL MEASUREMENT

Counting

The heart of the horizontal or X measurements is of course the X-counter. In order to achieve the desired quantization (~ 1000 parts) while achieving a reasonable sweep rate, it was deemed necessary to count at a five megacycle rate. This precluded use of a ripple counter since ripple propagation delays for existing circuitry are too great. (In order to successfully dump one would need flip flops with a switching time of less than 10 nanoseconds under the worst combination of temperature, power supply variation, and end-of-life component values. There are cheaper ways.) Use of a synchronous counter allows each stage to have up to 100 nanoseconds in which to toggle while still allowing time for the information to be dumped. An alternate method would be to have two X-counters, each of the ripple type. The first would be used to generate the control functions while the second supplied the data. In this case the second would be stopped when the dump appeared, then when enough time had elapsed for all ripples to have propagated, the information would be transferred. This approach deserves further study in the light of this counter's performance. The particular synchronous counter chosen utilizes the minimum number of components for the particular circuits available at the time it was designed. It is not recommended that this configuration be used for other than a laboratory environment. Even in the room temperature environment careful tailoring of loads and supply voltages was required. The clock supply is particularly critical, requiring pulses on the order of 15 nanoseconds in width and fall times of less than four nanoseconds. Careful tailoring resulted in a counter which at room temperature would work for supply voltage tolerances of ± 1 volt, including clock supply voltages. Therefore reasonable confidence may be felt in the present device, but a better method should be sought for future counters.

Correcting the Count

In addition to the eleven stages of the counter with their respective trigger-logic and output buffers, there are included provisions for resetting either the entire counter or the least significant seven stages. These resets are part of the scheme for reticulization. Also included is the self test flip flop ST1. This generates a one-bit time pulse at count 512 and is fed back through the star center pulse input to test the data processing. Note that it provides only a rudimentary check of the horizontal counter since the dump will occur with a reading of 513 whether or not it truly took 513 input counts to get to that point. The extra one is part of the dump logic delay.

The entire counter is reset by either V_0 or by count 1376 in Star, Disc Edge, and Calibrate other than V_0 . The latter possibility is to prevent lockup of the system if V_0 goes missing. It is required since the horizontal counter furnishes the reset for the horizontal deflection circuits. In calibrate V_0 the total reset is provided by tau.

The partial reset is used when one of the V-lines other than V_0 is encountered with a reading of less than 128 modulo 128. This condition is detected by ANDing the reticle pulse with CX7. In the event of a partial reset it is necessary to propagate a carry into stages CX8, CX9, and CX10. None is required into CX11 since V_7 is the last V-line. This carry is responsible for the double NORs on the trigger inputs to those three stages.

The current mechanization can only subtract one if the count is too high. At one point it was expected that this could be modified to allow up to eight counts to be subtracted. Unfortunately the data processor became an integral part of the system shortly thereafter and insufficient down time was available to make the modification. The technique was to have been as follows. If a V-line other than V_0 is encountered with a count between 0 and 8 modulo 128, the X-counter would be stopped and an auxiliary counter started. When the auxiliary counter equals the X-counter least significant three bits, enough counts have been skipped by the X-counter and it is restarted. This scheme could of course be extended to handle any number of erroneous readings up to sixty four. At sixty four it becomes difficult to know whether to add or subtract. Corrections of more than one are unnecessary of course due to the requirement that star data be recorded accurately 255 counts after any given V-line. Missing a V-line other than V_0 has no effect other than that caused by errors in the sweep rate. Missing V_0 results in the count being low by about 16 counts. This is corrected by the first V-line encountered. Extra reticle lines are disastrous since a single extra pulse can add up to 64 counts. Some protection can be gained by refusing to accept reticles which are not close to the expected position, but the tighter this masking, the more stringent are the requirements on the sweep circuits.

VERTICAL MEASUREMENT

The Y-counter is a normal ripple counter* utilizing the standard line of one megacycle flip flops. Ripple propagation time for the counter is less than 550 nanoseconds under worst case conditions including temperature. Counts are entered either at the end of the horizontal blanking or during the D-line section of the raster. Thus only a star at the extreme right of the screen or, in the calibrate V_0 mode, a V_0 which was at the extreme left of its tolerance range, could encounter difficulties with ripple propagation. These hazards can be eliminated with rather trivial modifications, but they do exist in the present mechanization.

As was mentioned before, the vertical reticulization depends upon the horizontal count being absolutely correct. If the horizontal is off, errors will be introduced into the vertical. While this is unfortunate, it stems from the fact that the vidicon is swept horizontally, the vertical "sweep" being a procession of horizontal lines.

*See footnote on page 43

The X-Y coincidence detector is one of several similar circuits used in this machine. The basic idea is that only the first moment of equality is needed. Extra signals after that do not matter. Use of this simplification cuts the number of logic circuits required in half. Due to the fact that D-lines are transposed 32 counts to the right only the least significant five of the seven bits meet the above requirements, bits six and seven requiring a full comparison. The logical product is denoted by Pi on the accompanying timing charts, Figures 4-6 and 4-7 which are found on pages 83 and 84 .

DUMP LOGIC

General

The dump pulse is a 200 nanosecond signal which depends upon nearly every control element in the data processor. The full equation for it is:

$$\text{dump} = \overline{\text{dp}} * \overline{\text{KK4}} (\overline{\text{CD6}} + \text{KS1} * \overline{\text{CAL}} * \overline{\text{KK3}} * \overline{\text{KK1}}) (\text{STAR} + \text{VP3}) (\overline{\text{CAL}} + \text{KS1} * \overline{\text{CAL}} * \overline{\text{KK3}} * \overline{\text{KK1}} + \overline{\text{CD7}} * \text{KS1}) * (\overline{\text{CAL}} + \text{KK6} (\text{KR1} + \text{CX6} * \text{CX9} * \text{CX11} + \text{KR2} * \text{KR3} (\text{cv0} + \text{"Reticle Off"}))) (\overline{\text{CX9}} + \overline{\text{CX11}})$$

where * denotes the logical "AND" and + denotes the logical "OR". In the Star mode this is equivalent to:

$$\text{dump}_{\text{star}} = \text{KS1} * \overline{\text{dp}} * \overline{\text{KK4}} * (\overline{\text{CD6}} * \overline{\text{CD7}} + \overline{\text{KK1}} * \overline{\text{KK3}}) * (\overline{\text{CX9}} + \overline{\text{CX11}})$$

In words this is:

Dump if there is a star center pulse and you aren't in data processing and display and you aren't in an odd state and you either have the noise gate open or you are in state zero and you're not between the horizontal blanking and V_0 .

In the Disc Edge mode the dump reduces to:

$$\text{dump}_{\text{D.E.}} = (\text{dump}_{\text{star}}) * \text{VP3} ; \text{ i. e., the same as that for the Star}$$

mode except for the inclusion of the VP3 term. This term says "go" if the vertical position is above that specified by the VERTICAL POSITION controls.

In the calibrate mode this reduces to:

$$\text{dump}_{\text{CAL}} = \text{KR1} * \overline{\text{dp}} * \overline{\text{KR4}} * \overline{\text{CD6}} * \overline{\text{VP3}} * \text{KK6} * (\overline{\text{CX9}} + \overline{\text{CX11}})$$

Thus in the calibrate mode KR1 replaces KS1, only the left side of the noise gate is used, and the KK6 flip flop must be on. The latter is set by the READ pushbutton and permits single readings to be taken. In the future this might be profitably included in the other modes as well. Note that while state zero bypasses the noise gate in the Star and Disc Edge modes, it does not in Calibrate. It should also be noted that many of the terms in the equation as mechanized never show up in the effective equations. This is due to "don't care" conditions being utilized to simplify the mechanization. A third observation is that several functions enter this equation indirectly. Thus the horizontal and vertical blanking signals are not listed since they are applied to the input to KR1 and KS1. This is also true of the "Self-test" feature and a bit of logic to eliminate a false reticle which is generated by the camera differentiating a star pulse.

Horizontal Gating

The noise gate was discussed under the Star mode of operation, and, as was pointed out at that time, the gate opens when $N(\text{CX}) = N(\text{RX})$. This condition is detected by the same type of coincidence detector used in the vertical reticulization. All bits satisfy the conditions here, thus ten NOR circuits are saved over what would be needed for a full comparison. The gate is open when both CD6 and CD7 are off. CD6 controls the left side of the gate; being turned ON by the horizontal retrace and OFF by the coincidence detector. CD7 controls the right or closing side of the gate. It is turned OFF one-bit time after CD6 turns on and is turned ON by the noise gate counter reaching the state specified by the GATE WIDTH switch.

The contents of the X-register are loaded as described above in the Star and Disc Edge modes. In the calibrate mode the contents are generated by setting the RETICLE switch. This switch selected number is loaded when the READ pushbutton is depressed.

Vertical Gating

The VERTICAL POSITION controls determine the starting point and duration of the single-shot SS1. By limiting the variation and utilizing a multi-turn potentiometer, the dial resolution is approximately 10^0 per vertical count. Excellent stability and repeatability have been experienced. When the single-shot turns off, it turns on VP2. Since this point is continuously variable in time, some method of enabling integral lines is needed. This is provided by VP3 which turns on for both CX11 and VP2 on. Both VP2 and VP3 then remain on until the end of the vertical frame. This latter facet has been criticized and it might prove advantageous to turn off VP3 after some finite period such as 20 or 30 lines. One could then truly control the vertical position rather than merely setting a lower limit to it.

Transferring the Data

Once the dump pulse has been generated, it is sent to the X- and Y-dump gates and to the sequencer. The Y-gates are merely a second set of transmission gates on the A-register flip flops, a condition made feasible by the relative immobility of the Y-counter. The X-gates are required to take their sample in considerably less than 200 nanoseconds. To accomplish this in spite of the delays through the several NORS needed to build up the dump logic and then amplify the dump pulse to drive twenty logic functions, special bias nets were built to permit a nor to drive directly into the base of the X-register flip flops. Twenty of these NORS then "and" the output of the X-counter with the dump pulse and set or reset the stages of RX directly. Despite this faster scheme it was necessary to tailor the delays. In the future it would probably be advisable to reclock the dump pulse as well. The dump logic seems particularly sensitive to power supply variation, but that may be due to one of the many input functions dying.

SOME FURTHER OBSERVATIONS

A rather cursory look was taken at the voltage profile for the data processor as a whole, and it appears that the tolerance on all three supplies is at least one half volt plus or minus if a center point of +11, +6.5, and -6.0 are used. The low "+12" is due to too low a Zener diode having been used in the shift driver circuits. The high "+6" increases the speed of the "30 Mc" circuits.

Using Fairchild and Signetics integrated circuits, the entire data processor could be reduced to cigar box size; a thought to be kept in mind, but tempered with the realization that such a reduction would in effect "freeze" the design. Its present "ugly duckling" packaging offers significant advantages for an evolving system.

The addition of a Friden "Flex-o-writer"/tape punch to the output would present the data in much more usable form. Such a device would provide a tape for direct input into a general purpose computer, thus expediting such operations as conversion from octal to decimal, "RMS"-ing the deviations of large numbers of readings, calculating the centers of ellipses, etc.

SUMMARY OF SIGNIFICANT CHARACTERISTICS

The Space Sextant Data Processor divides into two sections; the data averaging and display section, and the section devoted to position measurement and noise rejection.

POSITION MEASUREMENT AND NOISE REJECTION

Clock rate	5 megacycles
Operation	Synchronous
Control	Decision making sequential logic
Inputs	Reticle center pulses, Star Center Pulses, Vertical Blanking, Noise Gate Position, t, and TZ pulses, Samples Complete Signal
Outputs	x_i ; y_i ; the four possible processing codes f, no, tw, or dp; Horizontal Retrace, Horizontal Blanking, Simulated Vertical Blanking, the 1 Mc clock
Modes	Star, Disc Edge, and Calibrate
Transistors	approximately 400

DATA AVERAGING AND DISPLAY

Clock Rate	1 megacycle
Operation	synchronous, parallel input, serial internal
Control	wired program under external control
Inputs	x_i , y_i , processing codes, 1 Mc clock
Outputs	Noise Gate Position, t and TZ, Samples Complete, X_{average} , Y_{average}
Transistors	approximately 250

TOTAL POWER

+6.5 volts at 2 3/4 amps; +11 volts at 1 1/4 amps; -6 volts at 1/2 amp
+50 volts, 1 vac, 115 vac

FLIP FLOP SYMBOLS OR GLOSSARY

NAME	FUNCTION
AD1	add/subtract control
CB1, $\overline{\text{CB2}}$, CB3, $\overline{\text{CB4}}$, CB5	shift register section of bit time counter - counts modulo five by shifting a one through five positions
CB6, CB7	counter section of bit time counter - counts modulo three - entire counter counts modulo fifteen.
CC1	carry flip flop for adder subtractor
CD1, CD2, . . . , CD5	noise gate counter - uses recursive techniques
CD6, CD7	noise gate control
CL1, $\overline{\text{CL2}}$, CL3	clock counter - counts modulo five to generate 1 MC from 5 MC clock.
CW1, CW2, CW3, CW4	word time counter - ripple counter - counts modulo sixteen.
CX1, CX2, . . . , CX11	horizontal counter - synchronous - modulo 2048
CY1, CY2, . . . , CY11	vertical counter - ripple counter - modulo 2048
DV1	demarks period during which the division operation forms X_{avg} .
KB1	carry flip flop - increment adder - B-register
KK1, KK2, KK3, KK4	sequencing control
KK6	read control - calibrate mode

FLIP FLOP SYMBOLS OR GLOSSARY (Cont.)

NAME	FUNCTION
KR1, KR4, KR5	detects and synchronizes the start of each reticle pulse.
KR2, KR3	generate horizontal retrace and horizontal reset tau.
KS1	star center pulse synchronization
KS2, KS3	"STAR" indicator control
KV1, KV2, KV3	control vertical count input
KV4	vertical blanking synchronization
KV5	generates vertical reset
KX1, KX2	control RX shift
RA1, RA2, . . . , RA10	vertical buffer register
RB1, $\overline{RB2}$, . . . , RB5	sample register - holds N
RC1, RC2, . . . , RC16	accumulator for $\sum_{i=1}^N x_i$
RH1, RH2, . . . , RH10	horizontal display register
RV1, RV2, . . . , RV10	vertical display register
$\overline{RX1}$, RX2, . . . , RX10	horizontal buffer - holds coordinate of noise gate start
$\overline{RX11}$	part of horizontal buffer - holds sign of noise gate start coordinate

FLIP FLOP SYMBOLS OR GLOSSARY (Cont.)

NAME	FUNCTION
SC1	indicates sufficient samples have been taken in the DISC EDGE mode.
ST1	generates the self test input
TT1	modifies sequencing in CALIBRATE mode.
VP1, VP2, VP3	trigger and synchronize single shot SS1 to set minimum vertical in CAL and DE modes.
WT1	demarks period for calculation of Y_{avg} .

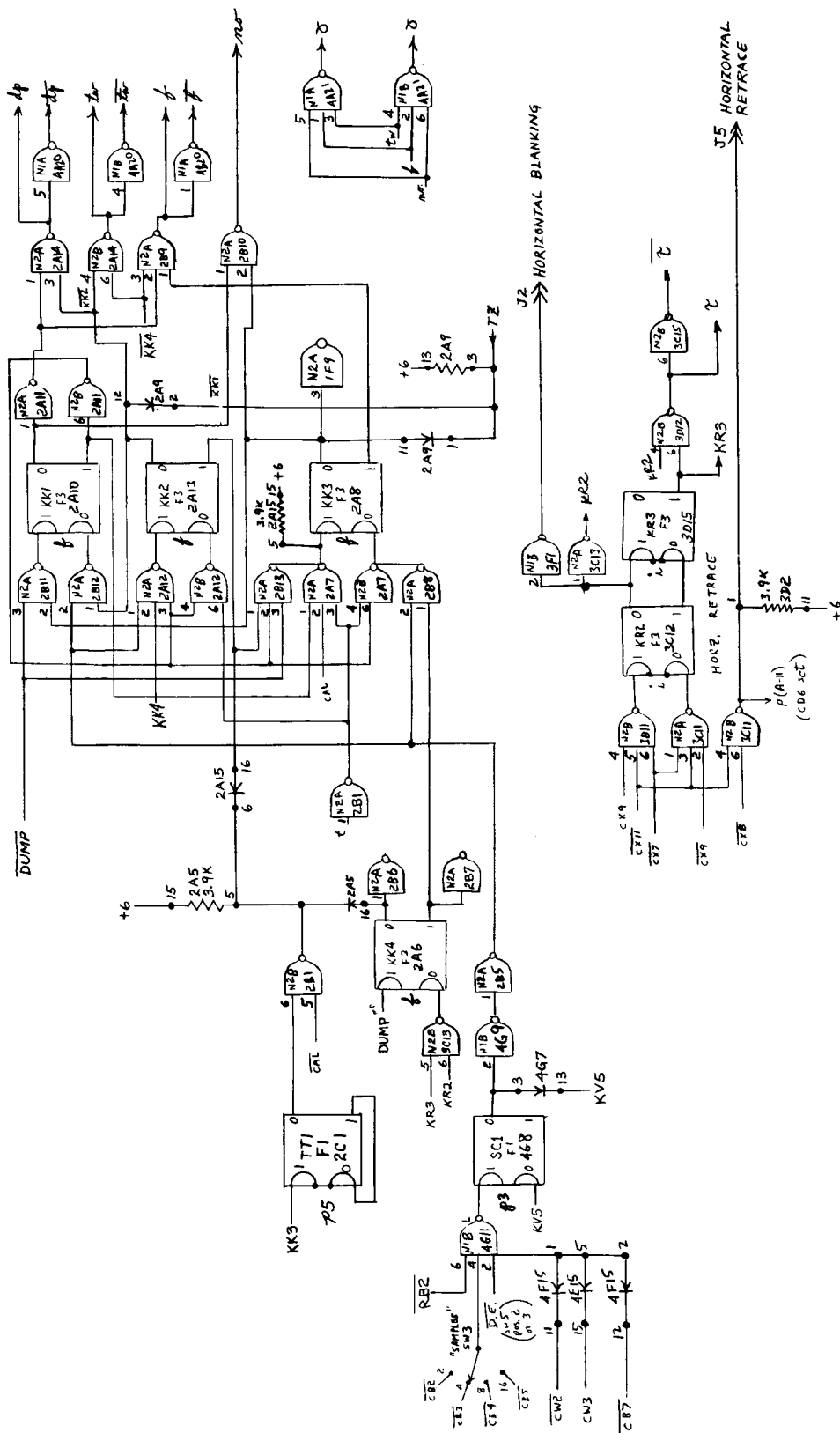
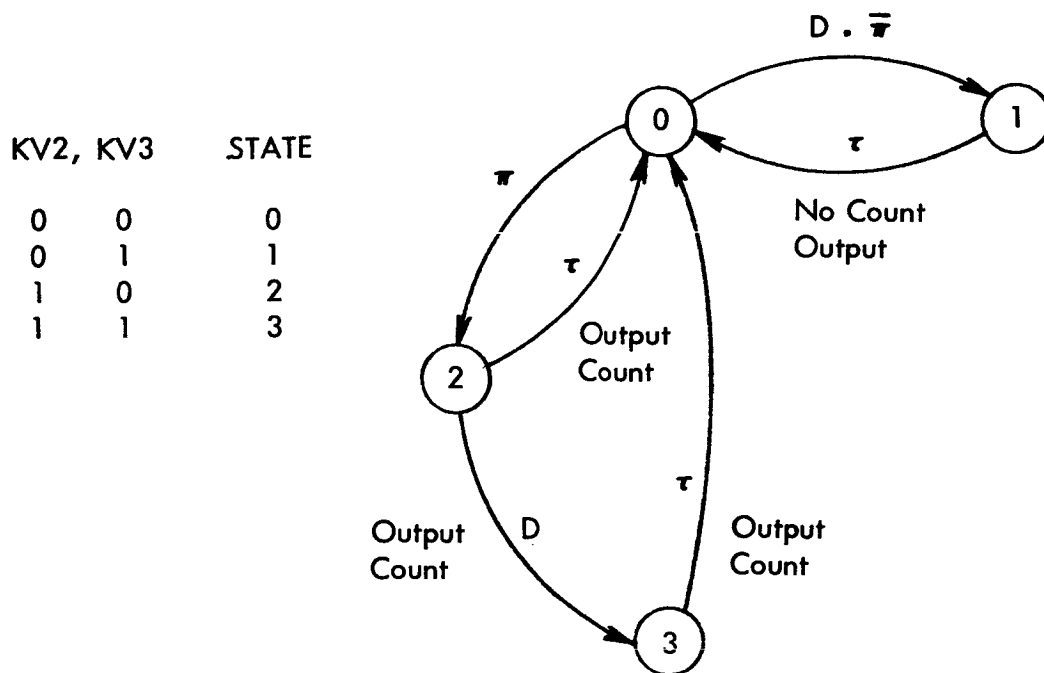


Figure 4-5. Sequencing



$\pi = 1 \Rightarrow$ LS7D of CX = LS7B of CY and D-lines in Sight
 $D = 1 \Rightarrow$ Reticle Center Pulse NOW and D-lines in Sight
 $\tau = 1 \Rightarrow$ Start of a New Horizontal Sweep

Figure 4-6. State Diagram - Vertical Reticulization Sequence

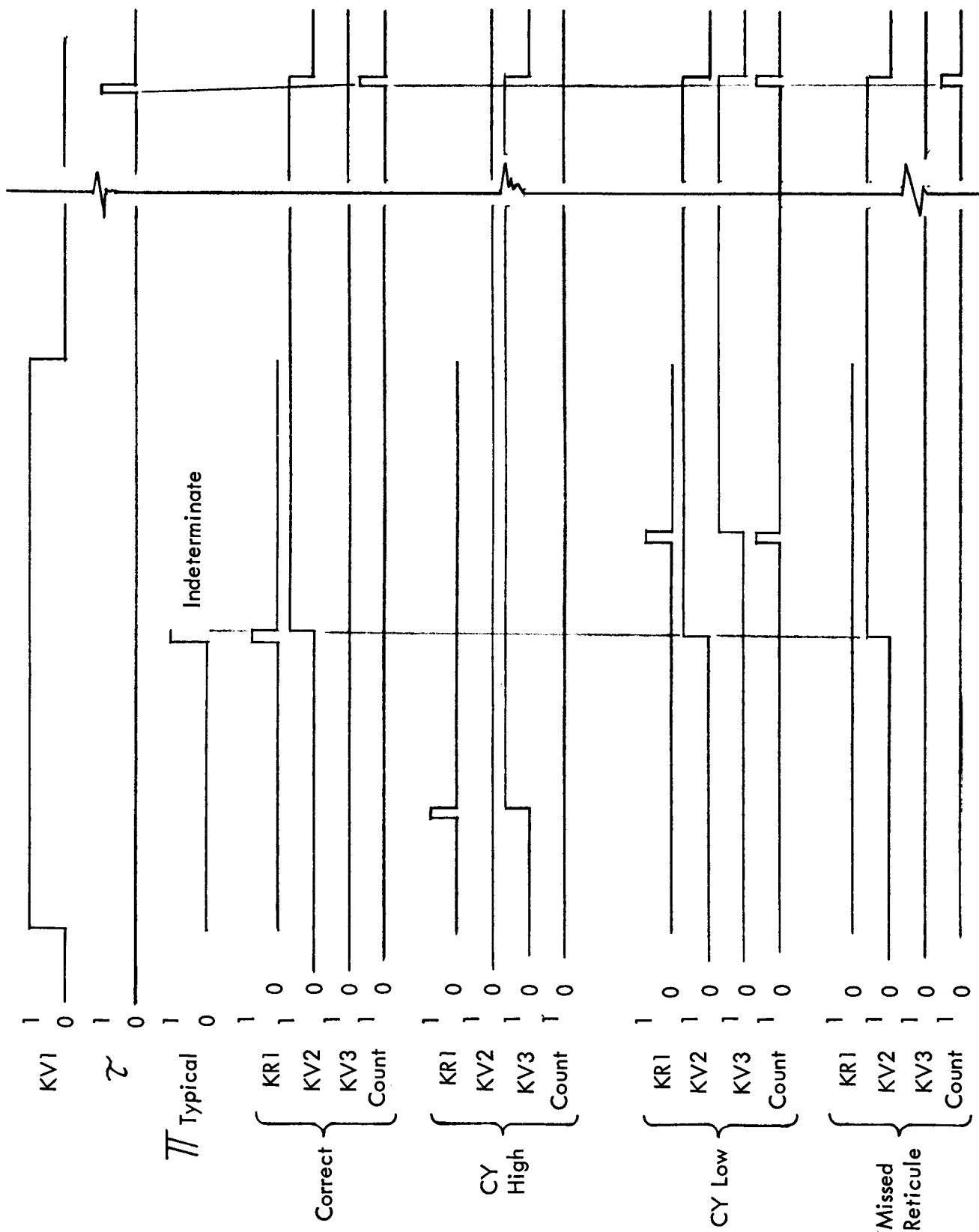


Figure 4-7. Timing-Vertical Reticulization

Section 5

ANALYSIS AND SYSTEM CONSIDERATIONS

INTRODUCTION

While this program was primarily hardware oriented several system considerations pertinent to future hardware developments were also explored. The significant results and ideas of a non-equipment nature that were developed are summarized in this section. For further information and a more detailed discussion of these areas refer to the following Space Sextant Project Memorandums:

- o Memorandum No. 15 - Optical Transfer Function Space Sextant Optics, Foley 1 February, 1964. Reference No. 17
- o Memorandum No. 8 - Study of Target and Image Characteristics, Foley. Reference No. 11
- o Memorandum No. 9 - Applications of an Orthogonal Scan System for All Space Sextant Modes of Operation, Welch, 27 August, 1963. Reference No. 12
- o Memorandum No. 13 - Techniques for Utilizing Space Sextant Data in a Self-Contained Space Navigator, Welch, 8 January, 1964 Reference No. 15

Each of the areas dealt with in these memoranda will be discussed briefly below.

OPTICAL TRANSFER FUNCTIONS OF THE SPACE SEXTANT OPTICS

The geometric optics built for the Space Sextant can be considered as a transducer which converts the angular relationship of a line-of-sight to a position in the image plane. This section examines this relationship for both the narrow field and the wide field optics. Thus, given an image plane location - the orientation of the line-of-sight with respect to an optically centered reference frame can be determined.

General Coordinate Relationships

The optics coordinate system will be as defined in Figure 5-1a.

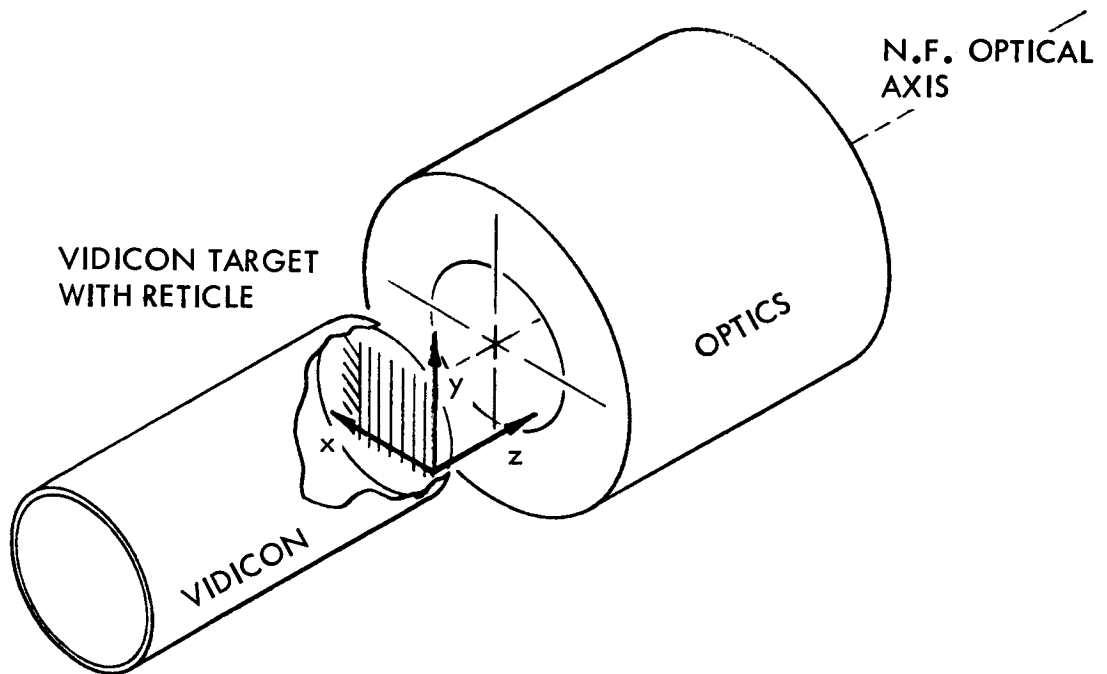


Figure 5-1a. Optics Coordinate System

The direction of the target ray can be related to this coordinate system as shown in Figure 5-1b. In this figure \bar{a} is a unit vector along the target ray pointing from the optics to the target.

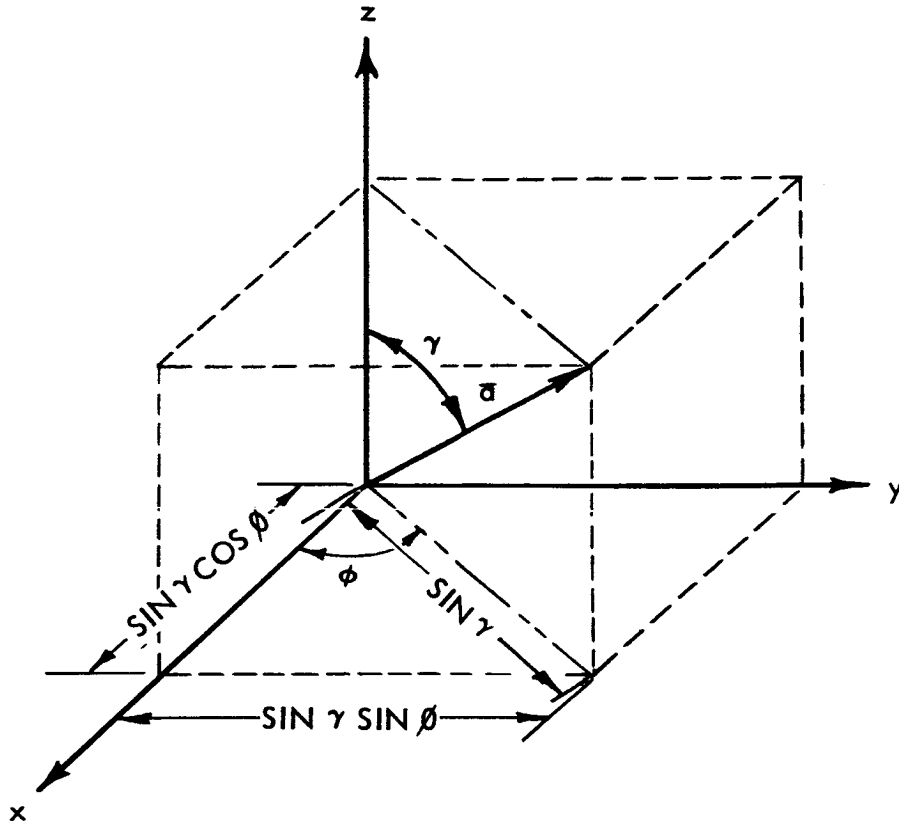


Figure 5-1b. Target Ray Geometry

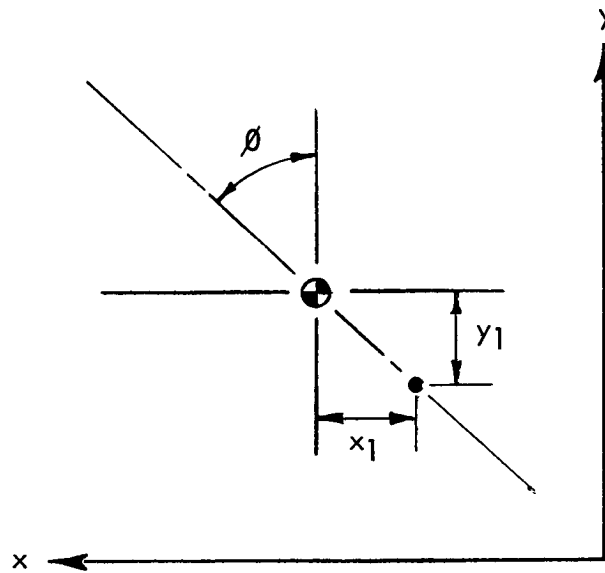
Defining a_x , a_y and a_z as the direction cosines of the target ray, in the x , y , z optics frame, from Figure 5-1b the following relationships can be developed

$$a_x = \sin \gamma \cos \phi$$

$$a_y = \sin \gamma \sin \phi$$

$$a_z = \cos \gamma$$

Corresponding to Figure 5-1b, the image plane presentation is as shown in Figure 5-1c. The displacement of the target image from boresight is indicated by the image plane coordinates x_1 and y_1 .



- = TARGET IMAGE
 ⊕ = CENTER OF RETICLE CORRESPONDING TO $\gamma = 0$, WITH
 COORDINATES x_0, y_0

Figure 5-1c. Vidicon Target Presentation Corresponding to Figure 5-1b.

From Figures 5-1b and 5-1c relationships can be developed for $\cos \phi$ and $\sin \phi$ in terms of x_1 and y_1 so that the expressions for the direction cosines become:

$$a_x = \sin \gamma \frac{(-x_1)}{\sqrt{x_1^2 + y_1^2}}$$

$$a_y = \sin \gamma \frac{(-y_1)}{\sqrt{x_1^2 + y_1^2}}$$

$$a_z = \cos \gamma$$

Narrow Field Transfer Functions

In the narrow field system where $\gamma \leq 1/2^\circ$ the simplifying approximation of $\sin \gamma = \gamma$ can be made. In addition the off-axis angle γ can be related to the location of the image in the image plane with a simple linear expression and:

$$\sin \gamma \approx \gamma = k_n \sqrt{x_1^2 + y_1^2}$$

For this case of $\gamma \leq 1/2^\circ$ a second simplifying approximation of the form of $\cos \gamma \approx 1.0$ can be made.

The transfer functions given in the previous section now become

$$\begin{aligned} a_x &= -K_n x_1 \\ a_y &= -K_n y_1 \\ a_z &= 1.0 \end{aligned}$$

K_n is a proportionality constant relating the off-optical axis angle to the off-center distance of the target in the image plane. If x_1 and y_1 are expressed in data processor readout counts (decimal), this constant is approximately:

$$K_n = 2.23 \text{ arc sec/count}$$

Wide Field Transfer Function

In the wide field system the angular range does not permit the simplifying approximations used in the narrow field transfer function development. The transfer function is, as previously given in the General Coordinate Relationship section:

$$a_x = \sin \gamma \left(\frac{-x_1}{r} \right)$$

$$a_y = \sin \gamma \left(\frac{-y_1}{r} \right)$$

$$a_z = \cos \gamma$$

$$\text{where } r = \sqrt{x_1^2 + y_1^2}$$

Based upon tests conducted using the wide field optics, the off-axis angle γ can be expressed as a function of r

$$\gamma = 90.19 - 5.430 \times 10^{-2} r^2 - 1.364 \times 10^{-5} r^2$$

where γ is in degrees

and r is in readout counts (decimal)

This expression for γ is parabolic in nature but the quadratic term is small. To a 30 arc min approximation a linear relationship could be employed.

STUDY OF TARGET AND IMAGE CHARACTERISTICS FOR THE WIDE ANGLE OPTICS

There are four important features to note about the wide angle system.

- A. For an off-axis viewing angle the object plane image is an ellipse. This is true of any wide field of view system and is independent of the optics. While it is conceivable that certain types of optics might produce a circular image from this object plane relationship, the present optics do not.

Consider the situation shown in Figure 5-2. The tracker is located at point "O" a distance "a" from the horizon plane of a spherical body of radius "R". The tracker axis is offset from the true local vertical by the angle " α ".

For convenience we establish an object plane for the tracker which is perpendicular to its axis at point "P" and intersects the local vertical at point "A".

The horizon image seen by the tracker can now be described as the curve of intersection between the conical surface subtended by the spherical body from point "O" and the object plane.

If $\alpha = 0$ the object plane and horizon plane coincide and this curve is a circle. For any other value of α the curve is an ellipse.

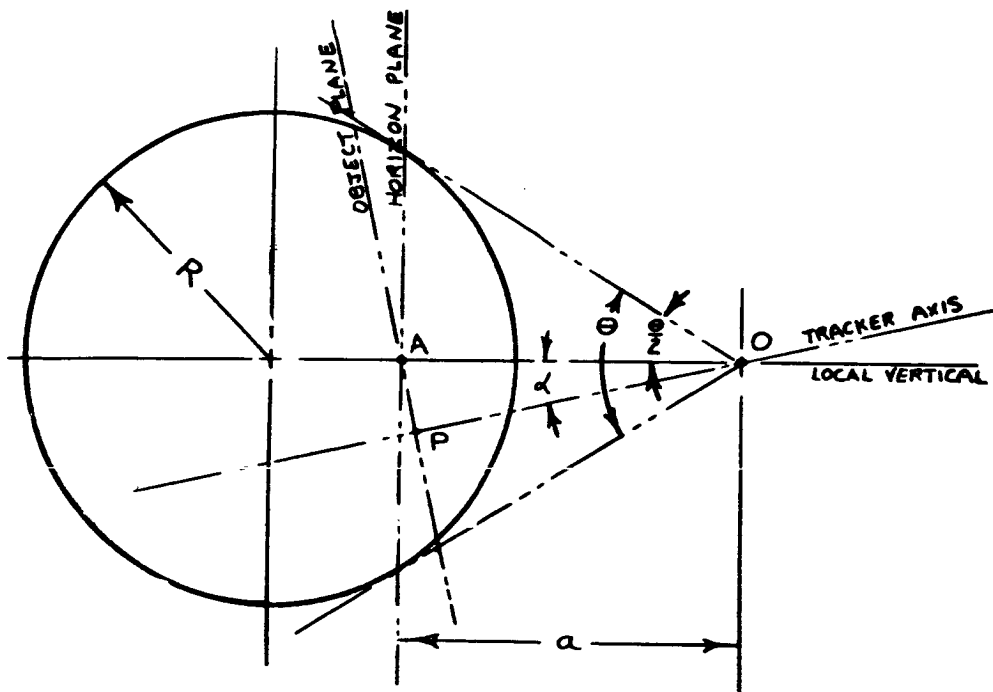


Figure 5-2. "Off Vertical" Horizon Geometry

- B. While the actual transfer function relating the off-axis angle (γ) to its image plane position (r) is parabolic, it can be closely approximated by the linear expression*.

$$r = 0.6 - 0.006 \gamma$$

where: r = radial position in image plane (inches)

γ = off-axis angle of the object (degrees)

- C. For an off-axis viewing angle the image of a spherical body formed by the wide mode optics is elliptical with an eccentricity which is a function of both altitude and off-axis angle. The center of this elliptical image is offset from the center of the image plane as a function of the off-axis angle.
- D. The operating range of the instrument, for continuous horizon images in the image plane, can be determined by subtracting four times the desired maximum offset angle from the angular range of the optics.

*Accurate to approximately ± 30 arc min.

This is necessary because the image will intersect with the outer edge of the image plane or it will be interrupted by the central obscuration should these angles be exceeded. These two cases are shown in figures 5-3 and 5-4. As an example, the wide mode optics which have a nominal angular range of seventy degrees (90 to 160°) could operate, for a ten degree offset, only in a thirty degree range (110 to 140°). If this range were exceeded image interruption would occur. Image interruption in itself is not limiting however. Should it occur a different mode of data reduction will be required.

SCAN TECHNIQUES FOR WIDE ANGLE MODE OF OPERATION

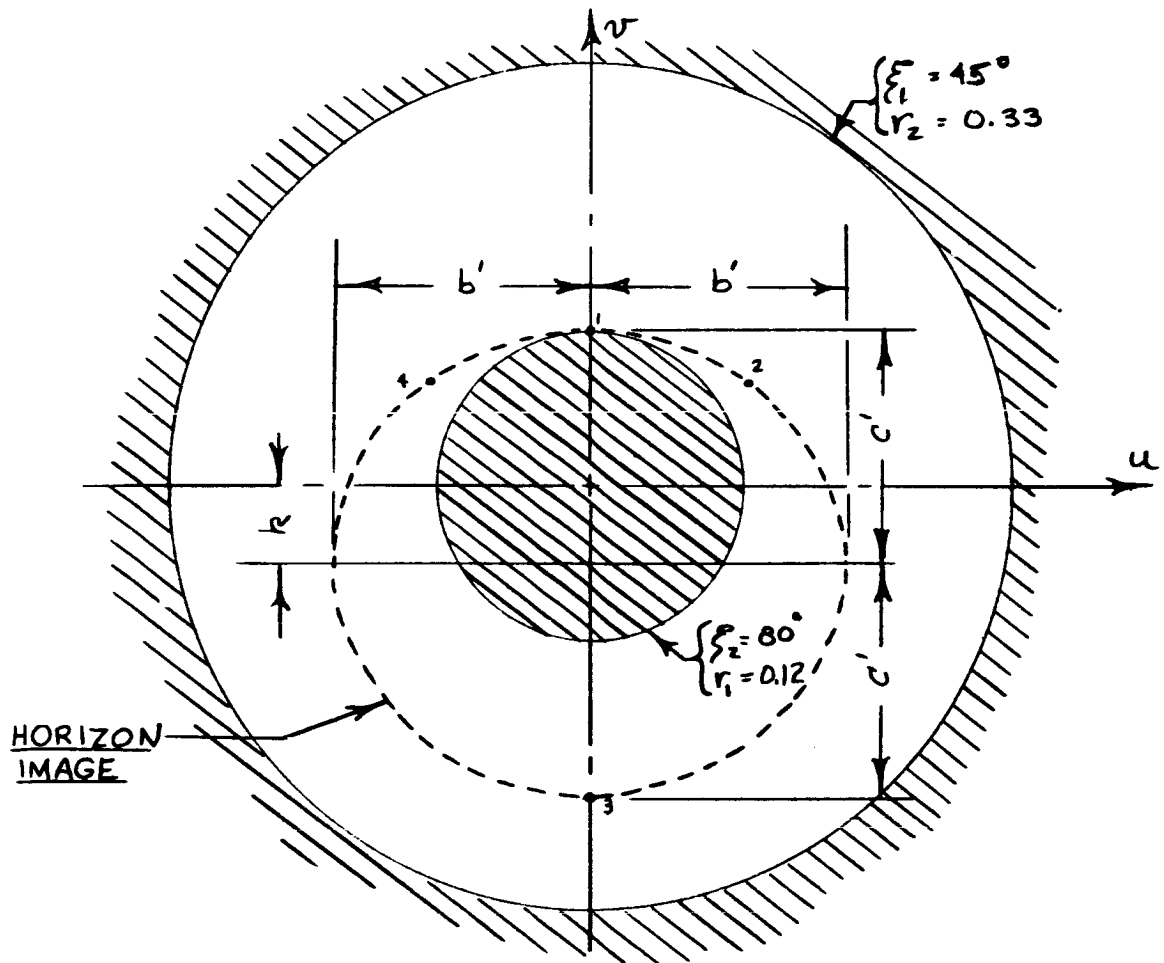
Three basic approaches to camera operation have been considered for obtaining navigation fixes while tracking planetary disks in the wide angle mode of operation:

- A. Spiral Scan
- B. Radial Scan
- C. Orthogonal Scan

The spiral scan is basically a polar scan technique which provides servo signals to null the tracker boresight reference at the center of a fully or partially illuminated disk. In the nulling mode the operation approaches a curve tracking function.

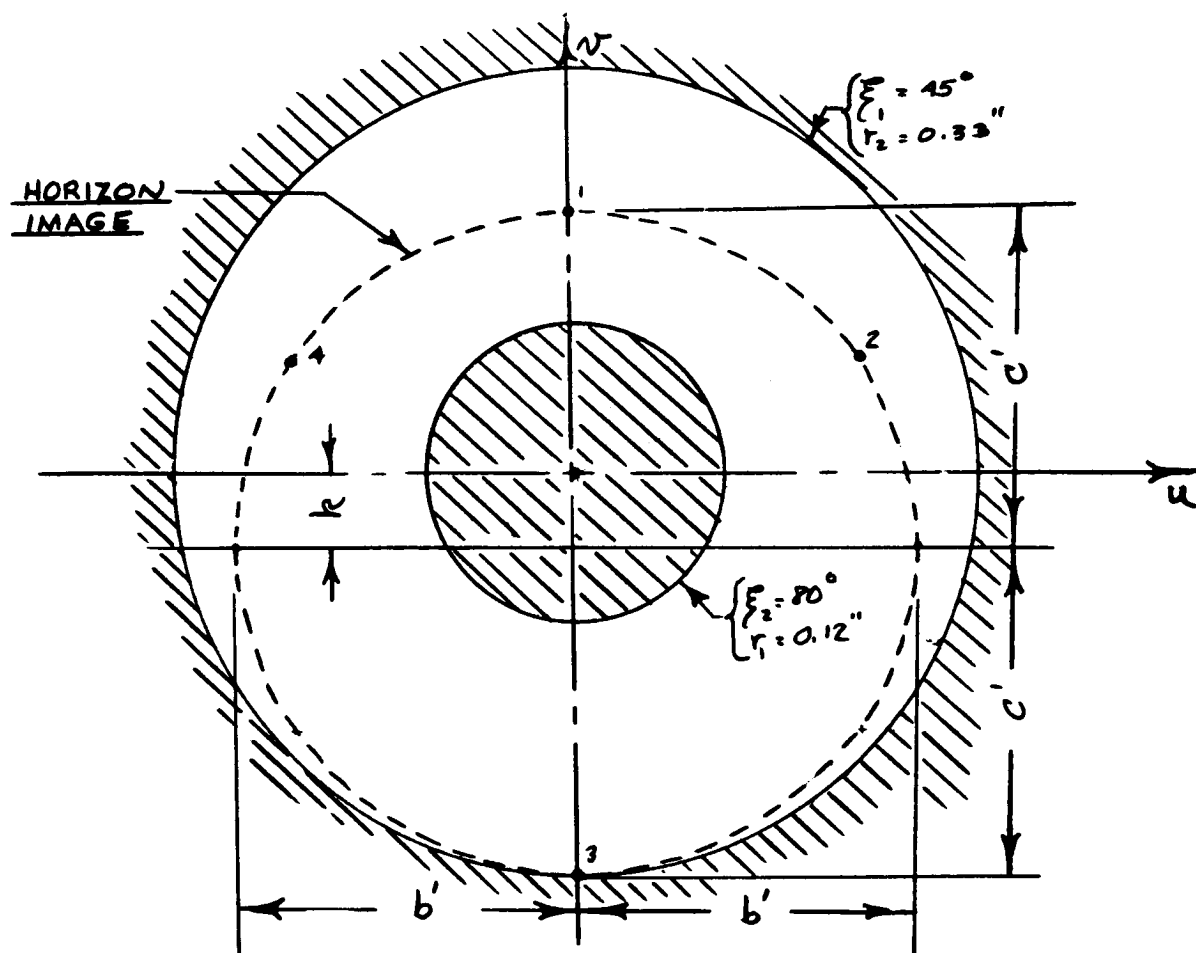
The radial scan is another polar scan technique which also operates best in a nulling mode. Servo signals for nulling are obtained by detecting the non-equal length of radial scan lines extending from the camera boresight reference to the planetary limb. The hardware constructed to produce this scan mode is discussed in Section 3 of this report.

The orthogonal scan technique uses the intersections of scan lines with the disk edge to obtain multiple, single-dimensional, (cylindrical) positional constraints. The angular orientation of the line of sight, relative to the sextant boresight frame, is determined by measuring the image intersection displacement relative to the camera reference frame. Since the camera reference frame can be related to a stellar frame by the technique of star tracking, it is possible to determine the orientation relative to a stellar frame of the cylindrical positional locus corresponding to the tracked point. The axial direction of this locus relative to the stellar frame, together with a record of the time at which the sighting was taken, is a fragmentary piece of navigation data of the type required by the statistical processing operation of the computer in determining the vehicle ephemeris.



VIEWING ANGLE $\theta = 140^\circ$
 OFFSET ANGLE $\alpha = 10^\circ$
 OFFSET OF CENTER OF IMAGE $= k = 0.06''$
 SEMI MAJOR AXIS $= b' = 0.20''$
 SEMI MINOR AXIS $= c' = 0.18''$
 ECCENTRICITY $= e = 0.40$

Figure 5-3. Image Plane Horizon



VIEWING ANGLE $\Theta = 110^\circ$
 OFFSET ANGLE $\alpha = 10^\circ$

OFFSET OF CENTER OF IMAGE = $r = 0.06''$
 SEMI MAJOR AXIS = $b' = 0.27''$
 SEMI MINOR AXIS = $c' = 0.28''$
 ECCENTRICITY = $e = 0.28$

Figure 5-4. Image Plane Horizon

relative to a stellar frame of the cylindrical positional locus corresponding to the tracked point. The axial direction of this locus relative to the stellar frame, together with a record of the time at which the sighting was taken, is a fragmentary piece of navigation data of the type required by the statistical processing operation of the computer in determining the vehicle ephemeris.

An important point to be noted is that the tracking of sufficient random points on an observed planetary limb will provide a navigation fix. There is no advantage, from a navigational point of view, in interposing the intermediate step of finding the center of a fully or partially illuminated disk.

Table 5-1 which follows provides a comparison of these alternative scan techniques.

UTILIZATION OF SPACE SEXTANT DATA FOR SELF-CONTAINED SPACE NAVIGATION SYSTEMS:

The primary function of the Space Sextant is to measure inter-celestial angles to obtain navigation fixes (e. g. angle between a stellar reference frame and a planetary center).

Two general approaches to data utilization may be classified as:

- A. The utilization of "predictable observable" data in well established mathematical techniques. A typical "predictable observable" will be the angle between a known star and the center of a known planet.

The Space Sextant can obtain this type of data at all planetary ranges and over a wide variation of planetary illumination conditions. This type of data can be utilized with well established navigation techniques such as the statistical prediction techniques using Kalman Filter Techniques, Maximum Likelihood Estimators, or Bayes Estimate Techniques.

- B. The utilization of "nonpredictable observables" such as the directionality of a randomly selected planetary limb point relative to a stellar frame. This approach to data utilization has certain advantages but will require different computational procedures.

It is emphasized that the Space Sextant can obtain conventional navigation data and utilize well developed mathematical techniques. The operation of the Space Sextant is not in any way contingent upon the development of new orbit determination techniques.

TABLE 5-1
A COMPARISON OF ALTERNATIVE SCAN TECHNIQUES

	Spiral Scan	Radial Scan	Orthogonal Scan
1. Primary Mode of Operation	Nulling of center of planetary limb on camera boresight.	Nulling of center of planetary limb on camera boresight	Off-axis readout of points on planetary limb and other fix points.
2. Mechanical Stability Requirement	Requires angular positional stability for nulling.	Requires angular positional stability for nulling.	Requires only moderate reduction of angular rates to permit camera image readout.
3. Off-Axis Readout Capability	Very complex	Requires computer operation for off-axis interpretation.	Requires computer operation for off-axis operation.
4. Primary Disadvantages	Requires implementation of special scan. Impractical for off-axis operation. Requires periodic discharge (erasure) of image tube. Not acceptable for crew monitoring or IP tracking in wide angle mode. Spiral scan electronics difficult to mechanize to produce uniform scan rate.	Requires implementation of special scan. Requires periodic discharge (erasure) of image tube. Not acceptable for crew monitoring or IP tracking in wide angle mode.	If verticality nulling is required for non-navigation purposes (e.g., for attitude control), then computer is required for obtaining vertical.
5. Primary Advantages	Readily adaptable to nulling mode without use of computer.	Readily adaptable to nulling mode without use of computer. Readily adapted to tracking partially illuminated disks.	Same scan and data logic for both optical modes. Orthogonal scan provides for crew monitoring and IP tracking in both in both optical modes. Orthogonal scan can take advantage of same reticle pattern for both optical modes. Since each randomly selected point on a planetary limb is treated as an independent data point and disk center is not computed explicitly camera/gyro data rate can be relaxed.

However, the Space Sextant does also permit the option of exploiting a new approach, to self-contained navigation having certain advantages. This alternative approach would require different mathematical techniques.

SUMMARY

- A. The Space Sextant Design permits a wide range of data processing techniques ranging from relatively elementary techniques to more complex complete orbit determination procedures which are even capable of solving the "I am lost!" problem.
- B. The data processing techniques to be selected bear heavily upon the optical modes to be used. In designing a specific mission optical fields of view can be selected which will permit selection of the most suitable data processing mode.
- C. Crew operation can greatly simplify the computational operation for the manual vehicle case. Likewise, if desired, for the unmanned probe, the digital camera and gyro data can be telemetered to earth based stations in order to avoid all on-board computations.
- D. An attempt to classify computational techniques is presented in Table 5-2. In this table the optical modes referred to are as follows:
 - o Optical Mode No. 1 - Wide angle mode.
 - o Optical Mode No. 2 - Narrow angle mode with angle subtended by sighted planet greater than angular field of view of narrow angle mode.
 - o Optical Mode No. 3 - Narrow angle mode with the angle subtended by the planet less than view angle of narrow field system.

TABLE 5-2
COMPARISON OF CERTAIN DATA UTILIZATION MODES

Data Utilization Mode	Optical Mode Applicability	Optical Mode Non-Applicability	Comments
1 - Processing of simultaneously obtained limb point data obtained in a single camera frame.	Applicable to Optical Modes No. 1 and No. 3.	Not applicable to Optical Mode No. 2	Computation of planetary disk center is a simple, separate, short period computation. Navigation computation proceeds as in any technique involving planet vertically tracking.
2 - Processing of near simultaneously obtained limb point data obtained with short period with camera and E/S gyros.	Most applicable to Optical Mode No. 2.		Similar to above but definitely require multiple gyro readouts.
3 - Processing of non-simultaneously obtained limb point data using "angle perturbation" techniques.	Applicable to all Optical Modes.		Probably provides the simplest computation but will have some reduced accuracy unless special effort is used for selecting the tracked limb point. *
4 - Processing of non-simultaneously obtained data using simulated "stellar occultation" techniques.	Applicable to all Optical Modes.		Similar to No. 3 but uses time increment as input to perturbation technique.
5 - Processing of non-simultaneously obtained limb point data to compute vehicle ephemeris by "explicit" techniques based on concept of "non-predictable observables."	Applicable to all Optical Modes.		This is the most general approach with potential for the greatest flexibility. This looks like the "most interesting" technique for very advanced application as it can simplify the "measurement" problem. It also requires no pre-planning or pre-computation for navigation purposes and permits mission changes, abort maneuvers, recovery from completely "lost" conditions etc., without restriction from the navigation system. Computation may generally be more complex than is desirable for some space missions.

* Techniques for mechanizing this method have not as yet been completely developed

Section 6

SYSTEM TESTS AND RESULTS

INTRODUCTION

The work statement for the Space Sextant Phase A contract lists three major goals:

- A. Capability to detect $+2.0 M_v$ stars under good seeing conditions with a $S/N = 10$ minimum.
- B. Narrow field angular accuracy of ± 3 arc sec on boresight and 3 arc sec plus 0.3% of the off-axis angle elsewhere in the field.
- C. Wide field angular accuracy of 5 minutes-of-arc on boresight using idealized extended images.

The tests proposed to establish the degree of accomplishment of these goals were of three general types:

- A. Optics and Camera Sub-System Evaluation Tests
- B. Off-Axis Angular Readout Accuracy Tests
- C. Photometric Tests

The first two of these test types were performed entirely in the Optics Lab at our Johnson City Installation. The test setups and facilities used are shown in Figures 6-1-2-3.

The third type, to determine signal to noise ratios for typical celestial targets, was performed both at Johnson City and the General Electric Company's Photo-electric Observatory in Schenectady.

The facilities used and the tests performed at the Optics Lab at Johnson City, New York are described in the following paragraphs.

FACILITIES

- A. Star-Simulator: A tungsten arc focused on a 0.0005" dia pinhole which is located at the principal focus of an 8 inch $f/8.0$ parabolic, $1/4$ wave mirror, served as the simulated star. Color temperature is approximately 3200°K , (Reference Figure 6-4).

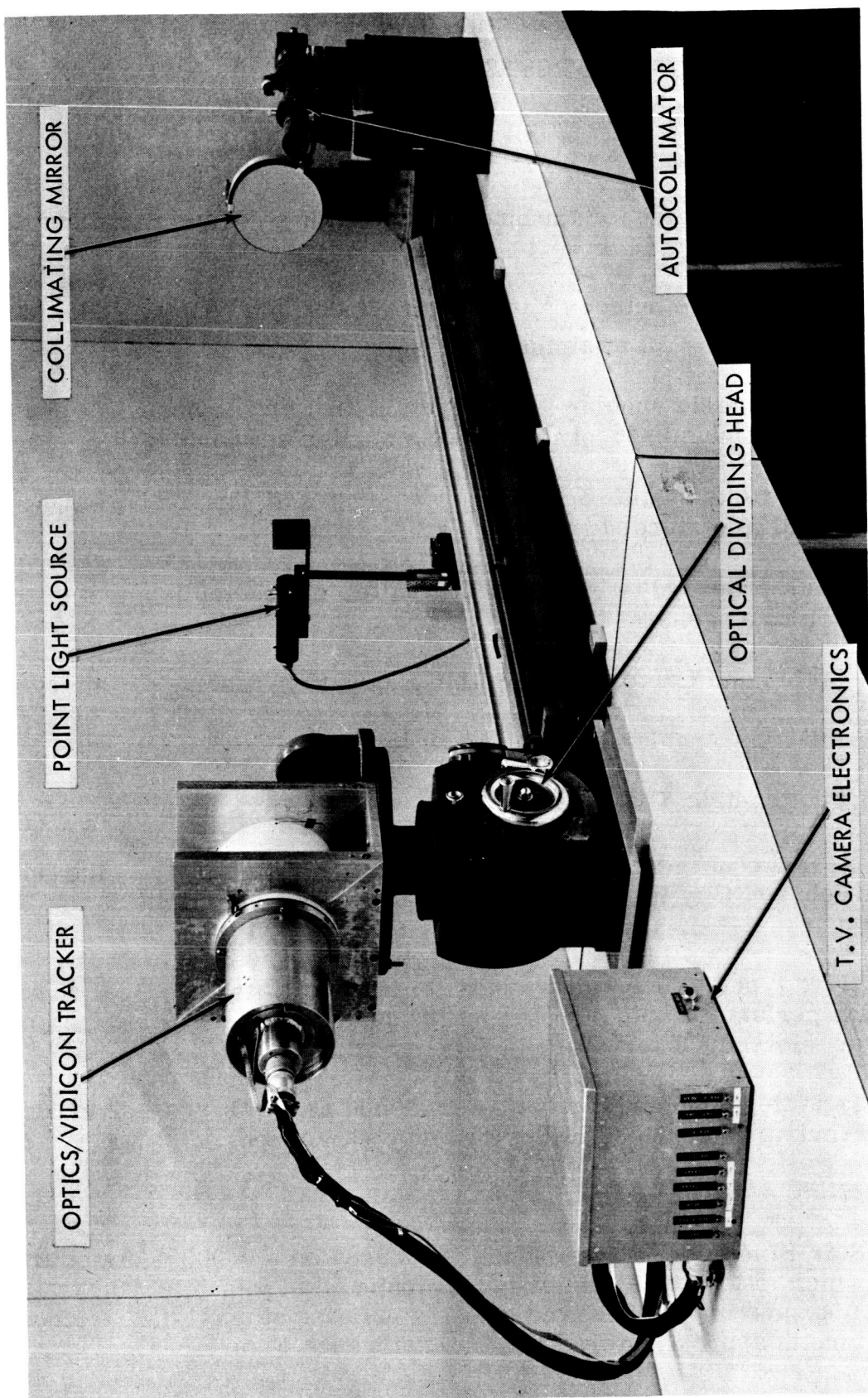


Figure 6-1. Angularity Test Setup (Narrow Mode)

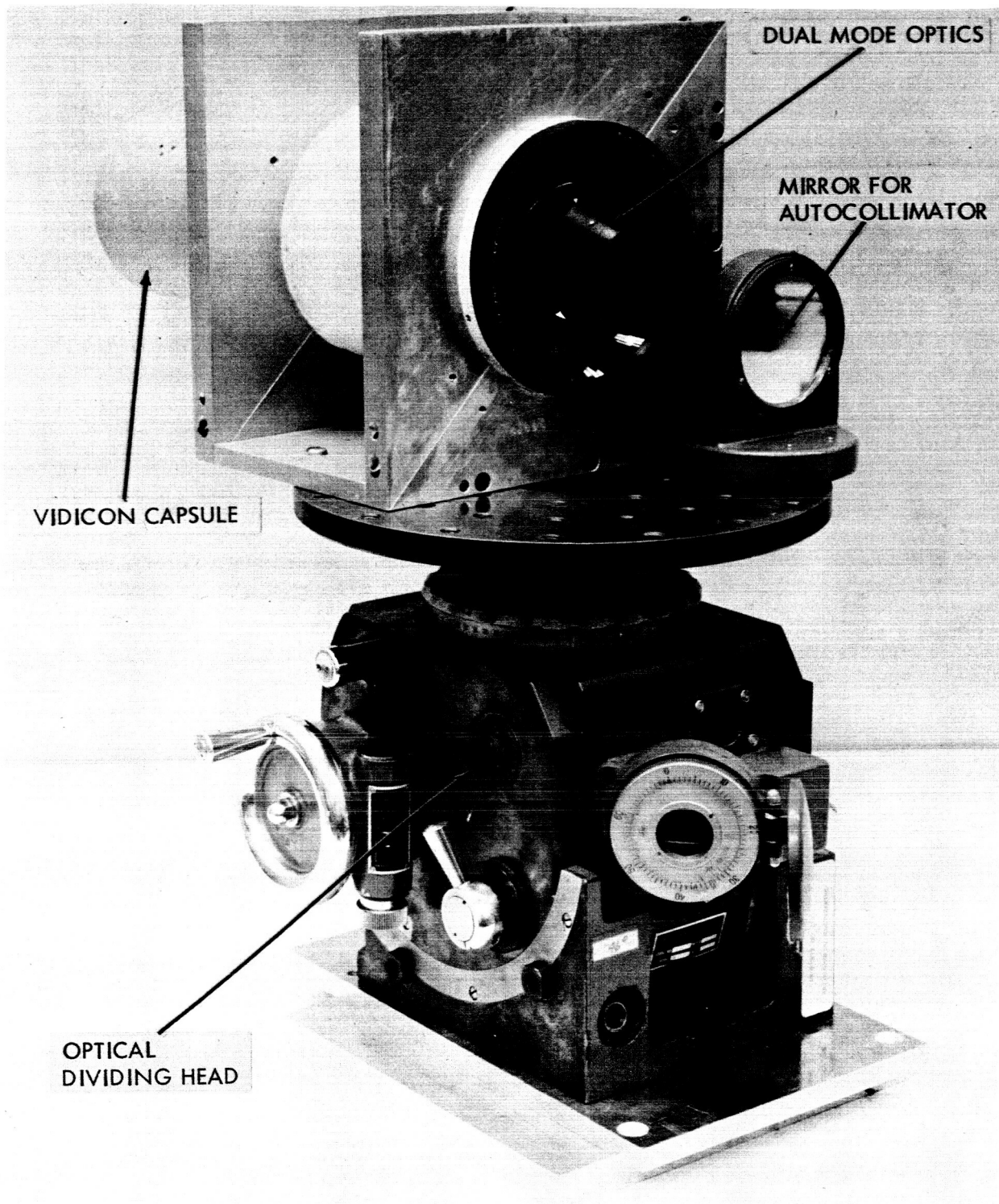
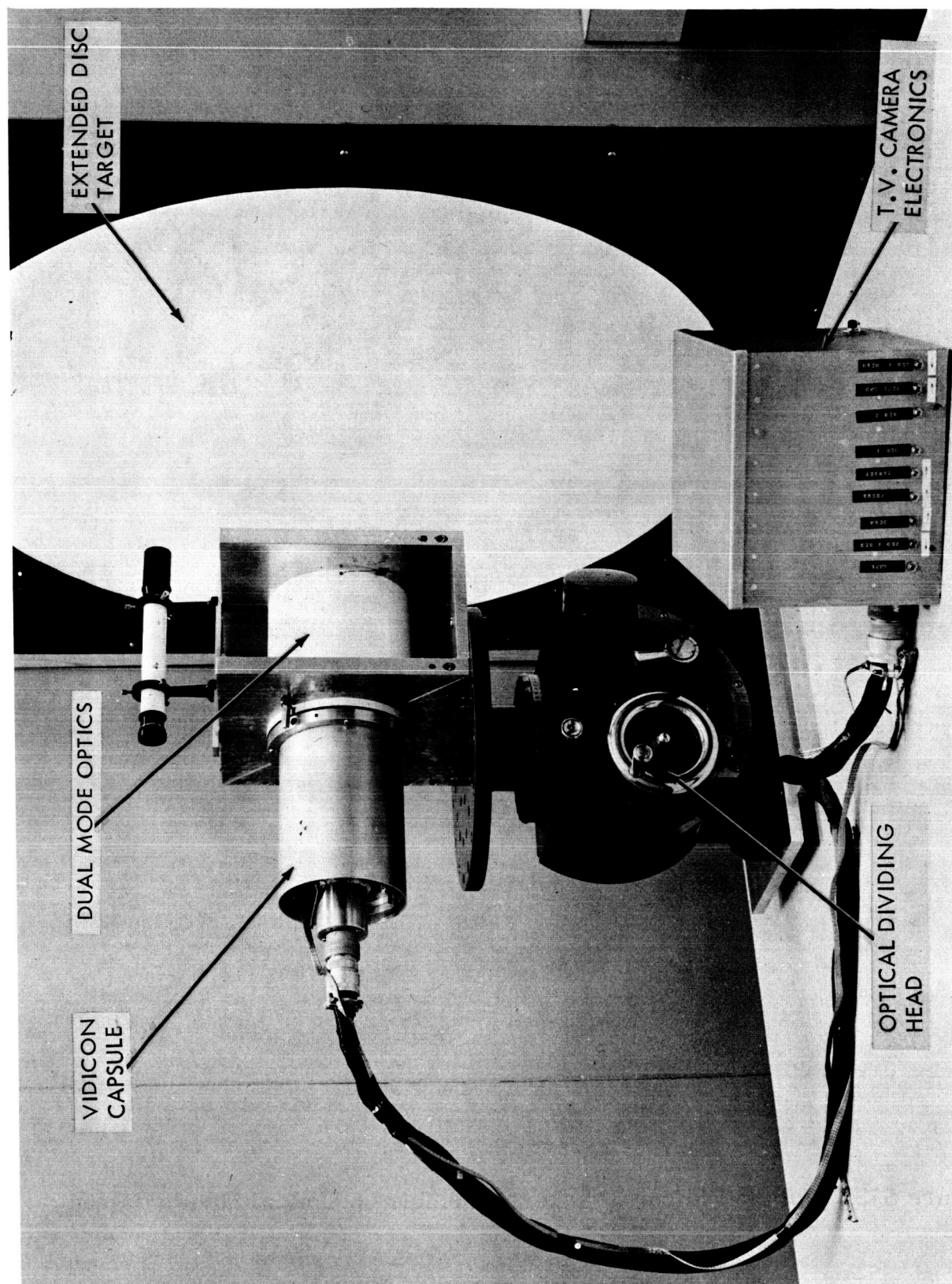


Figure 6-2. Optics-Vidicon Tracker Assembly on Optical Dividing Head



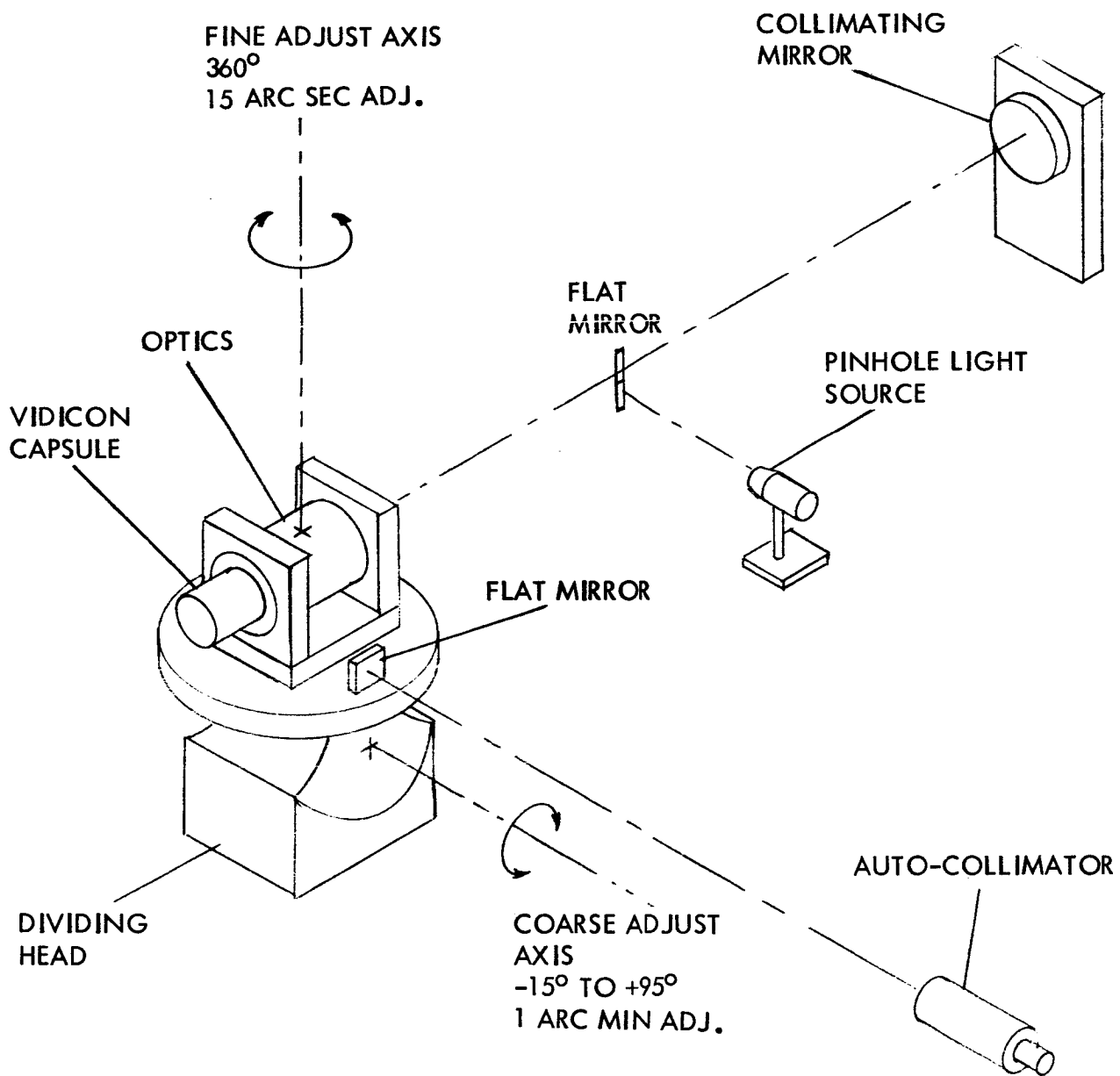


Figure 6-4. Test Setup Off-Axis Angular Evaluation Tests

- B. Planet Disc Simulator: A translucent screen, back-illuminated with a circular spot from a slide projector, served as the primary target. The projector lamp, a 350 watt tungsten bulb, has a color temperature of approximately 3200°K. A Macbeth Illuminometer was used to establish the brightness levels and the deviations of the target from an ideal Lambert surface.
- C. Angular Adjustments: A Griswold Model OPL Dividing Head served as the primary angular adjustment mechanism, (Reference Figure 6-2). This device has two orthogonal axes of adjustment. The first can be rotated thru 360° with a built-in angular readout with a resolution of 15 arc-seconds. The second can be rotated through -15° to +95° with a readout resolution of 1 arc-minute.
- D. High Accuracy Angular Readout: For precision readout, a Hilger and Watts Microptic Auto-Collimator was employed, (Reference Figure 6-1). This device has a 10 arc-minute range with a readout resolution of 0.1 arc-seconds.

This high accuracy was applied to one coordinate of the image plane at a time and this coordinate was selected by physically re-orienting the optics/vidicon assembly on the dividing head.

The x-axis accuracy tests were performed by orienting the assembly so that the raster lines were parallel to the surface of the dividing head. The y-axis accuracy tests were performed by reorienting the optics/vidicon so that the raster lines were perpendicular to the surface of the dividing head.

EVALUATION TESTS - VIDICON RETICLE PATTERN

To obtain a precise digital readout from the vidicon tube a reticle pattern was added to its target. The specification for this pattern is given below.

- A. Reticle Pattern: The reticle pattern consists of 8 vertical lines and 9 diagonal lines (the first of which is shorter than the other 8) located in a square area at the center of the vidicon target (reference Figure 6-5).
- B. Positioning of the Reticle: The reticle will be positioned on the vidicon target with sufficient accuracy to allow the complete reticle to be included in a square raster scan pattern. This square raster will begin 0.004" to the left of the first vertical line.

The reticle pattern will be oriented so that the vertical lines are perpendicular to the vidicon's scan lines within $\pm 3^\circ$.

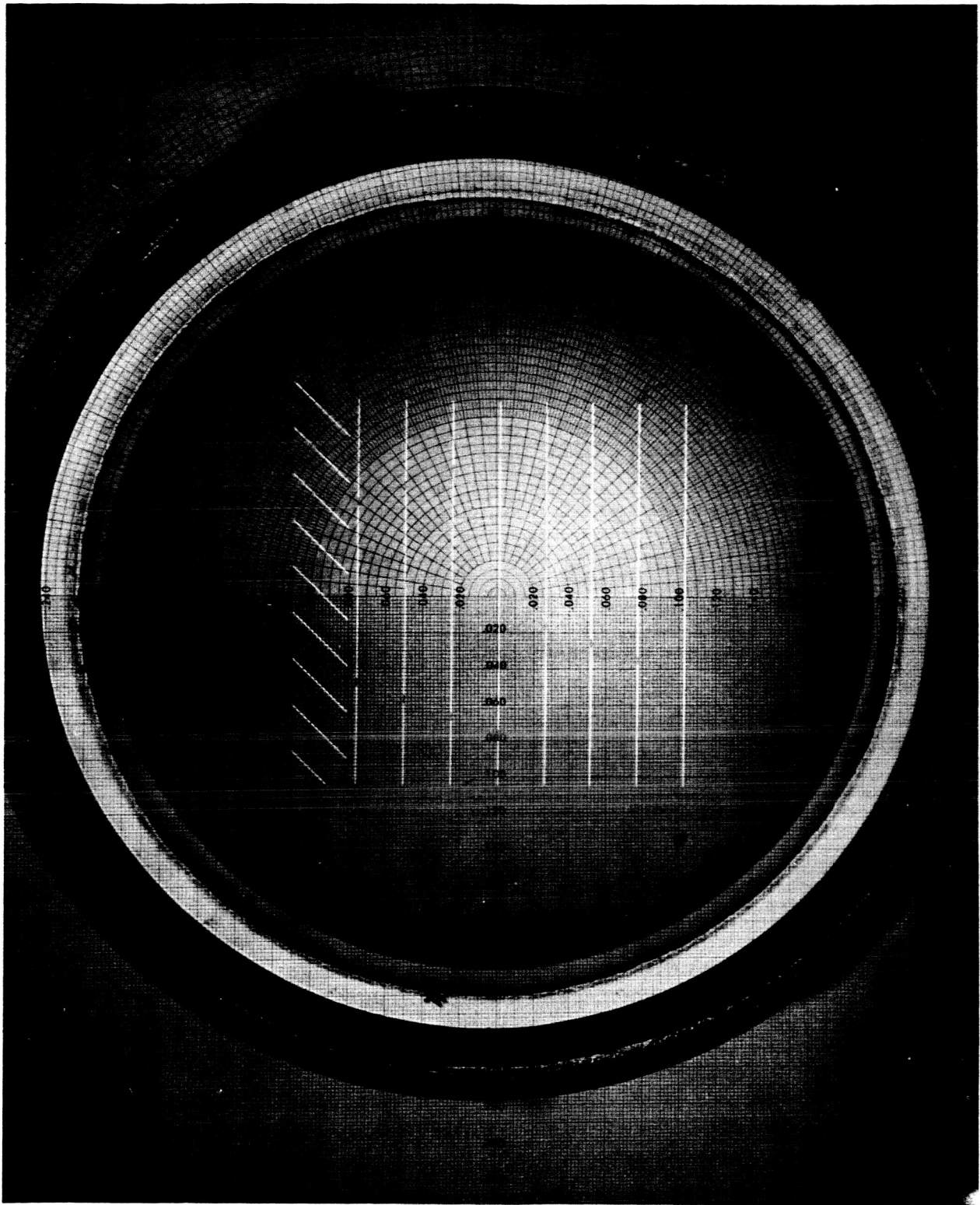


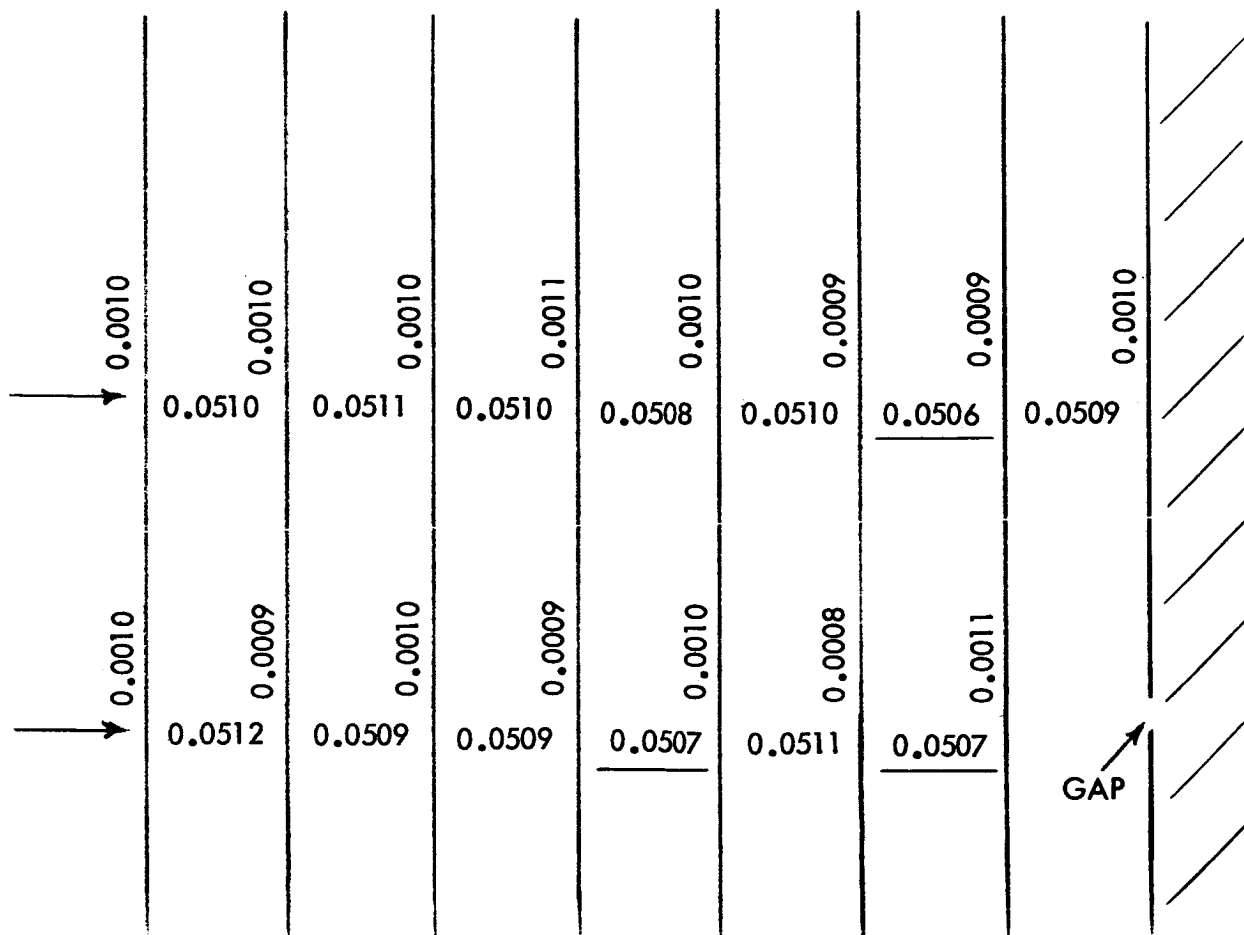
Figure 6-5. Optical Comparator Presentation of Reticle Pattern on Vidicon

- C. Line Spacing Tolerance: Line spacing will be 0.051 ± 0.0001 inches.
- D. Interruptions in Reticle Lines: To allow for mechanical rigidity of the mask used in fabrication of the reticle, 0.010" gaps may be included in the vertical lines subject to the following:
1. There shall be no gaps in the first vertical line.
 2. There shall be no more than three gaps on any one vertical line.
 3. There shall be no more than one gap scanned by any one horizontal raster line. (Therefore, the gap spacing must take into account the angular positioning tolerance discussed in the paragraph above on the "Positioning of the Reticle.")

To determine the actual mechanical quality of the reticle as received¹ a series of evaluation tests were performed.

- A. Optical Comparator Inspection: Utilizing an Excello optical comparator at a 50 x magnification, the photo in Figure 6-5 was obtained. While the accuracy (± 0.004 inch) of the comparator was insufficient to allow a precise check of the line widths and spacings it provided an excellent means of examining the over-all reticle pattern for size and quality. Multiplying the indicated coordinate numbers by 2 yields dimensions in thousandths of an inch.
- B. Microscope Tests: To obtain more precise measurements of the reticle, a microscope, cross slide, and dial indicator were used. The results for two typical measurement tests across the tube are shown in Figure 6-6. About 95% of the line thicknesses are within specifications (0.001 ± 0.0001 inches). The other 5% fail to meet specifications by less than ± 0.0003 . About 75% of the line spacings meet specifications with the remainder being ± 0.0004 of the nominal as opposed to the ± 0.0001 specified.

¹The manufacturer of the vidicon with reticle was the General Electrodynamics Corp. of Garland, Texas.



NOTE:

MEASUREMENTS MADE WITH DIAL INDICATOR
 ± 0.0001 AND MICROSCOPE

Figure 6-6. Vidicon Reticle Measurements

CALIBRATION OF LABORATORY STAR LIGHT SOURCE

The laboratory "star" light source is shown in Figure 6-7. The tungsten arc which forms the primary light source is a Sylvania Model C2T with the following catalog specification:

Mean Source Dia = 0.007 inch

Average Brightness = 11300 candles/in²

Color Temperature = 3200°K

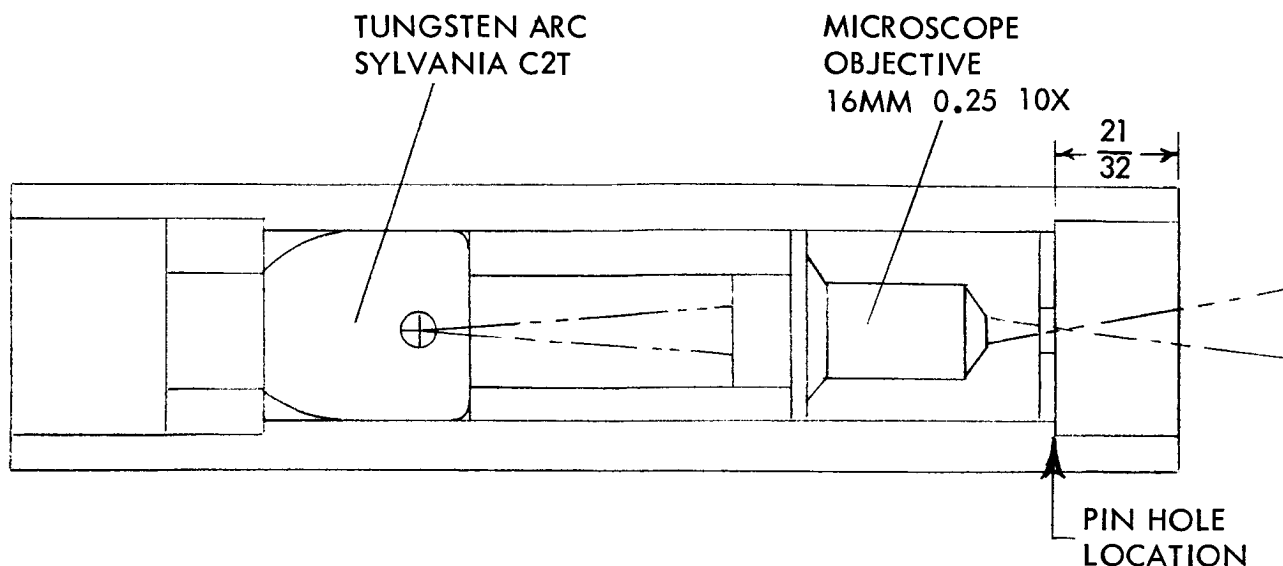


Figure 6-7. Laboratory Star (Full Scale)

By inserting neutral density filters between the microscope objective and the pinhole it is possible to make step changes in intensity without degrading the image quality.

Using the optics/vidicon assembly as a photometric tool the results in Table 6-1 were obtained.

TABLE 6-1
CALIBRATION TEST OF LABORATORY STAR

Neutral Density Filter (1)	Percent Transmission	Peak Video Signal (volts)
None	100	0.9
0.3	50	0.75
0.6	25	0.45
0.9	12.5	0.16
1.2	6.25	0.09

- (1) The numbers listed are the densities of the filters where

$$\text{density} = \log_{10} \left(\frac{1}{\text{Transmittance}} \right)$$

These results are plotted in Figure 6-8. During the photometric tests at the ATL Observatory a peak signal of 0.3 volts was observed for a +2.44 M_V star (Ursa Major β). Referring to Figure 6-8 this indicates that, to a reasonable approximation, the arc light with a 0.9 filter will produce the same effect on the vidicon as a +2.0 M_V star. Figure 6-9, which illustrates the amount of illumination produced on the Earth's surface by various magnitude stars is included for reference.

EVALUATION TESTS NARROW FIELD OPTICS

These tests were conducted on a setup as shown in Figure 6-4.

To prevent distortion due to localized stresses, the optics were mounted in an aluminum frame which clamps the optics outer tube about its full circumference. This frame is mounted on the Griswold dividing head that provides two degrees of rotational freedom (360° about the vertical axes and $+90^\circ$, -15° about the horizontal axis). This enables scanning the collimated light beam over the field of view of both the wide and narrow angle systems. To obtain precise angular measurement of the angle turned through, a flat mirror is mounted on the dividing head and an auto-collimator is utilized for precise angular readout. Refer to Figures 6-1 and 6-2.

- A. Image Quality: In evaluating the narrow mode system image quality, a point source of light of 0.0005 inch diameter was utilized. Considering the relative focal lengths of the source mirror and the optics and assuming perfect optical elements, the smallest image obtainable would be:

$$0.0005 \text{ inch} \times \frac{\text{F. L. (Optics)}}{\text{F. L. (Mirror)}} = 0.0005 \text{ inch} \times \frac{17.2}{64}$$

$$= 0.00015 \text{ inch}$$

The image actually obtained on the field flattener at various positions across the optics is shown in Figure 6-10. Subsequent tests have shown that this image size is not degraded significantly by removal of the field flattener and since off-axis linearity was enhanced by this removal, the field flattener was discarded.

- B. Angular Range: The angular field of view of the narrow angle system imaged on a 0.63 inch portion of the image plane is $1^\circ 9'$.
- C. Linearity: Linearity measurements were made without the field flattener in place and compared with the predicted results for the complete system with the field flattener. The results are shown in Figure 6-11. The measurements were made by rotating the dividing head through an angle of five minutes-of-arc as determined

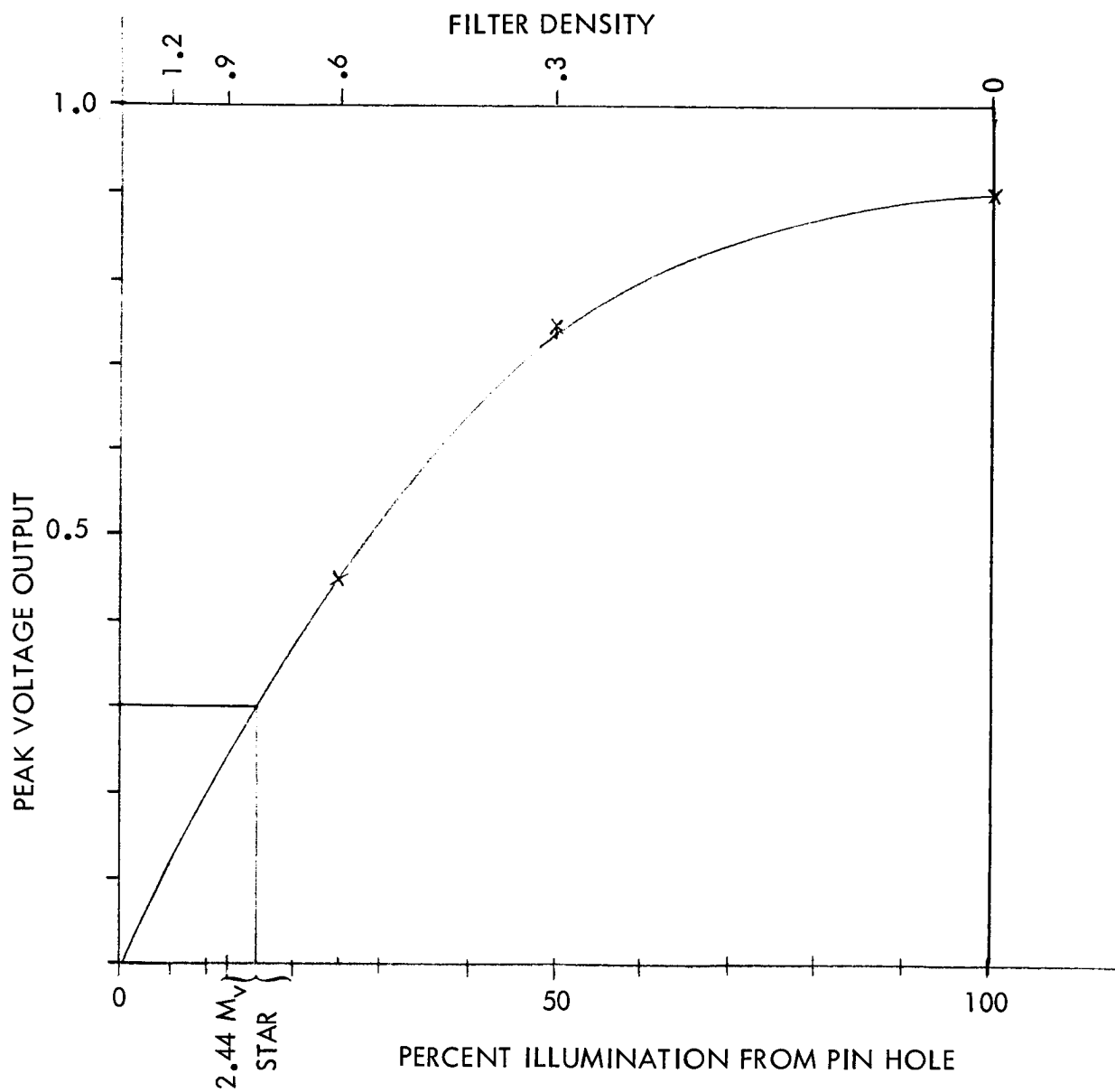


Figure 6-8. Test Results-Calibration of Laboratory Star

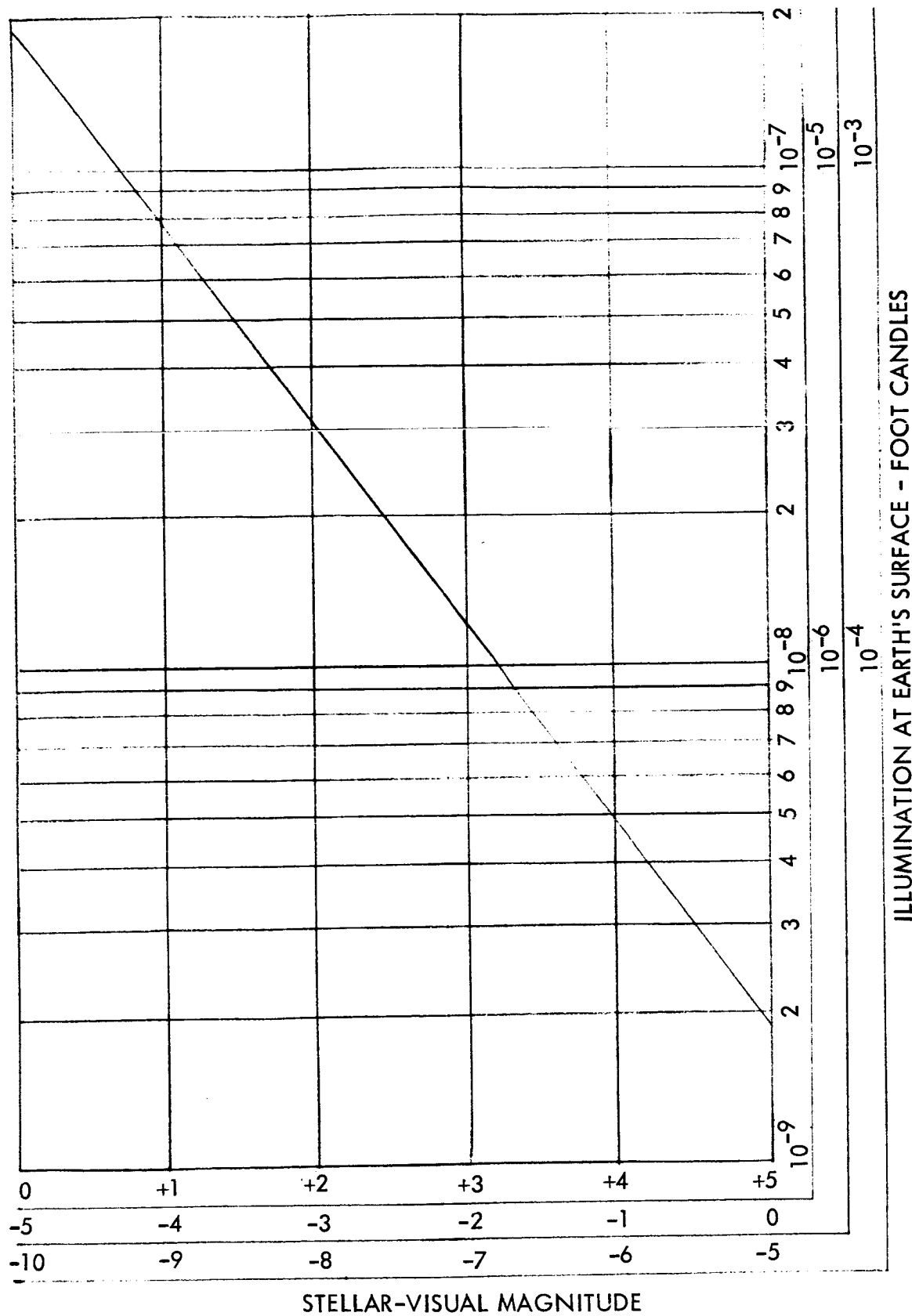


Figure 6-9. Earth Surface Illumination by Stars

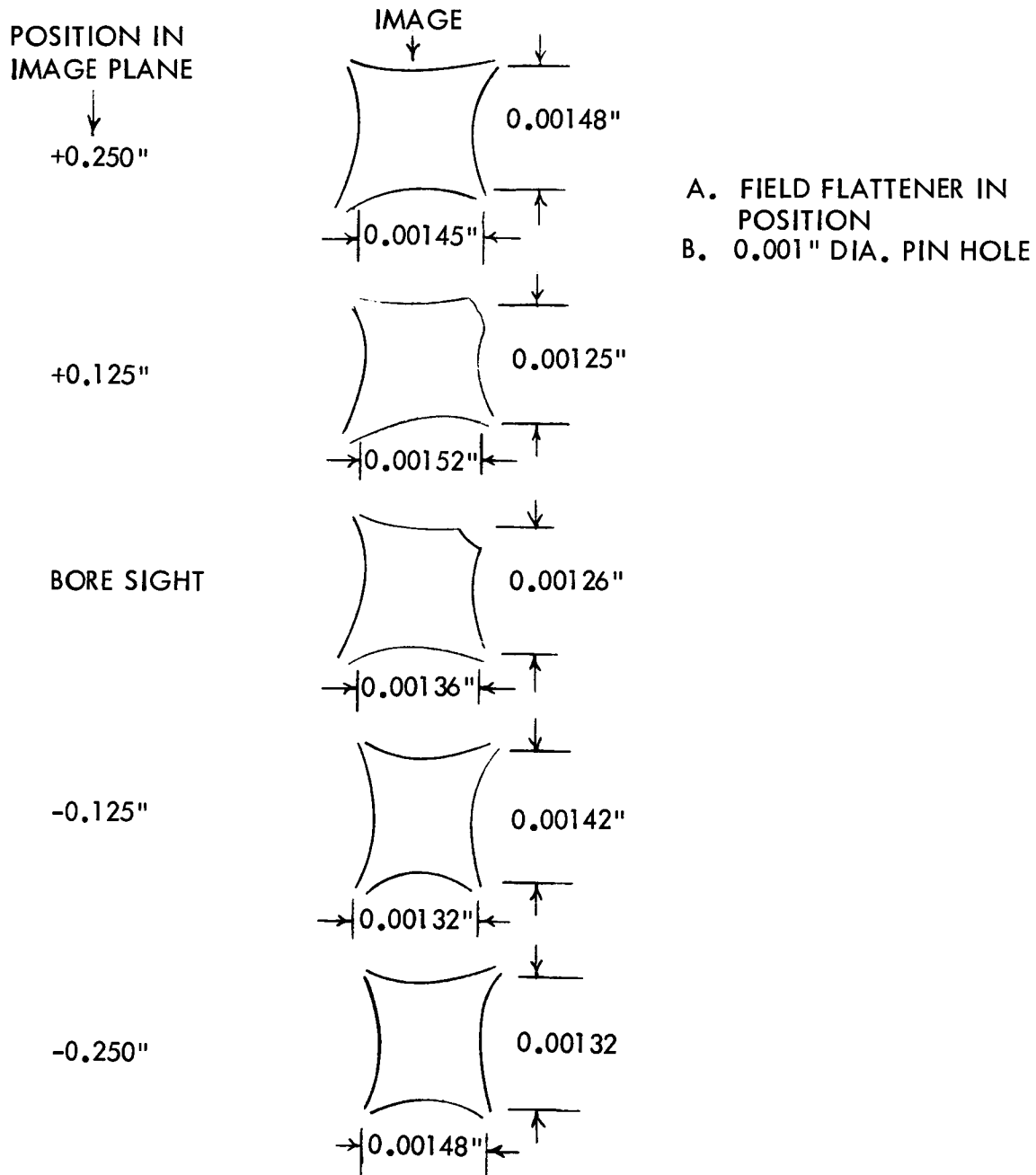


Figure 6-10. Image in Narrow Field System

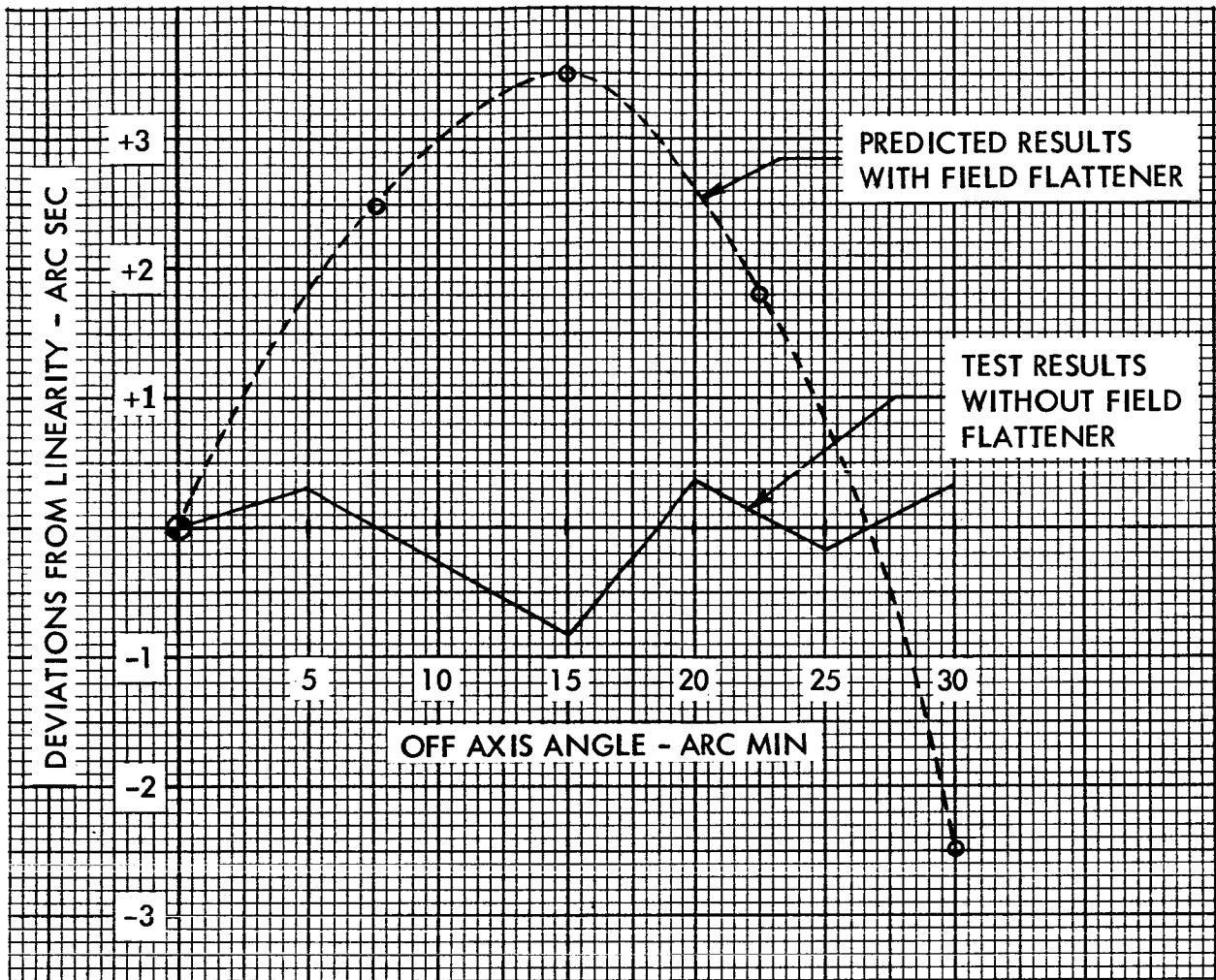


Figure 6-11. Linearity Deviations in Narrow Angle System

with the auto-collimator and measuring the displacement of the point source image in the optics image plane with a microscope.

EVALUATION TESTS WIDE FIELD OPTICS

The Evaluation Tests on the Wide Field Optics are described below.

- A. Image Quality: The image quality tests were run with a 0.007 inch diameter tungsten arc at the prime focus of the 8 inch, f/8.0 mirror.

The wide field system operates as if it had a focal length of approximately 0.3 inch. Thus, to a first approximation the ideal image in the image plane, would be a round spot with a diameter of:

$$d = 0.007 \times \frac{0.3}{64} = 3.3 \times 10^{-5} \text{ inches}$$

Therefore, the source employed is sufficiently small so that it will not, in itself, appreciably influence the results. The results of the test are shown in Figure 6-12.

The image quality tests shown in this figure illustrate the astigmatic nature of the system. Best focus was chosen as the tangential plane. However, it is seen that radial width is a function of position. Thus, it would be expected that images near the outer edges of the field would be capable of higher resolution. Since this outer diameter corresponds to the minimum angle in the Wide Field system, this result is fortuitous. Wide angles in planet tracking correspond to low altitudes where horizon noise is the accuracy limit and a high accuracy in the tracker is not as useful.

- B. Range and Linearity: Tests were now run on the range and linearity with results as shown in Figures 6-13 and 6-14.

The off-axis angular transfer function is essentially parabolic in nature. A linear relationship can be assumed which is accurate to within 30 arc-minutes but in order to achieve 5 arc-minutes accuracy the parabolic approximation is required. The deviations in this figure include the operator errors in performing the tests but in general fall within the ± 5 arc-minute limits except at the edges of the field where measurements become less accurate.

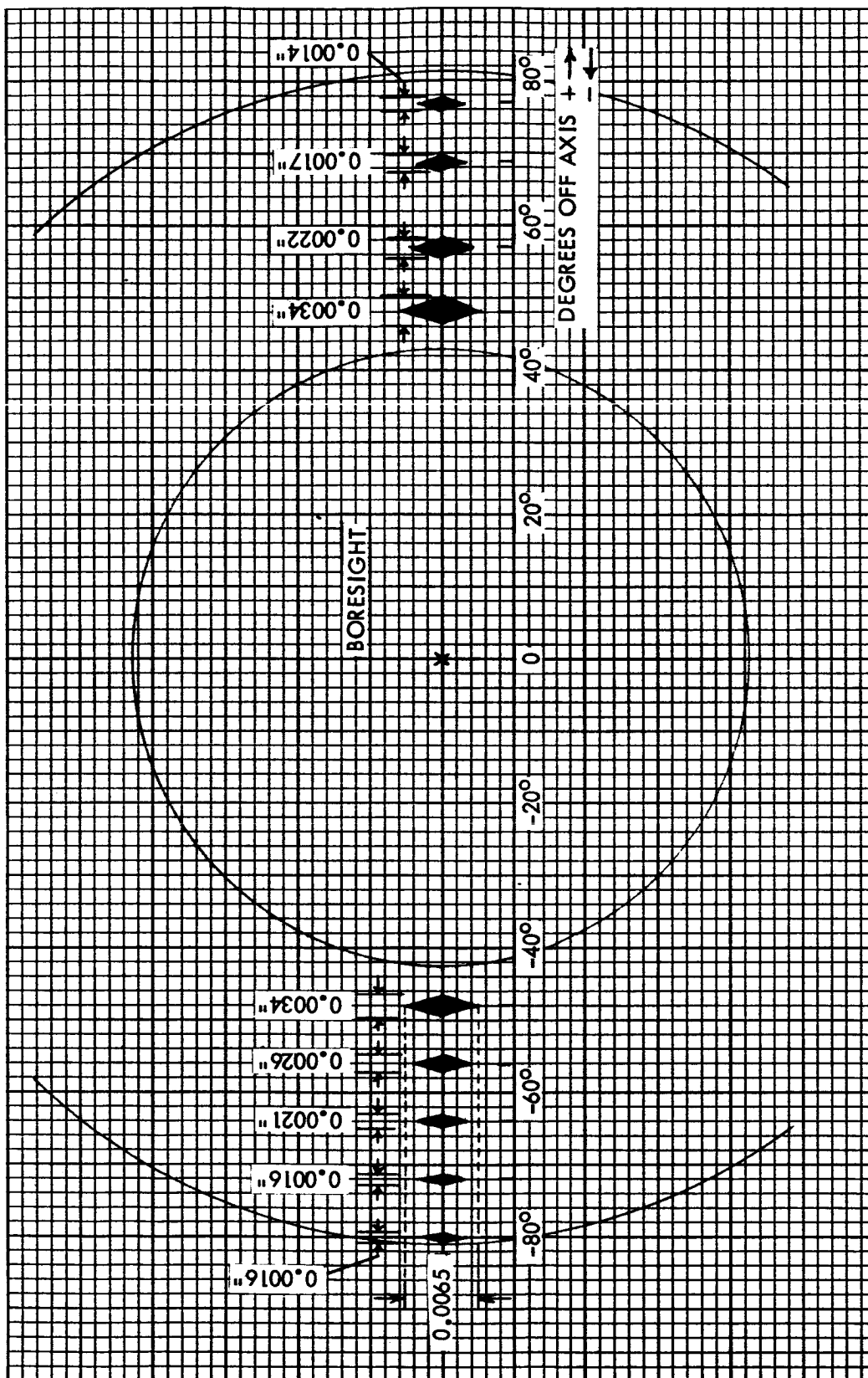


Figure 6-12. Image in Wide Field System (Source Diameter 0.007 inch)

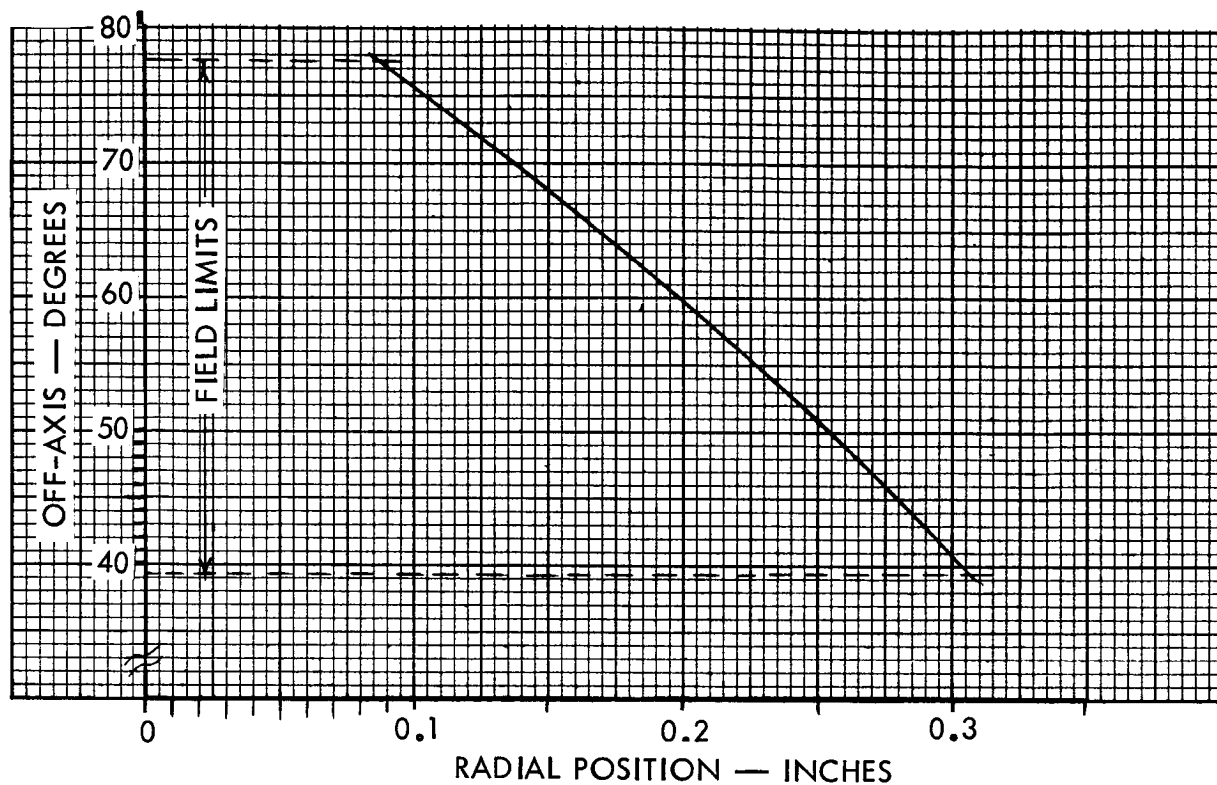


Figure 6-13. Off Axis Angle vs Radial Position of Image - Wide Field

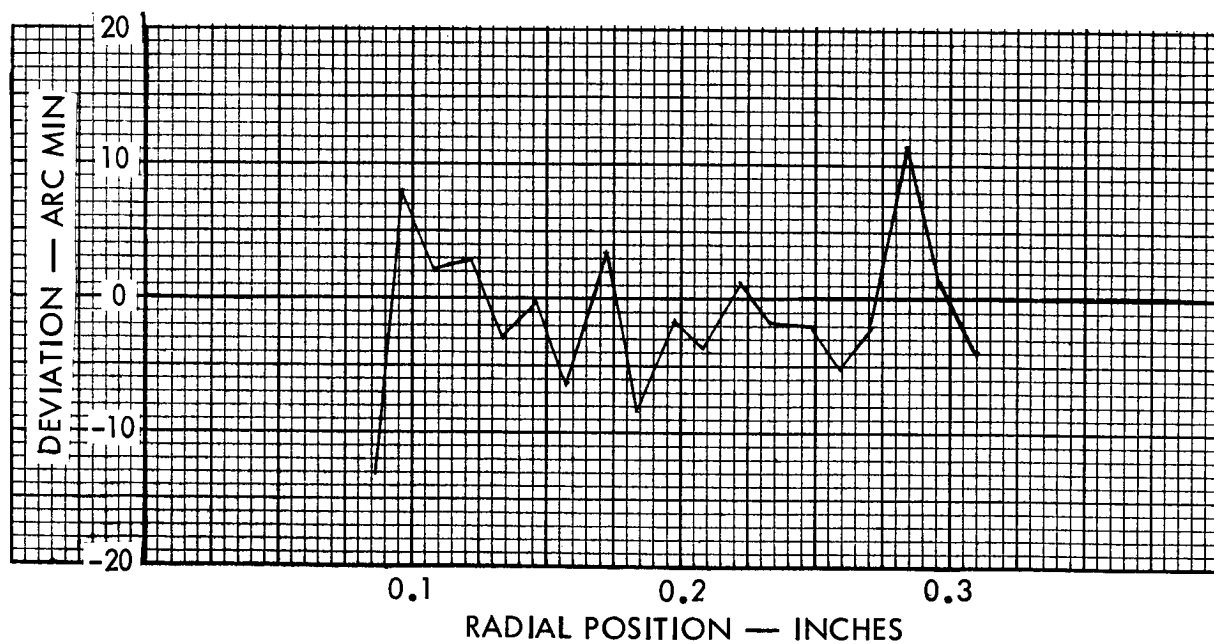


Figure 6-14. $(\theta - \theta_0)$ vs R — Wide Field (where $\theta_0 = 90.19 - 136.3r - 85.94r^2$)

PHOTOMETRIC TESTS AT OBSERVATORY

To establish the basic "seeing" sensitivity of the optics/vidicon chain the system was set up at the General Electric Company's Advanced Technology Labs observatory in Schenectady.

Figure 6-15 illustrates the equatorial mount with sidereal drive on which the Sextant was mounted. Figure 6-16 is a view of the Sextant in its mounting. This photo also shows the camera electronics and the inter-connecting cable.

The tests were conducted on the night of February 12 between 8:00 PM and 11:00 PM. The viewing conditions, in the opinion of the ATL astronomer J. Spalding, were down 1/2 to 1 visible magnitude from ideal.

Sightings were made on four stars and photographs taken of the oscilloscope presentation of the video signal. These photos are shown in Figures 6-17 through 6-20. Table 6-2 below lists the numerical results.

TABLE 6-2			
NUMERICAL RESULTS OF STAR SIGHTINGS			
Star	M_v	Signal/Noise Ratio	Illumination Foot Candles x 10^8
Canis Minor β	3.09	3.7, 6.7, 4.1	1.15
Ursa Major β	2.44	9.1, 10.5, 10.5	2.0
Orion ϵ	1.75	11.1, 9.9, —	3.8
Orion α	0.92	16.5, 17.5, 17.5	8.2

These results are plotted in Figure 6-21 along with a sketch of the definition of S/N used in this report. The dotted curve is an approximation based upon the general shape of the dynamic range curve experienced in lab tests and discussed previously in Figure 6-9. The rms noise level is estimated at 1/3 the ptp value of the noise as seen on the oscilloscope.* The deviation of ϵ Orion from this curve seems reasonable considering the estimate of viewing conditions.

Referring to Figure 6-17 it can be seen that there is a good deal of coherent interference in the noise, which could presumably be reduced by additional shielding, change of test site, etc. This reduction however has not been factored into the S/N measurements.

* This is an estimating number based on previous test experience. Using both an oscilloscope presentation and actual measurement of the rms value of a noise signal, it was found that the rms/ptp ratio can vary between 1/6 and 1/3 depending on the intensity level of the oscilloscope. It is felt that the use of 1/3 is a conservative estimate.

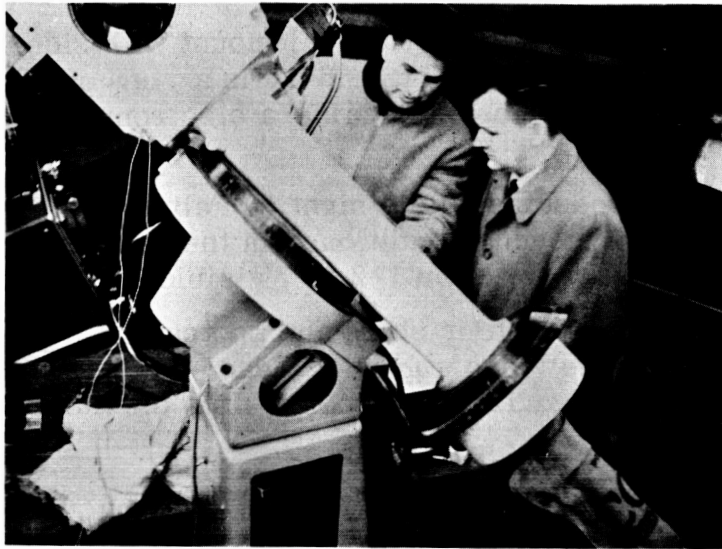


Figure 6-15. Equatorial Mount ATL Observatory



Figure 6-16. Space Sextant on Equatorial Mount

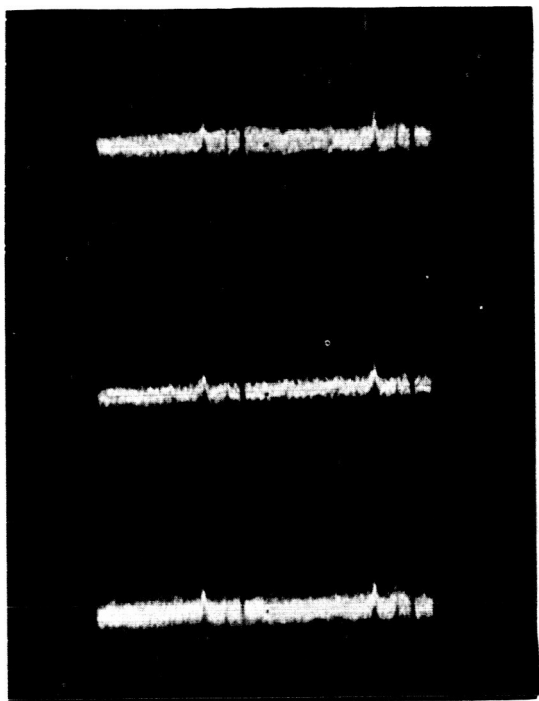


Figure 6-17. Canis Minor β

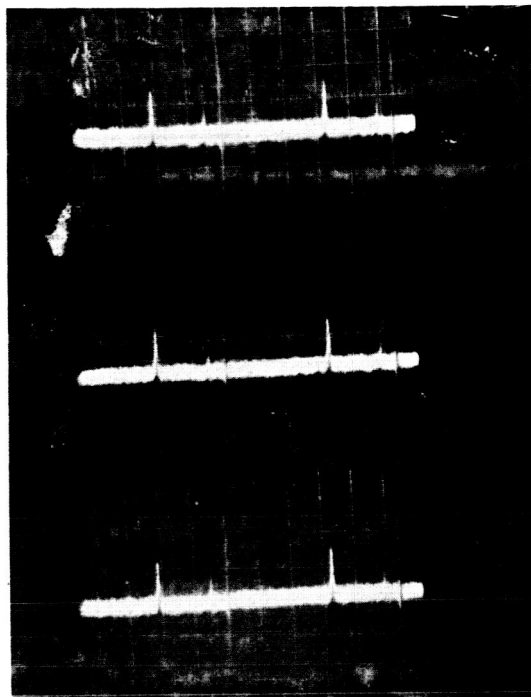


Figure 6-18. Ursa Major β

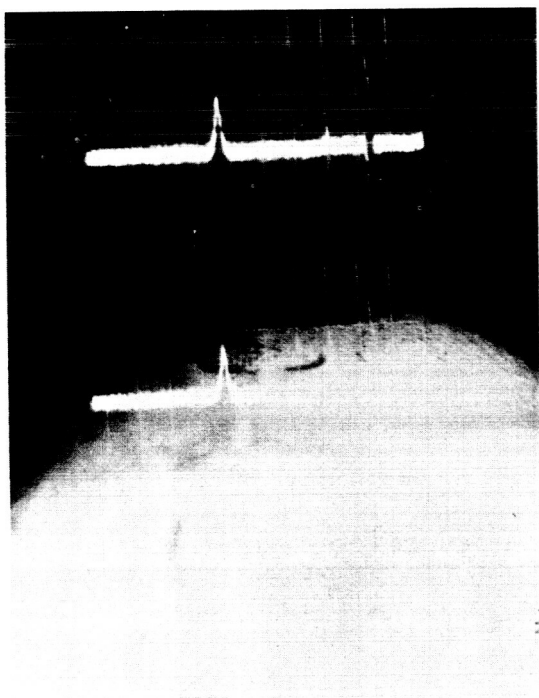


Figure 6-19. Orion ϵ

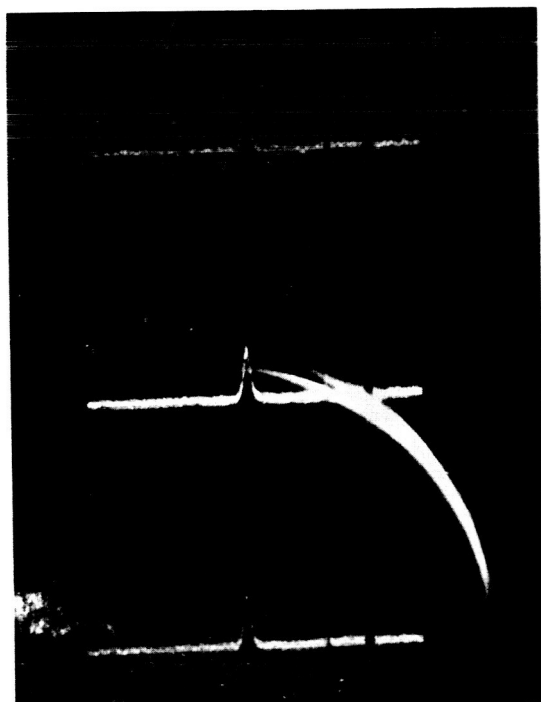


Figure 6-20. Orion α

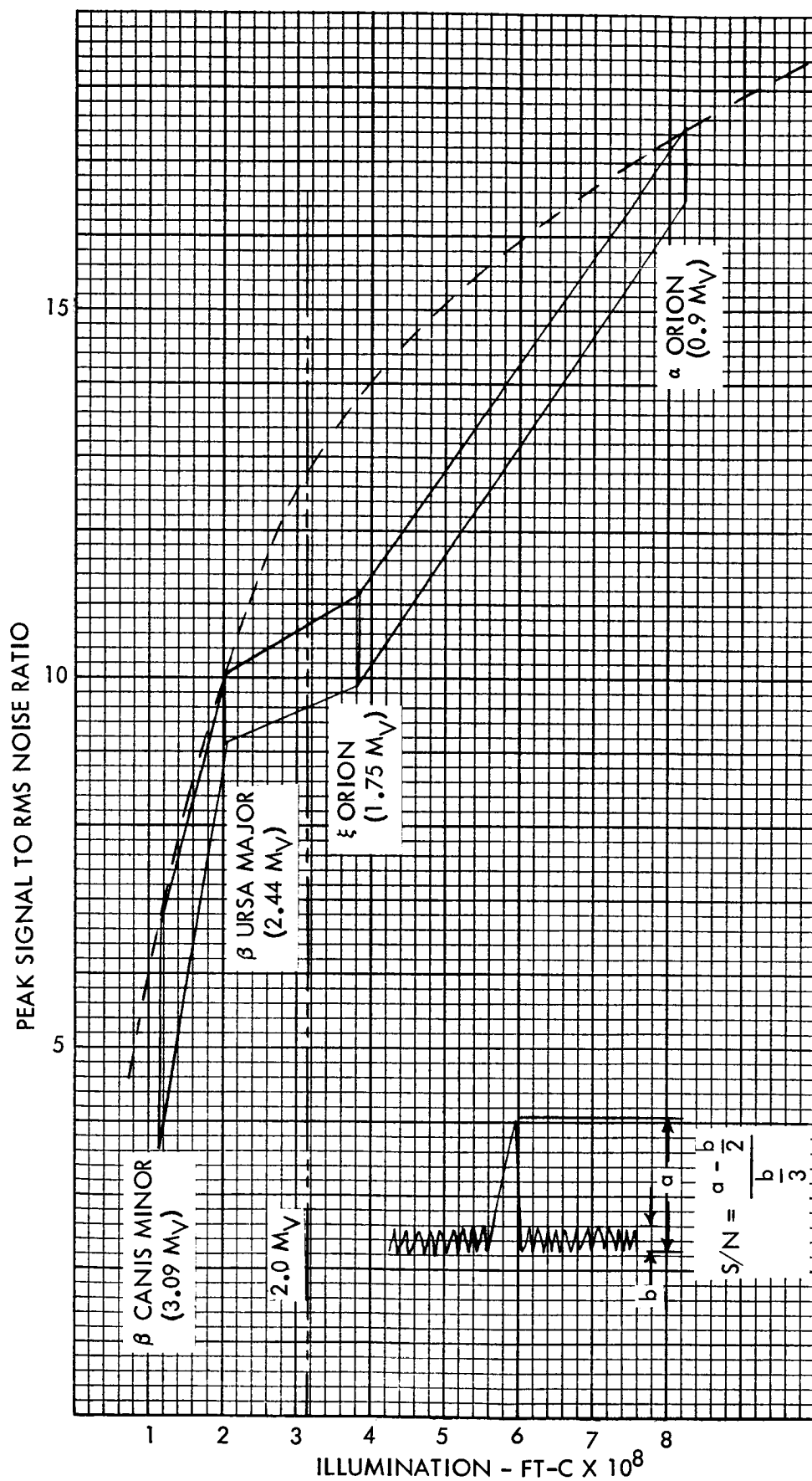


Figure 6-21. Photometric Test Results

The illumination level corresponding to a 2.0 M_v star is also shown in Figure 6-21. It is evident that a S/N ratio of 10/1 was achieved even on a conservative estimating basis.

OFF-AXIS ANGULARITY TESTS NARROW FIELD

The off-axis angularity accuracy tests were conducted in two steps.

- A. The optics/vidicon head mounted on the dividing head with the reticle lines parallel to the azimuth axis.
- B. The head mounted so that the reticle lines were parallel to the elevation axis.

The first setup was used to determine the X-axis accuracy (position along the T.V. raster lines). The second was used to determine the Y-axis accuracy (determination of the T.V. raster line passing through the center of the image).

The target used was the arc lamp, pinhole and collimating mirror, previously described.

Due to the uneven dark current level experienced in the video signal, even after processing through the noise cancellation circuits, it proved difficult to detect all reticle patterns reliably. In particular the diagonal reticles, which control the Y sweep correction, were detected intermittently. As a result it was necessary to run with X-axis correction only. This difficulty is discussed more fully in the Introduction and T.V. Camera Sections.

For comparison purposes, however, the Y-axis tests were run without correction.

Figure 6-22 illustrates the location of the test points on the vidicon target.

The ratios relating the angular displacement to the vidicon target coordinates are defined as:

$$M_x = \frac{\theta}{dp_x} = 2.415 \quad (1)$$

$$M_y = \frac{\theta}{dp_y} = 2.506 \quad (2)$$

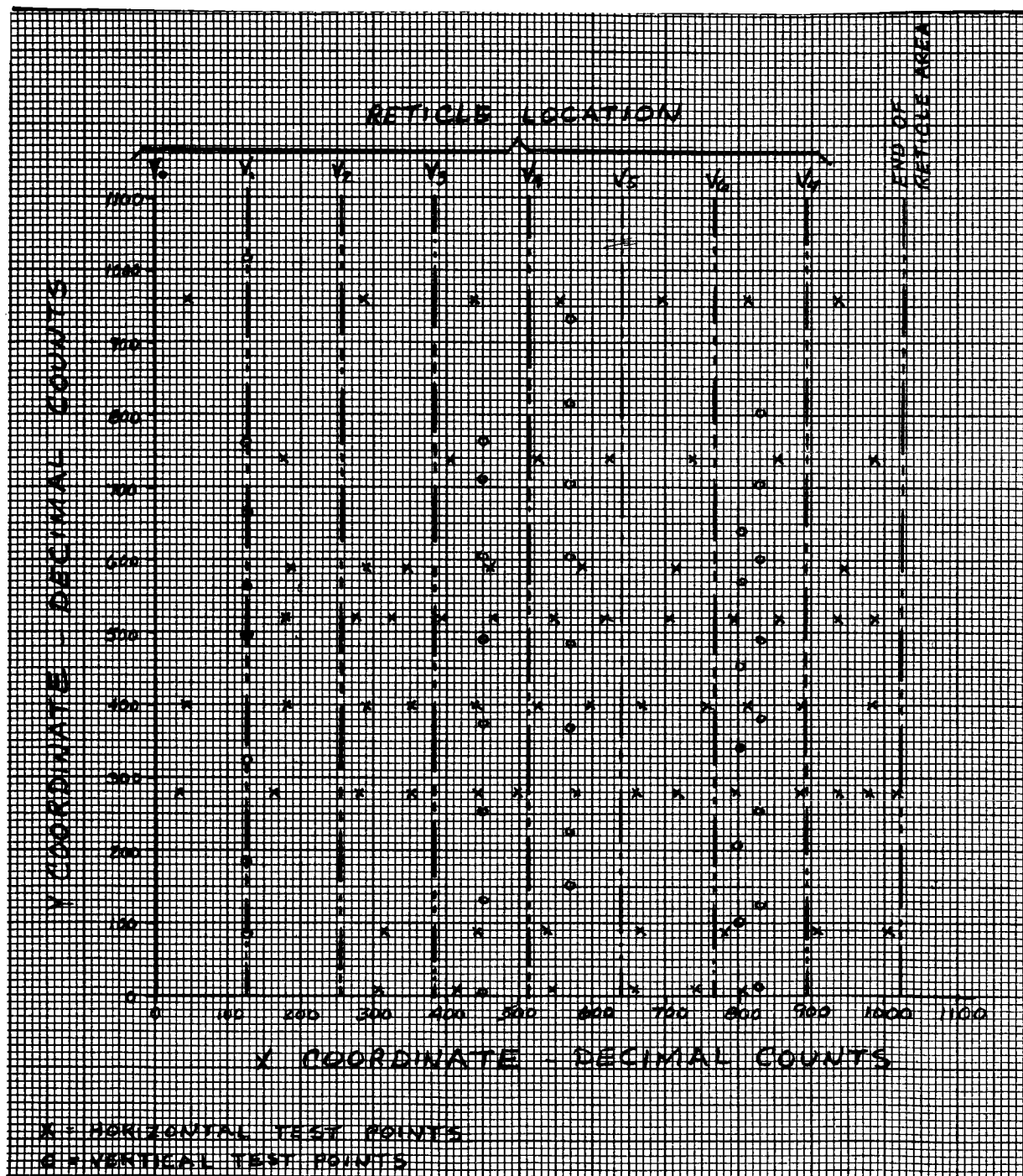


Figure 6-22. Test Point Location X & Y Angular Accuracy Tests

Where: θ is the displacement angle in arc-seconds

dp_x is the X coordinate given by the data processor (converted to decimal)

dp_y is the Y coordinate (decimal)

The values differ due to the fact that the Y tests were run with no reticle corrections. Using equations (1) and (2) the field of view represented by Figure 6-22 is *:

$$\theta_x = 2.415 \times 1024 = 2473 \text{ arc-seconds}$$

$$\theta_y = 2.506 \times 1024 = 2566 \text{ arc-seconds}$$

These values compare favorably with the predicted value of 2545 arc-seconds for a square raster in a 3600 arc-second circular field.

There are 111 test points shown in Figure 6-22, 73 for X tests and 38 for Y tests. At each test point 10 recordings were taken of the data processor readout, and were averaged.

The results of the X-axis tests are shown in Figure 6-23 sheets 1 and 2. These figures show the deviations of the angular readings, taken with the auto-collimator, from an ideal straight line with a slope of $M_x = 2.415$.

The bottom graph in Figure 6-23, sheet 2 illustrates the results of a brief statistical analysis of the results. The results generally follow a normal distribution curve with a standard deviation of approximately 4.2 arc-seconds. Checking the raw data tends to confirm this since 49 of the 73 test points, or 67.7% fall under the ± 5 arc-second limit.

The results of the uncorrected Y-axis tests are shown in Figure 6-24. The shape of these curves indicate the slight nonlinearity of the vidicon sweep which was not removed by the data processor. In general, as would be expected, these results do not follow a normal distribution. However, for purposes of comparison to the X results it is noted that 27 of the 38 test points, or 71% fall under a 16 arc-second limit.

It would therefore appear as a result of these tests that the X accuracy, with reticle correction, is 3 to 4 times better than the Y accuracy without correction.

* The vertical (Y) sweep was apparently fast, on the average. A given displacement took a shorter period of time and thus, produced a smaller coordinate count in the data processor.

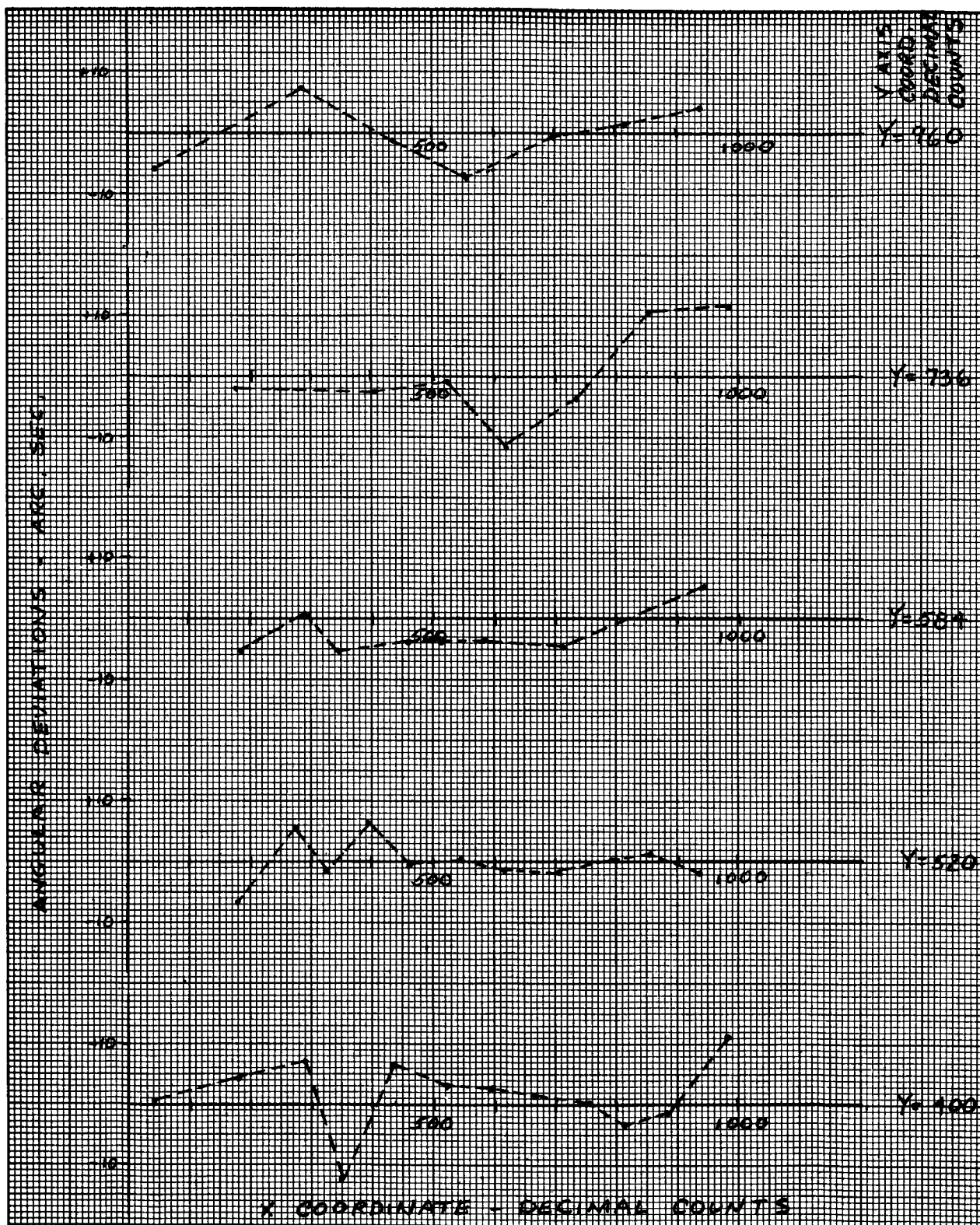


Figure 6-23. X-Axis Angular Accuracy Test Results (Sheet 1 of 2)

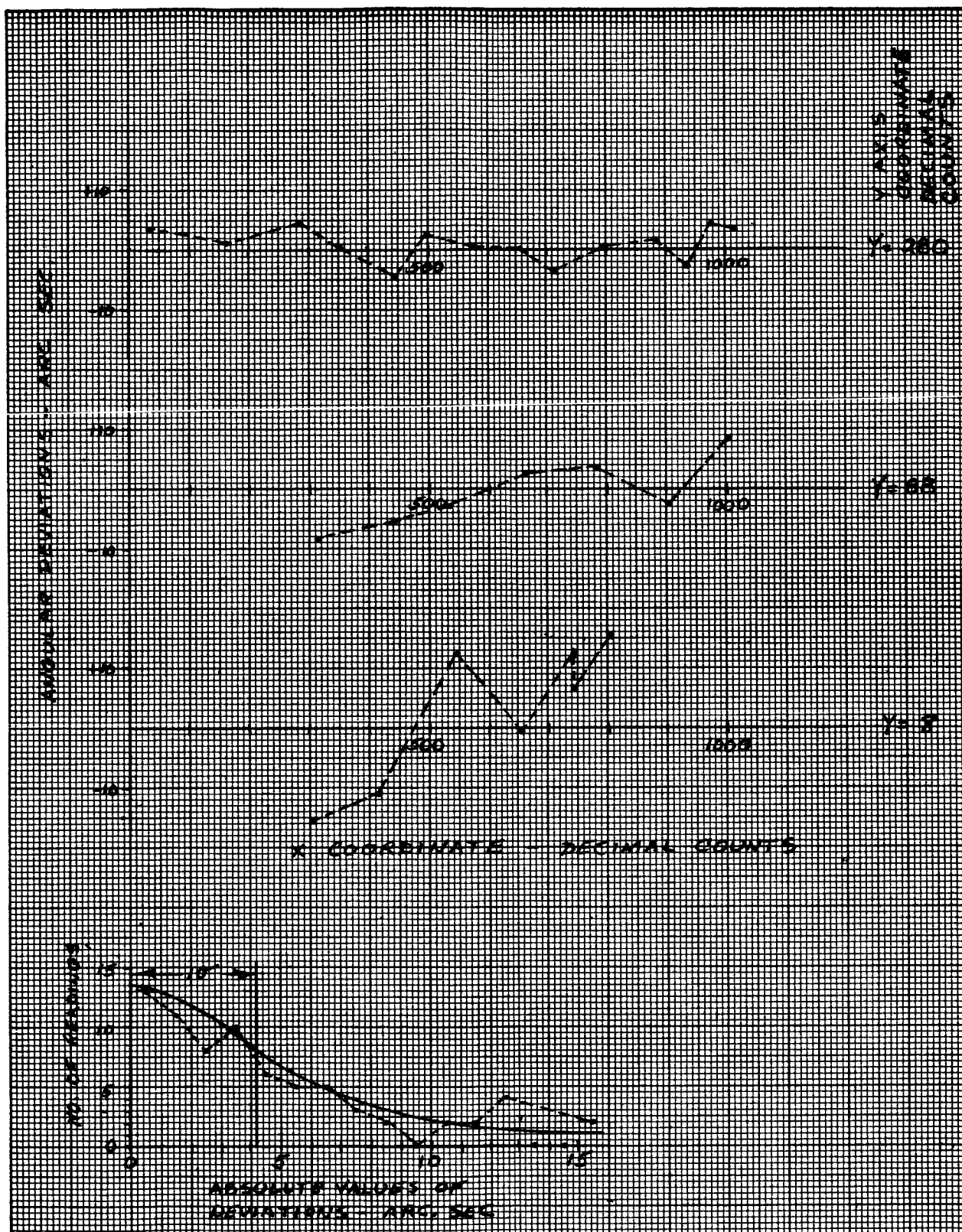


Figure 6-23. X-Axis Angular Accuracy Test Results (Sheet 2 of 2)

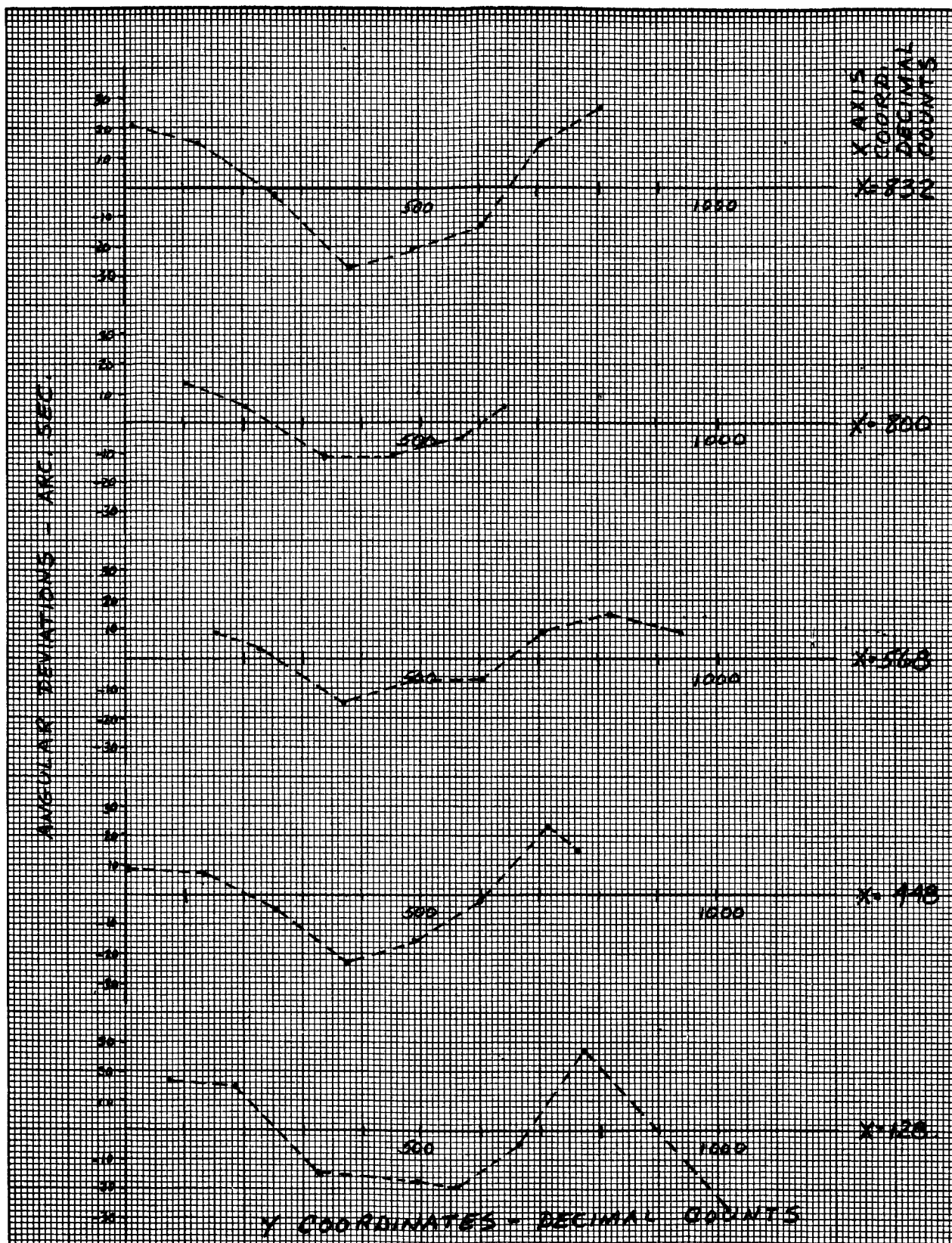


Figure 6-24. Y-Axis Angular Accuracy Test Results

EXTENDED IMAGE TESTS - WIDE FIELD

Angle Transfer and Image Quality Tests - Wide Field

Extended image tests, as opposed to point image tests, were run using the wide mode optics with an illuminated half-disc target as shown in Figure 6-25.

² This test setup is almost identical to that described in the interim report² and is mentioned further in the wide mode photometric test results later in this section.

The optics/vidicon assembly was mounted on the optical dividing head, previously described, and the off-vertical angles read directly from the dividing head's dials.

Three series of tests were conducted

- o 0° off-vertical (boresight)
- o 5° off-vertical (boresight)
- o 10° off-vertical (boresight)

To allow the two-dimensional target to correctly represent a spherical body presentation it was necessary to translate the target to a new position for each off-vertical angle so that the optical boresight passed through the center of the target.

In order to test the transfer function of the optics on a specific point on the disc edge, such as point B in Figure 6-25, it is necessary to determine the angle to this point, α in Figure 6-26, as a function of the off-vertical angle θ .

Referring to the geometry of the setup as given in Figure 6-26, it can be shown that the desired relationship is:

$$\cot \alpha = \frac{d}{R} \frac{1}{\cos^2 \theta} - \tan \theta$$

Where $d = 6.75$ inches
 $R = 17.75$ inches

²Reference 2 pp 36-42

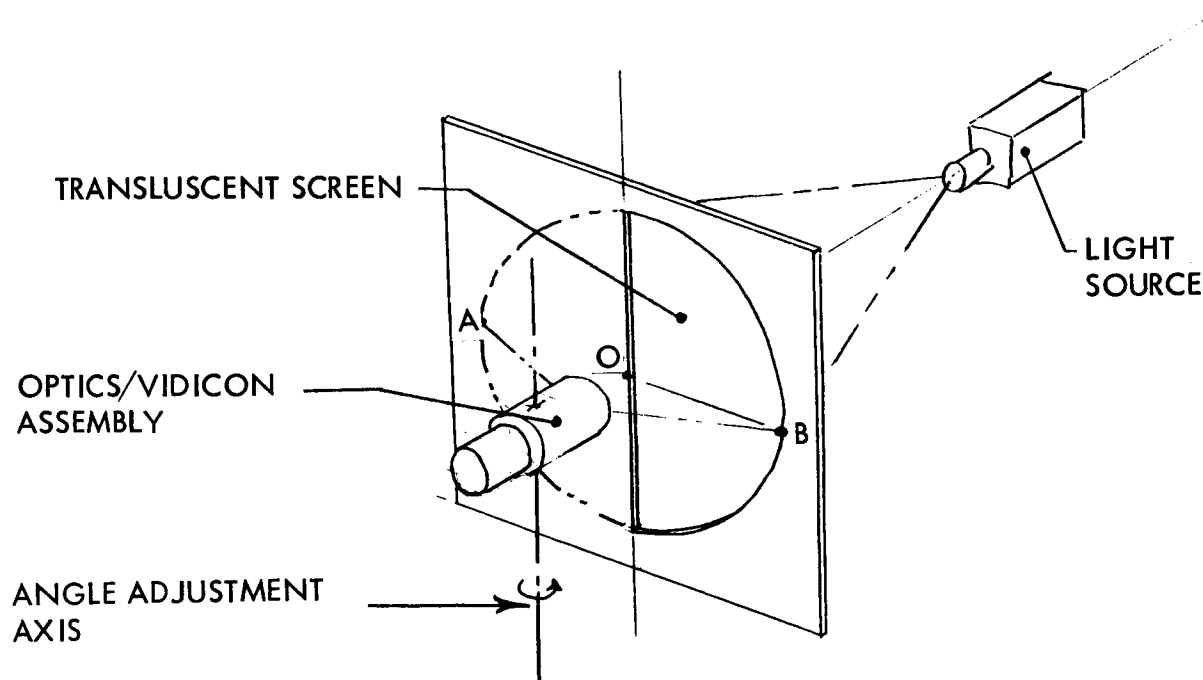


Figure 6-25. "Half-Moon" Wide Angle Test

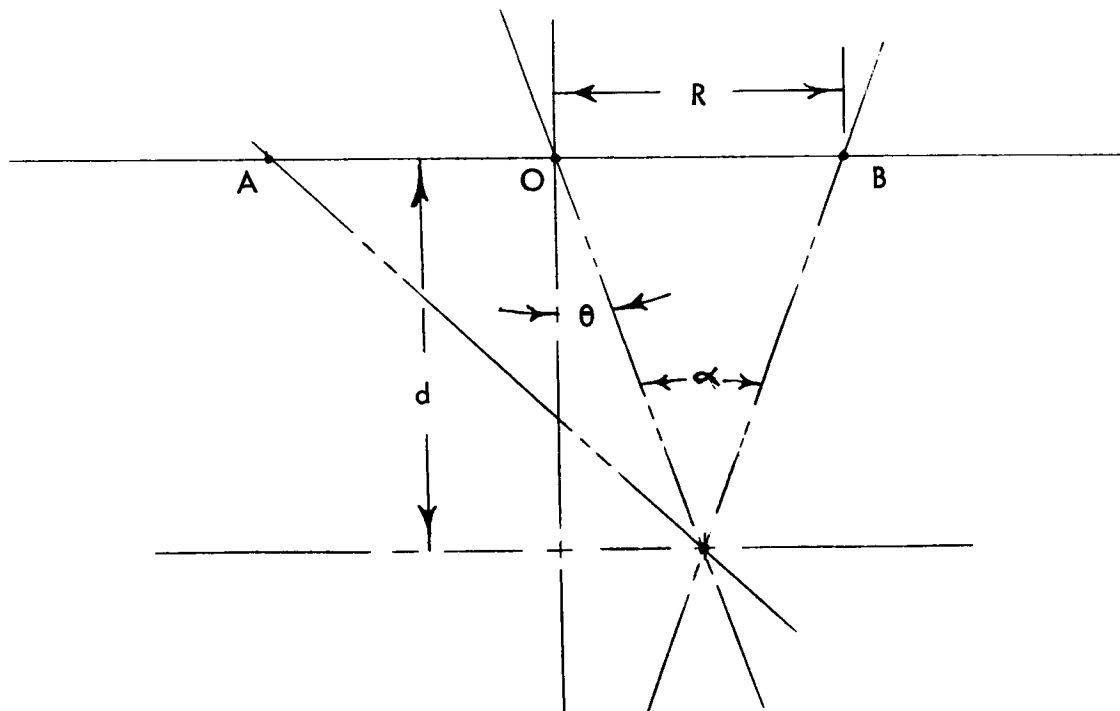


Figure 6-26. Off-Axis Angle Relationships

At the three test points employed the desired values of α are given in Table 6-3 below.

TABLE 6-3

θ	α	
0	69°	11'
5	73°	31'
10	77°	50'

For each off-vertical condition a series of test points were run to determine the resulting image on the vidicon target. For these test points the vertical, Y, target coordinate was selected manually on the data processor's control panel and both the X and Y coordinates of the point were obtained from the data processor's readout display.

At each of the test points, 10 readings were taken and averaged.

Figure 6-27 is a photograph of the oscilloscope presentation of the edge crossing data sent from the T. V. camera electronics to the data processor for the boresight test. This is not a complete video presentation so that the area to the right of the edge crossing is dark rather than bright. The displacement of the terminator towards the outer edge of the raster illustrates the radial inversion of the wide field optics.

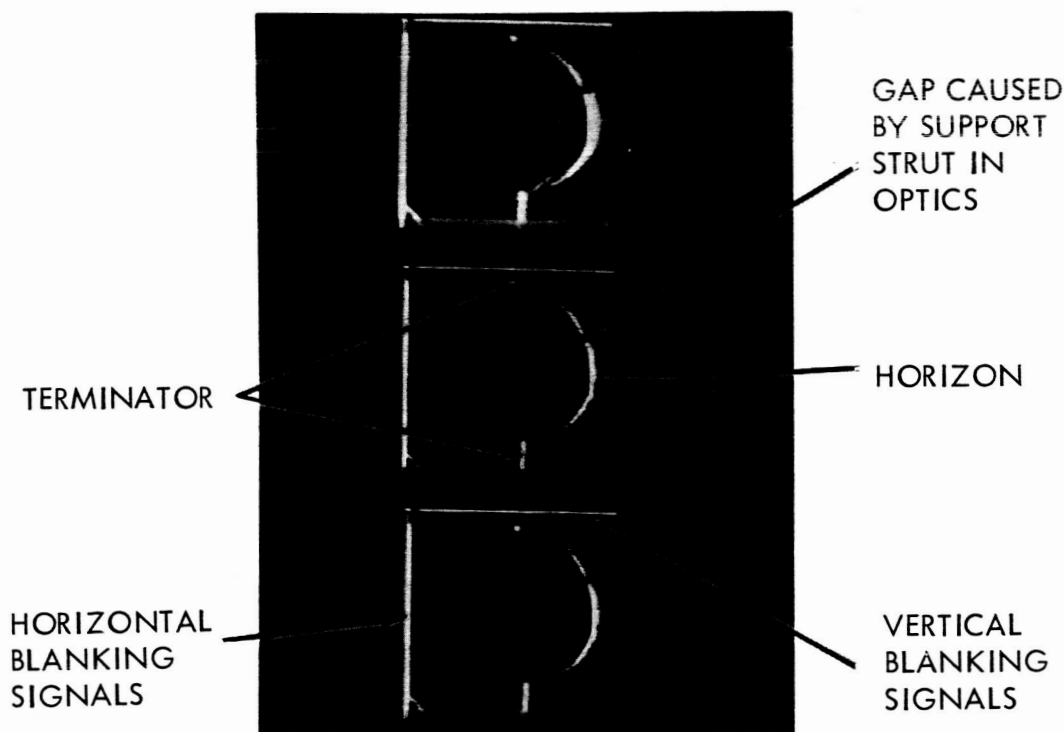


Figure 6-27. Data Processor Input, Wide Mode Boresight Test (Oscilloscope Test)

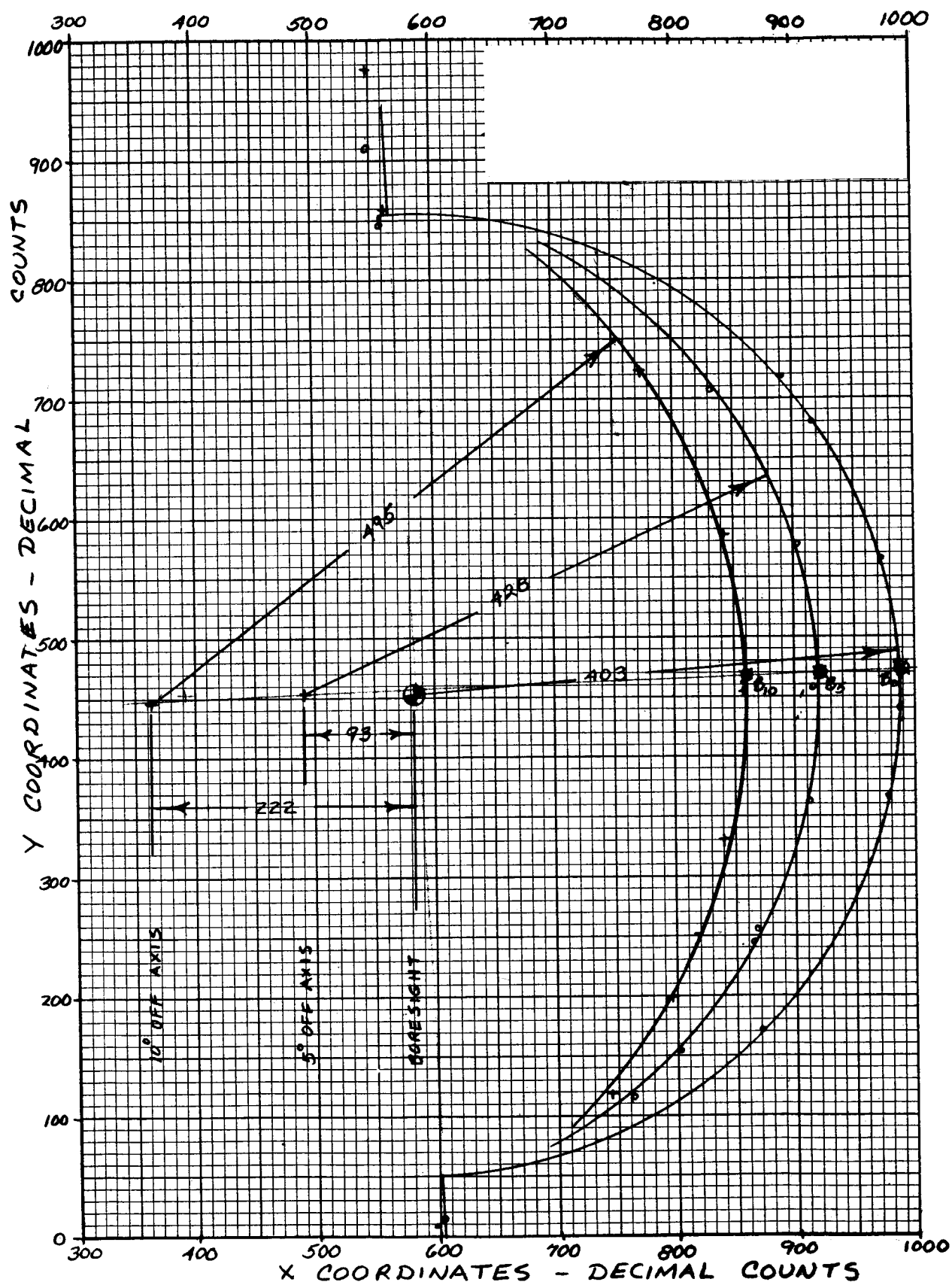


Figure 6-28. Disc Images Wide Mode Optics

The horizontal width of these signals is caused by the action of the pulse center detector on a disc edge crossing. The data processor uses only the leading (left-hand) edge of these signals.

Figure 6-28 is a graph of the vidicon target images obtained by plotting the X and Y coordinates for the test points.

The boresight image is circular with a center calculated to be at the point $X = 584.8$, $Y = 450.2$ with a radius of 402.7.

The images for the two off-vertical tests are elliptical, as expected. However the eccentricity of these ellipses is sufficiently small, for the angles used, that to a close approximation they can be described by circles with centers and radii as shown in Figure 6-28.

Figure 6-29 illustrates the shift of the image centers as a function of off-vertical angle. It is interesting to note that this relationship is non-linear and tends to amplify the shift. This was anticipated in the analysis covered by Memorandum No. 8.³

Figures 6-30, 6-31 and 6-32 illustrate the test point deviations from the assumed circular images. The polar angles in these figures are used as a convenient tool to locate the test points along the image. These angles are not related in any way to the off-vertical angle.

The edge crossing points B, of Figures 6-25 and 6-26 are shown in the target images in Figure 6-28. Using the results of Table 6-3 these points are plotted as a function of off-boresight radius in Figure 6-33.

As a result of previous analysis⁴ a transfer function for the wide angle optics was developed in the form

$$\gamma = 90.19 - 136.3r - 85.94r^2 \quad (4)$$

Where: γ is the off-axis angle in degrees

r is the position radius of the image in inches

Using this relationship a second set of points is plotted in Figure 6-33.

Comparison of the two lines indicates the need for a calibration procedure to eliminate the bias shift. In other respects however the agreement between predicted and actual results appears satisfactory.

³Reference No. 11

⁴References No. 16 and 17

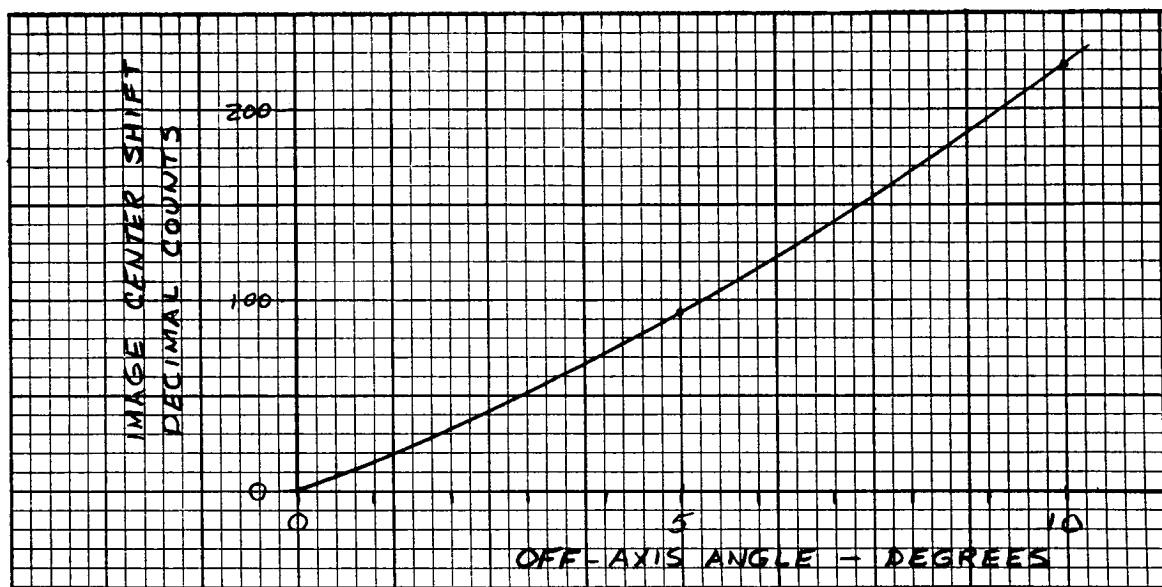


Figure 6-29. Image Shift vs Offset Angle

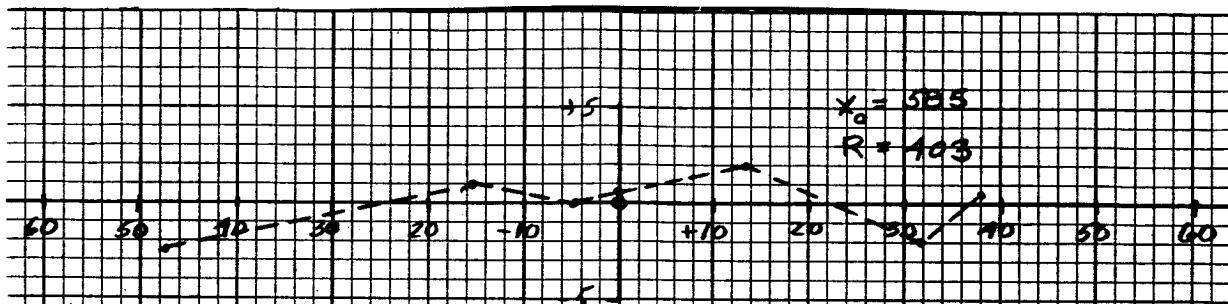


Figure 6-30. Deviations from Circle-Boresight

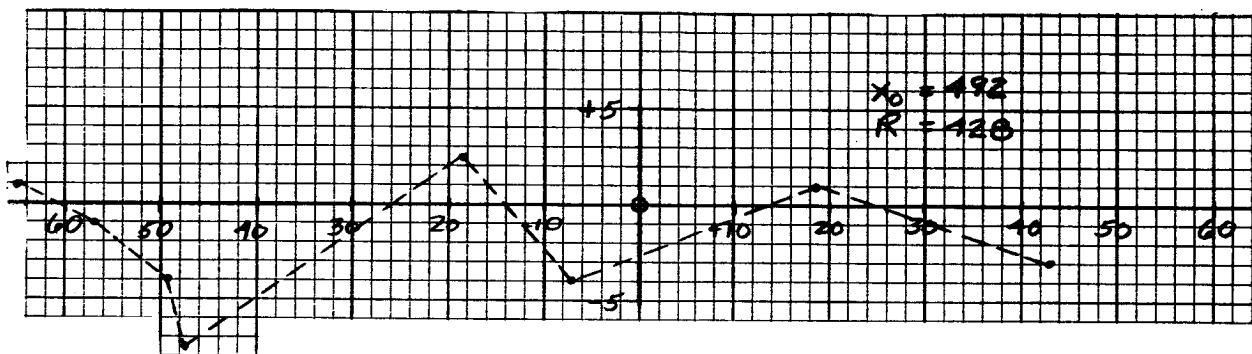


Figure 6-31. Deviations from Circle-5° Offset

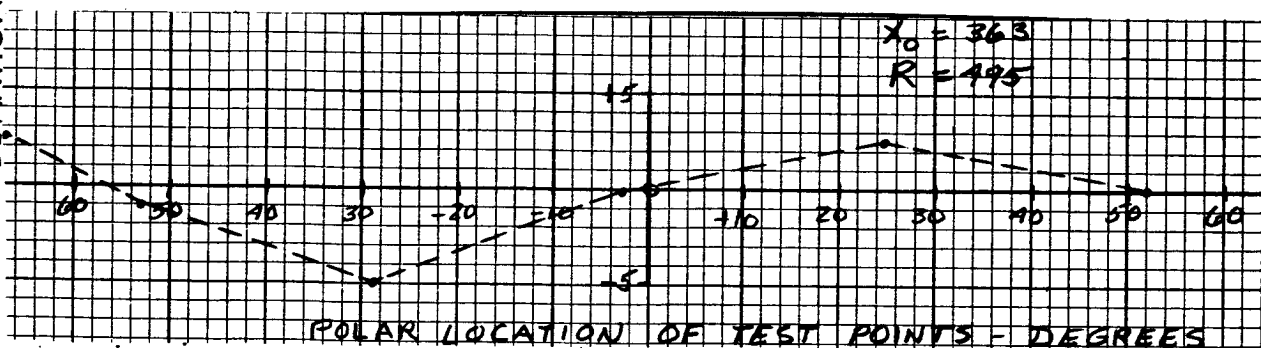


Figure 6-32. Deviations from Circle-10° Offset

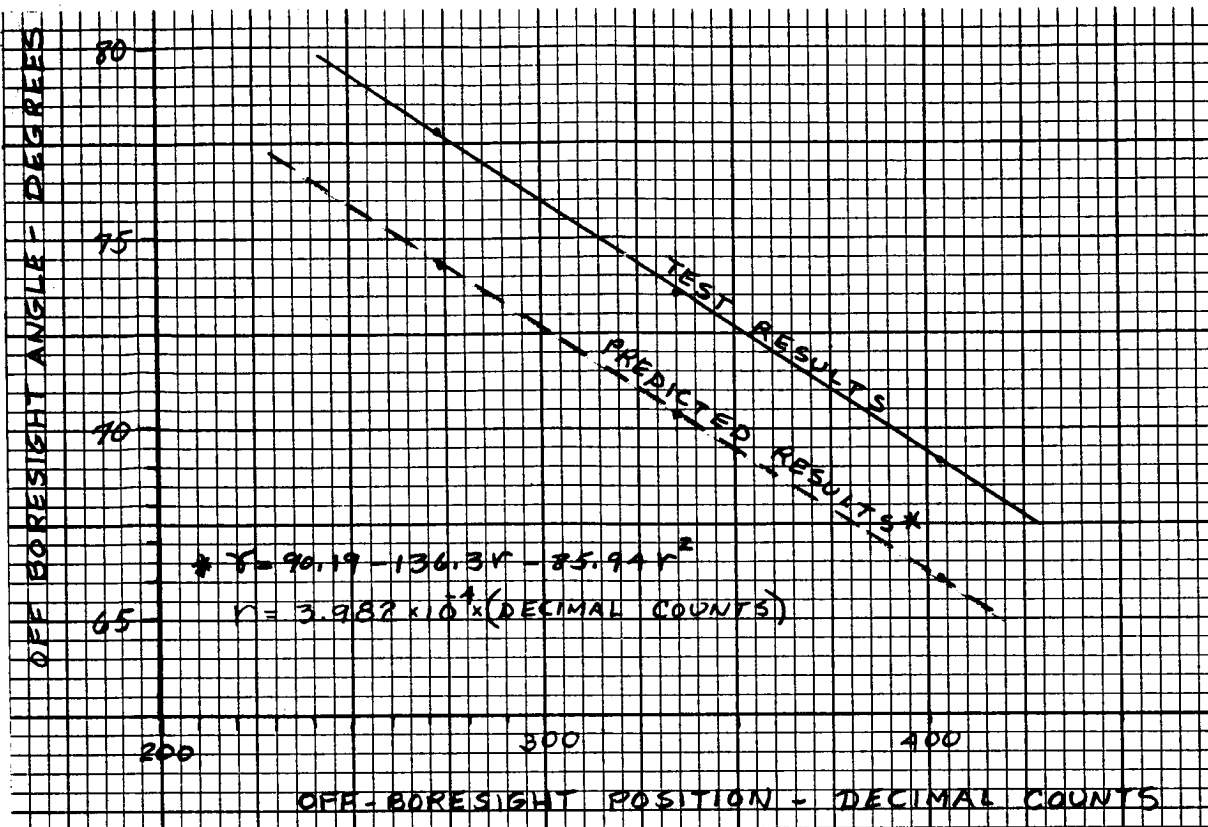


Figure 6-33. Image Location vs Off-Axis Angle Edge Crossing "B"

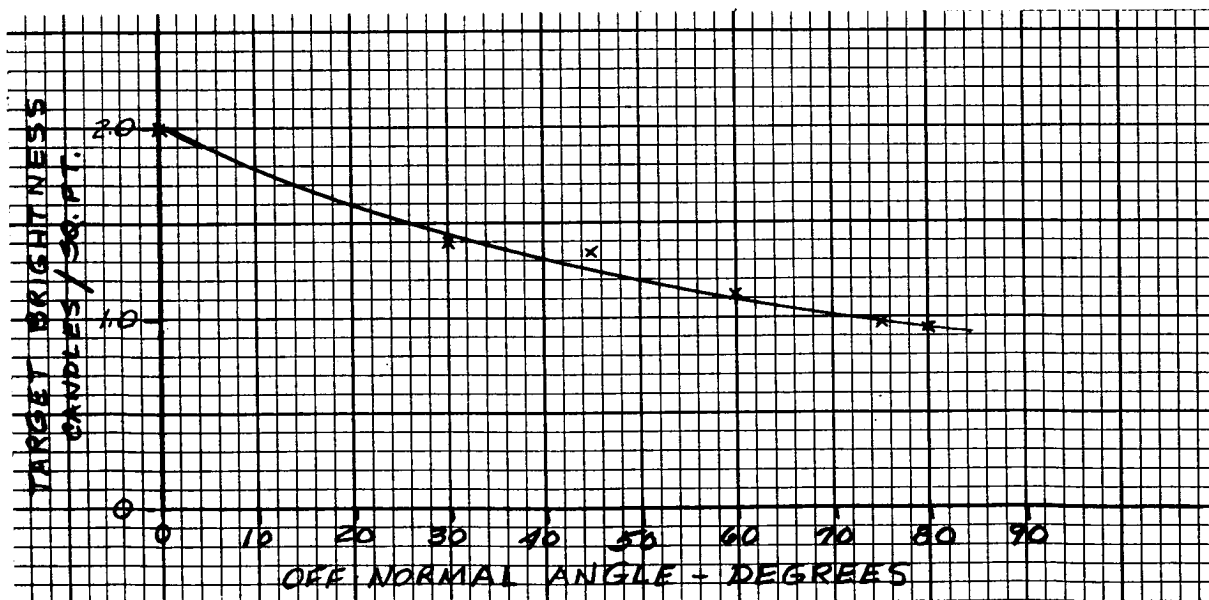


Figure 6-34. Brightness Measurements Wide Angle Target

Photometric Tests - Wide Field

Using a MacBeth Illuminometer the brightness of the extended disc target was determined to be approximately 2.0 candles/sq ft for a normal reading. Since the surface is non-lambert, off-normal readings fall below this value. The relationship determined by these tests is shown in Figure 6-34.

The video signal at the output of the video amplifiers (input to the pulse center detector circuits) is shown in Figures 6-35A and B. Both figures are for the boresight condition so the edge crossings occur at approximately 69° off-axis. Referring to Figure 6-34 this point had a brightness of approximately 1.0 candles/sq. ft.

Figure 6-35A is a raster line approximately $3/7$ of the distance up the raster. This signal was obtained with the reticle illumination turned on and the reticle lines are apparent in the picture. The estimated peak signal to rms noise ratio is $8/1$.

Figure 6-35B is a raster line approximately $1/2$ of the distance up the raster. This signal was obtained without reticle illumination. The estimated peak signal to rms noise ratio is again $8/1$.

To relate Figure 6-35A and B to Figure 6-28 the reversal of the oscilloscope camera must be accounted for and the video signals read from right to left.

Since the specification target for the wide angle system is the moon, which has a minimum brightness of approximately 37 candles/ft.^2 across a phase-angle range of 135° - 0° - 315° , the system has more than adequate sensitivity.

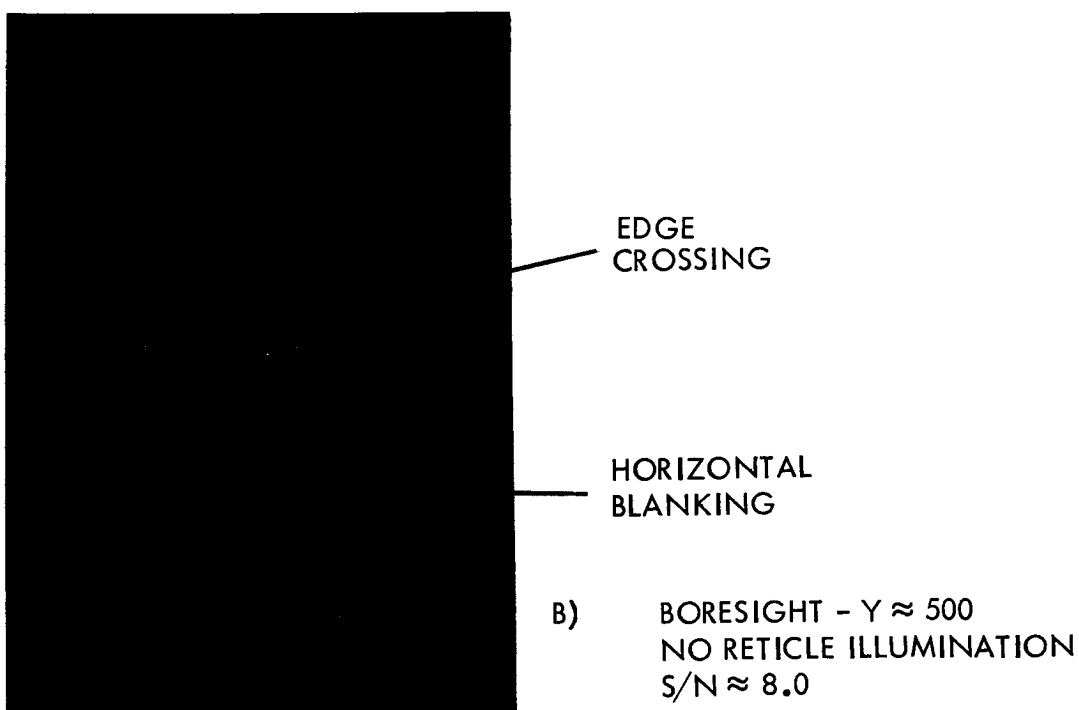
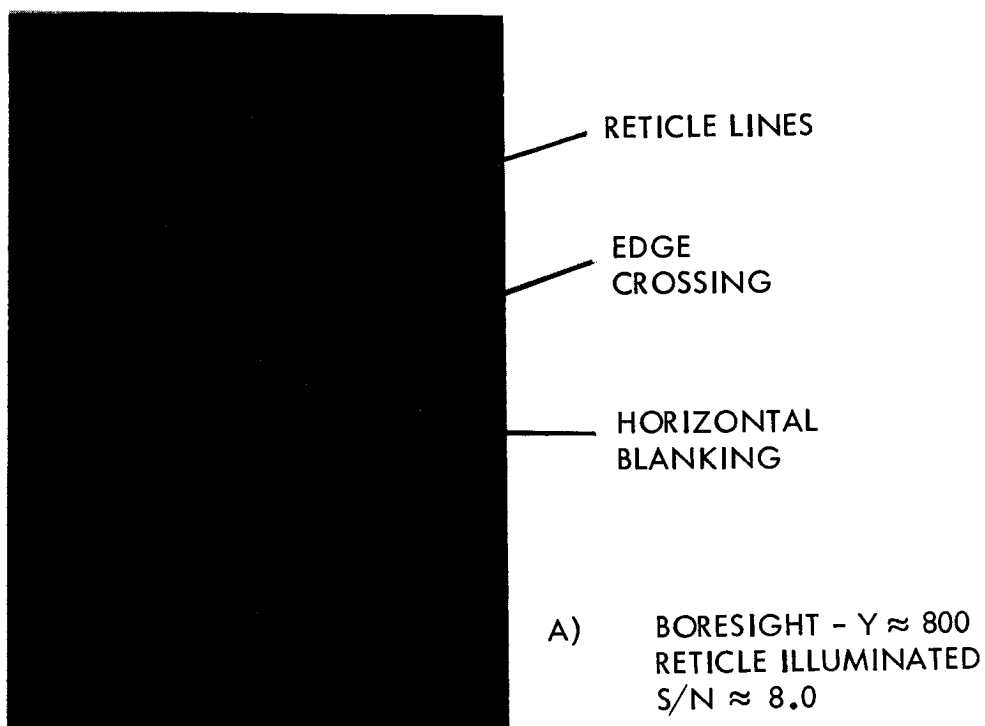


Figure 6-35 Video Signals - Wide Mode Tests

REFERENCES

1. Brunelle, H.E., Willey, R.R., Jr., "Coaxial Dual Field Optics for a Space Sextant," Applied Optics, Vol. II; No. 12; (December 1963), pp. 1265-1269 .
2. Optical- Inertial Space Sextant for an Advanced Space Navigation System-Program Progress Report, 7 January to 10 April, 1963; Contract No. NAS2-1087, Control No. 37974001.
3. Foley, W.D., Alignment and Initial Evaluation of Company Funded Optics for Space Sextant Project Memo No. 2, 13 February, 1963.
4. Welch, J.D., Preliminary Performance Specifications of Optics, Project Memo No. 3, 15 February, 1963.
5. Rosenberg, N., Extreme Wide-Angle Optics for Space Sextant Applications, Project Memo No. 3A, 4 March, 1963.
6. Foley, W.D., Discussion of Readout-Narrow Field-of-View, Project Memo No. 5, 10 May, 1963.
7. Merz, D.M., Determining Star Coordinates Within a Frame, Project Memo No. 6, 22 May, 1963.
8. Merz, D.M., Minimum Computer for Processing Noise-Free Tracker Data, Project Memo No. 7, 10 June, 1963.
9. Merz, D.M., Minimum Computer for Processing Noise-Free Tracker Data, Project Memo No. 7A, 1 July, 1963.
10. Colter, G.J., Sweep Circuit Development for Vidicon Star Tracker, Project Memo No. 7B, 8 July, 1963.
11. Foley, W.D., Study of Target and Image Characteristics, Project Memo No. 8, July 1963.
12. Welch, J.D., Application of an Orthogonal Scan System For all Space Sextant Modes of Operation, Project Memo No. 9, 27 August, 1963.
13. Barber, W.D., Camera Tube Reticles, Project Memo No. 10, 23 September, 1963.
14. Brunelle, H.E. Neutral Density Filter for Space Sextant, Project Memo No. 11, 14 October, 1963.
15. Welch, J.D., Techniques for Utilizing Space Sextant Data in a Self-Contained Space Navigator Project Memo No. 13, 8 January, 1964.
16. Gates, W.D., Geometric Optics - Test Results, Project Memo No. 14, 30 December, 1963.

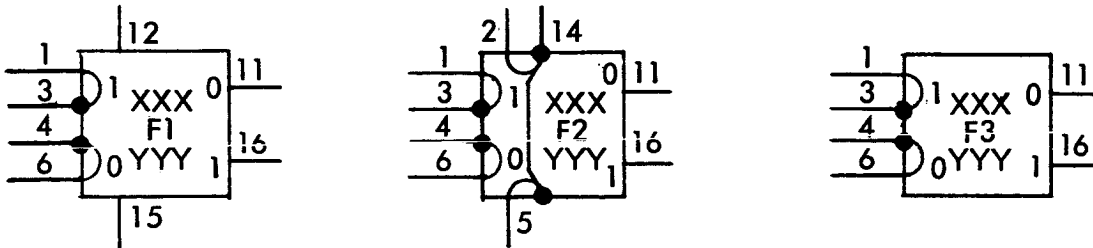
REFERENCES (Cont'd)

17. Foley, W.D., Optical Transfer Function Space Sextant Optics, Project Memo No. 15, 21 January, 1964.
18. Gates, W.D., Evaluation Tests -Vidicon Reticle Pattern, Project Memo No. 16, 7 January, 1964.
19. Foley, W.D., Calibration of Lab "Star" Light Source, Project Memo No. 17, 13 January, 1964.
20. Welch, J.D., An Advanced Optical-Inertial Space Navigation System, Paper presented at the annual summer meeting of the American Institute of Aeronautics and Astronautics, Los Angeles, Calif, 17 June, 1963.

APPENDIX I

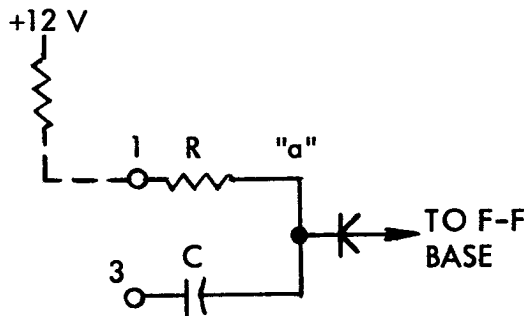
LOGIC ELEMENTS

All memory in the data processor is mechanized with flip flops. Although there are three types of circuits used two are logically equivalent, and the third is quite similar. The three symbols are:



XXX is the flip flop name and YYY is its location; board, row, column. F1 and F3 are logically equivalent, the difference lying in the speed of the input gates and the power requirements.

These flip flops incorporate the basic R-S flip flop plus a pair (two pair for F2) of input "transmission" gates. These gates supply a second bit of storage momentarily thus permitting shift registers and counters with one flip flop per bit. The transmission gate circuit is:

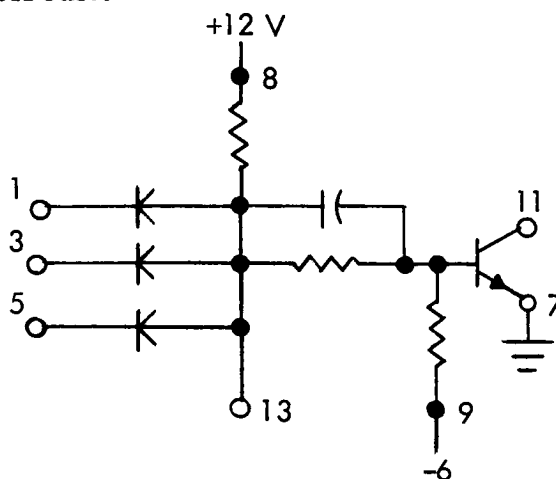


If pin one is grounded the signal on pin 3 is differentiated and the "ground-going" (negative here) portion is sent to the flip flop base, changing its state. If pin one is not shorted to ground, the external load resistor pulls pin one to +12v back biasing the diode and preventing signals from reaching the base. Note that before point "a" responds to a change on pin one, a finite time must pass. This time is determined by the product of R and C and this "integration" of the input effects the additional storage mentioned above. The integration also effectively blocks transient noise spikes on pin one from affecting the flip flop. Pin one's signal is called the "steering" and pin three's the "AC" input.

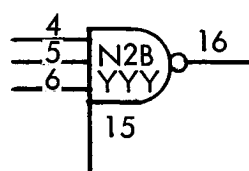
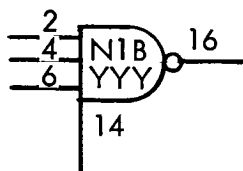
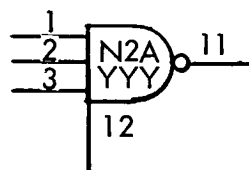
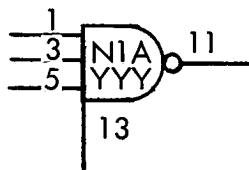
While the sketch shows the "set" transmission gate, the other gate's action is identical. The AC input is denoted by the black dot, the pin numbers being understood in many cases.

Throughout the discussions a short to ground is defined as a "one," and a grounded emitter transistor is in the "one" state when it is "on," i.e., conducting.

The above definition causes the following circuit to correspond to a logical "or" followed by an inversion or "not" circuit. This is commonly referred to as a "NOR" circuit.

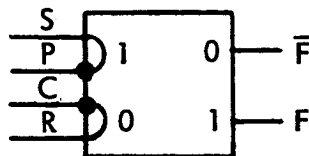
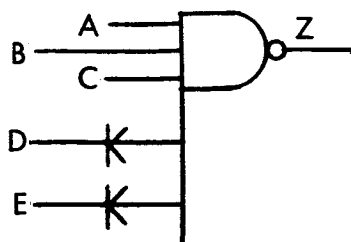


The symbols used for a NOR circuit are:



The circuit for the N2 is logically equivalent to that of the N1. The difference lies in the speed of operation. The N1 cubes include 3.9K resistors connected from pins 12 and 15 to the +12v supply internally. Thus if a NOR feeds a transmission gate, pins 11 and 12 will be tied together. This is denoted by an L placed above the NOR's output.

The logical equations for the NOR and flip flop are:



$$Z = \overline{A} \cdot \overline{B} \cdot \overline{C} \cdot \overline{D} \cdot \overline{E} \cdot \dots$$

$$F_i = S \cdot P + F_{i-1} \cdot \overline{R \cdot C \downarrow}$$

$$(S \cdot P \downarrow) \cdot (R \cdot C \downarrow) \equiv 0$$

where \downarrow signifies going to ground.

The inverter is merely an inverting power amplifier which fully utilizes the entire NOR output. The shift-driver is an inverter with an additional transistor to pull the output back positive, rapidly. The bias net or coupling net performs no logic function.

APPENDIX II

GEC 7522 VIDICON

The GEC 7522 electrostatic focus and deflection vidicon was designed to provide a small pickup tube requiring low operating power in equipment of minimum size and weight. Deflection is accomplished by a Deflectron, a revolutionary electrostatic deflection device. Resolution of 500 lines is obtained with 300 volts beam acceleration. Power requirements and operating voltages are designed for operation with completely transistorized circuits.

DATA

GENERAL:

Operating Position	Any
Focusing Method	Electrostatic
Deflection Method	Electrostatic
Maximum Useful Image Area Diagonal measurement of 4 x 3 aspect ratio	0.625 in.

ELECTRICAL CHARACTERISTICS:

Heater Voltage (AC or DC)	$6.3 \text{ V} \pm 10\%$
Heater Current	0.3 A
Spectral Response (See Fig. 4)	S-18
Direct Interelectrode Capacities	
Signal Electrode to all others	4 uuf
D1 to D2 (Horizontal Plates)	6 uuf
D3 to D4 (Vertical Plates)	6 uuf

ABSOLUTE MAXIMUM RATINGS:

Grid No. 1 Voltage	
Negative Bias	300 V
Positive Bias	0 V
Heater to Cathode Peak Voltage	
Heater Negative with Respect to Cathode	125 V
Heater Positive with Respect to Cathode	10 V
Grid No. 2 Voltage	750 V



ABSOLUTE MAXIMUM RATINGS, Continued:

Faceplate	
Illumination	1000 ft-c
Temperature	71° C.
Signal Electrode Current	0.6 uA

TYPICAL OPERATION:

Scanned Area	0.500 x 0.375 in.
Faceplate Temperature	30° to 35° C.
Optimum Signal Output Current	
(Less Dark Current, with uniform 2870° K Tungsten illumination on faceplate.)	
5 ft-c and greater	0.2 uA
0.2 to 0.5 ft-c	.05 to .1 uA
Signal Electrode Voltage	20 to 100 V
Average Gamma of Transfer Characteristic over Signal Output Current Range of .05 to 0.2 uA	.55
Grid No. 5 Voltage	300 V
Focus Electrode Voltage	0 to 50 V
Grid No. 2 and Grid No. 4 Voltage	200 V
Grid No. 1 (For signal cutoff with no blanking on G1)	-45 to -100 V
Minimum Blanking Voltage (Peak to Peak)	
When applied to Grid No. 1	30 V
When applied to Cathode	10 V
Deflection Voltages (Peak to Peak)	
Horizontal (D1 to D2)	60 V
Vertical (D3 to D4)	50 V
Horizontal Plates DC Voltage	200 V to 250 V
Vertical Plates DC Voltage	200 V to 250 V

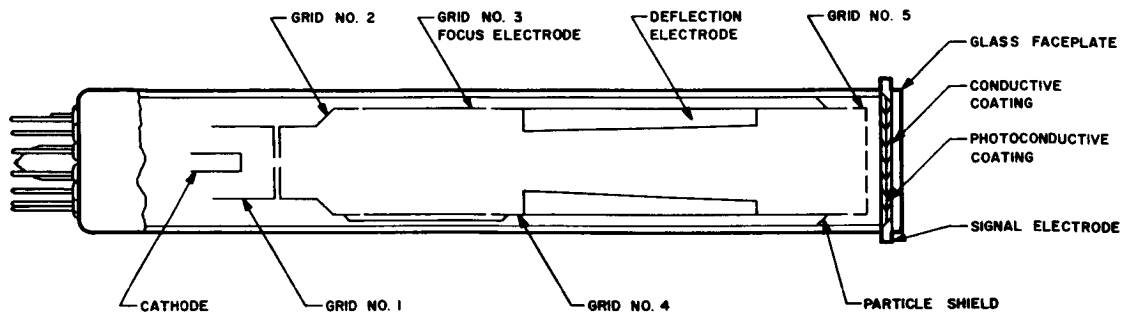


FIG. I

PRINCIPLES OF OPERATION

Basic Vidicon Operation

The GEC 7522 vidicon is a photoconductive imaging device using electrostatic focus and deflection. The vidicon faceplate inside surface is coated with a transparent conductive coating as shown in Figure 1. Over this a layer of photoconductive material is deposited. This material when dark is a reasonably good insulator but increases in electrical conductivity when exposed to light. The electron beam scans the back surface of this photoconductor.

In operation, the photoconductor front surface is held at a positive potential with respect to the cathode, by applying voltage to the transparent conductive coating. The scanning electron beam deposits a negative charge on the photoconductor back surface. Where the photoconductor is dark and its resistance high, a negative charge accumulates until the back surface reaches cathode potential.

Where light from the scene falls on the photoconductor, conductivity increases, reducing negative charge at the illuminated point. Negative charge reduction at any point is proportional to the illumination on that point. The photoconductor therefore becomes charged much like a capacitor in a pattern conforming to the scene image. As the electron beam scans the photoconductor, it will release electrons into the less negatively charged areas and the resultant varying electron flow through a load resistor constitutes the video signal.

The vidicon has the ability to store the image for an entire scanning cycle. The image is "photographed" in a pattern of varying charge on the photoconductor back surface and is accumulated there for one complete frame. By this process the vidicon produces usable signal output from dimly lighted scenes.

Field Correction

A special mesh electrode, G5, is incorporated in the 7522 to assure flat field output and to compensate for beam landing error and optical lens distortion. The potential of this mesh can be varied independently of the other electrodes.

Focus

Electrostatic focus is accomplished in a saddle field lens arrangement composed of G2, G3, and G4, with G3 as the variable focusing electrode.

Deflection

Electrostatic deflection in the 7522 is accomplished through the use of a specially designed deflection plate configuration called the Deflectron. The conventional crossed pair deflection plates causes the electron beam to be deflected sequentially; that is,

PRINCIPLES OF OPERATION, Continued:

in passing between the first set of plates it is deflected in one plane and then when reaching the second set of plates is deflected in the other plane. The Deflectron causes the beam to be deflected both horizontally and vertically simultaneously as in magnetic deflection. This common center of deflection reduces the undesirable effects of fringe fields, defocusing and other distortion found in conventional deflection plate scanning.

Physically the Deflectron is a tube of insulating material, the inside of which contains the printed deflection plate pattern. The pattern of the Deflectron is illustrated laid out on a flat plane in Fig. 2. If the pattern is rolled to connect Side A to Side B, four individual electrical paths can be traced.

OPERATING CONSIDERATIONS

Installation

The GEC 7522 may be operated in any position, however, it must be oriented to place the horizontal deflection axis parallel to the horizontal image plane. The horizontal deflection axis is essentially parallel to a line through base pins 2 and 9. (See Fig. 7) The 13 pin socket for the 7522 is Type GEC 52-01 or equivalent.

Shielding

The 7522 should be shielded during operation from the effects of stray magnetic or electrostatic fields by the use of a suitable magnetic shield.

Deflection Circuits

The 7522 may be driven by standard electrostatic deflection circuits incorporating DC centering. The Deflectron elements are operated at a variable DC potential of from 200 to 250 volts positive with respect to cathode that will permit critical adjustment for minimum astigmatism.

Video Amplifier

The video amplifier design for use with the 7522 should incorporate all of the characteristics of an amplifier for a standard vidicon - low noise, high gain, aperture correction and high peaking. A typical transistor video preamplifier is shown in Fig. 3.

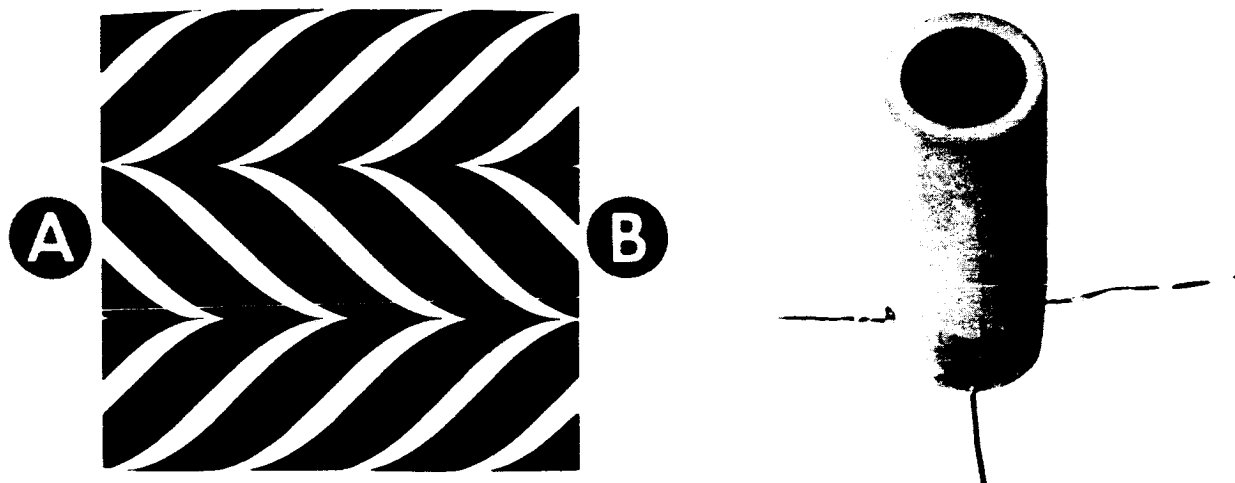


FIG. 2

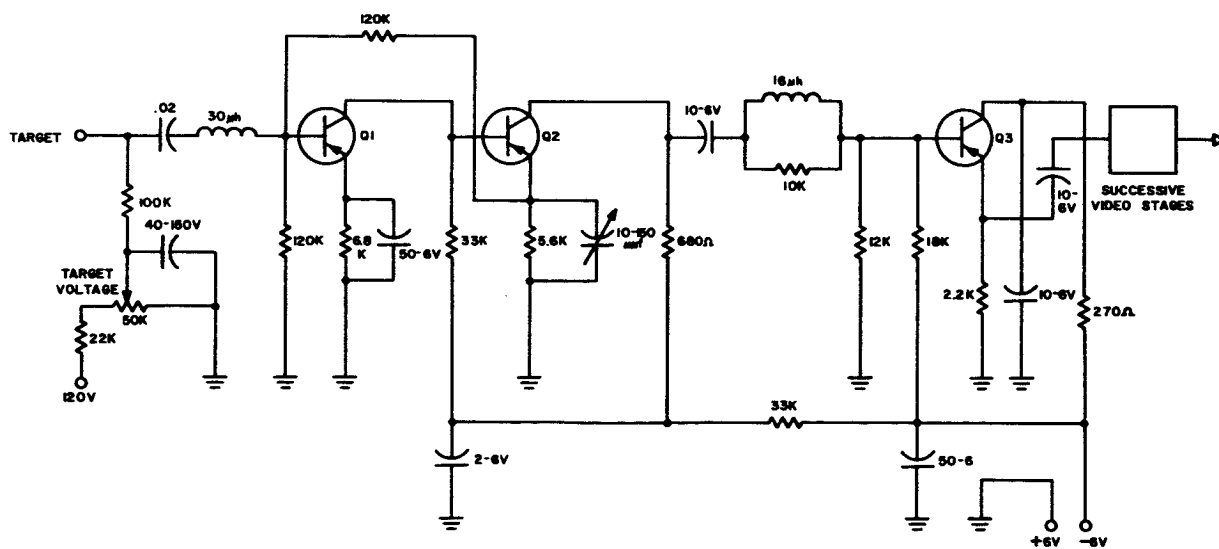
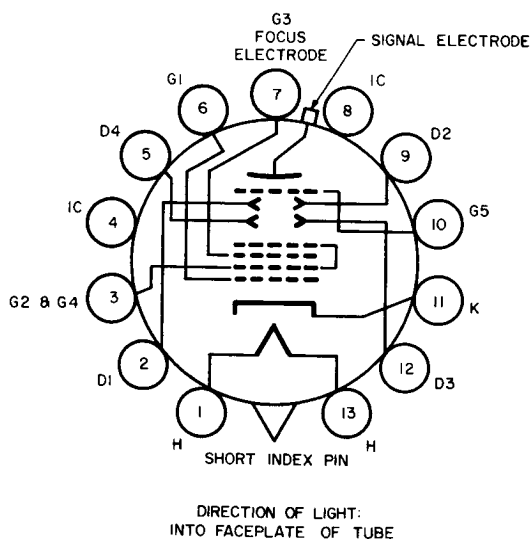
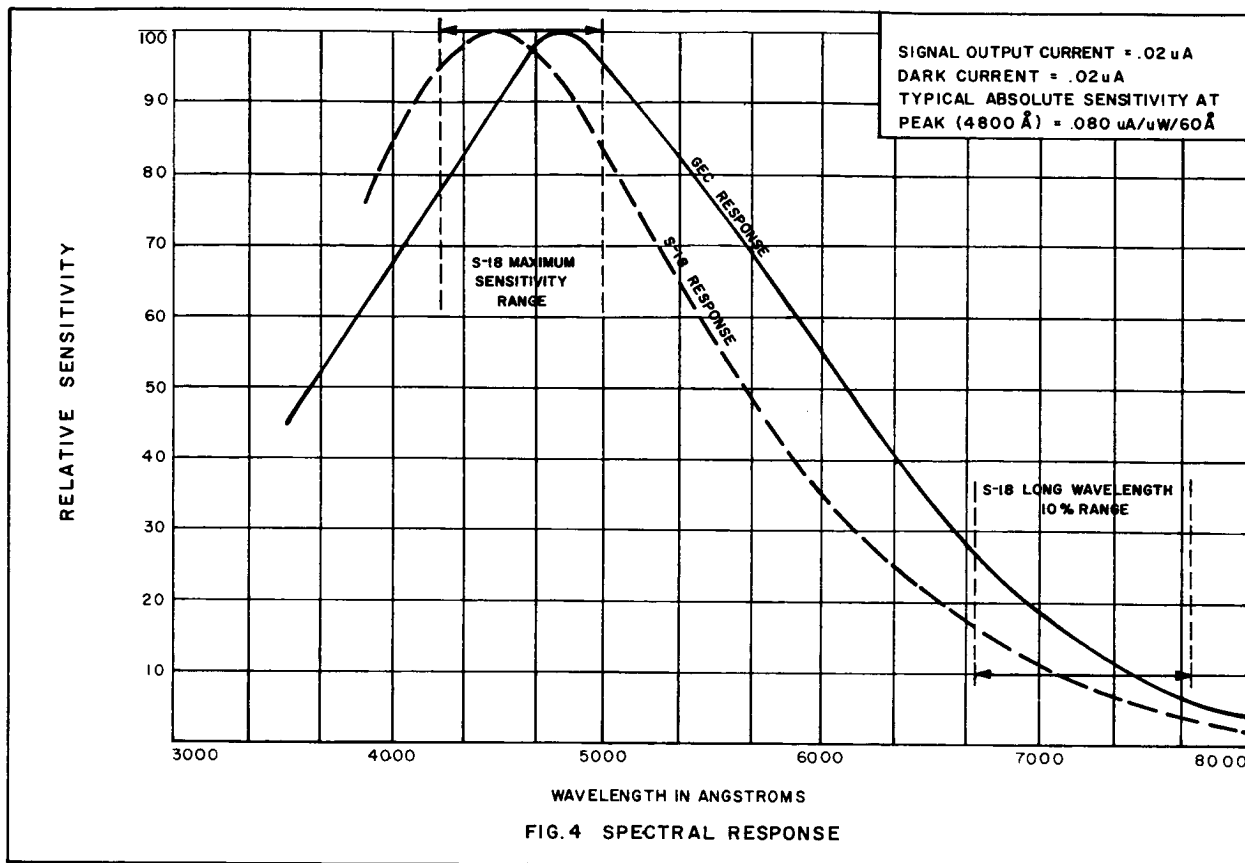
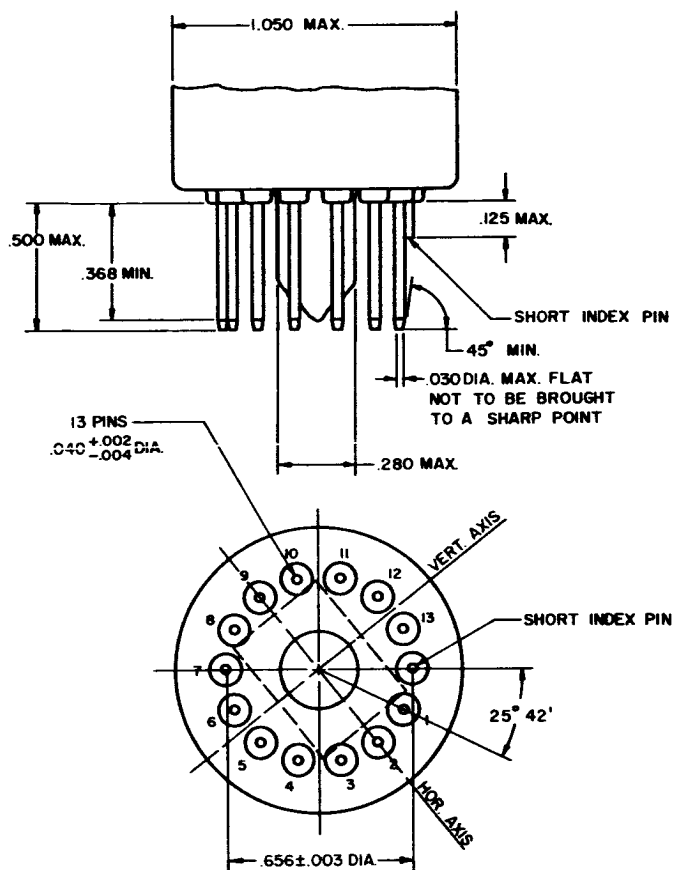
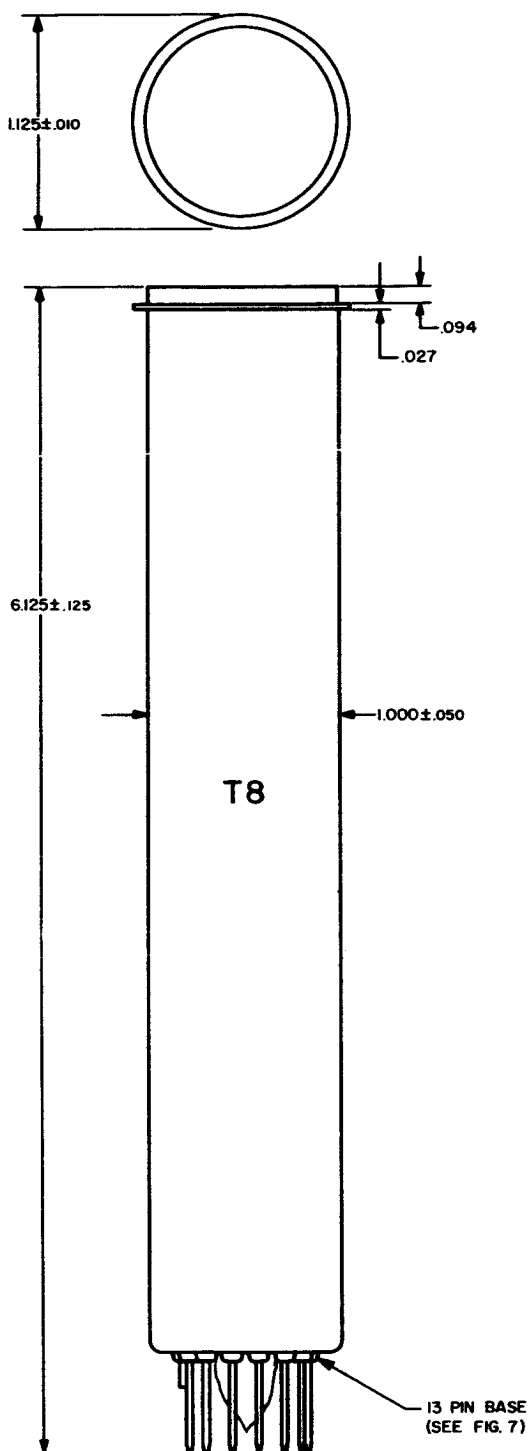


FIG. 3 TYPICAL TRANSISTOR VIDEO PRE-AMPLIFIER



- PIN 1: HEATER
- PIN 2: D1 HORIZONTAL DEFLECTION PLATE
- PIN 3: GRID NO. 2 & 4
- PIN 4: INTERNAL CONNECTION--DO NOT USE
- PIN 5: D4 VERTICAL DEFLECTION PLATE
- PIN 6: GRID NO. 1
- PIN 7: G3 FOCUS ELECTRODE
- PIN 8: INTERNAL CONNECTION--DO NOT USE
- PIN 9: D2 HORIZONTAL DEFLECTION PLATE
- PIN 10: GRID NO. 5
- PIN 11: CATHODE
- PIN 12: D3 VERTICAL DEFLECTION PLATE
- PIN 13: HEATER
- SHORT INDEX PIN: INTERNAL CONNECTION--DO NOT USE
- FLANGE: SIGNAL ELECTRODE

FIG. 5



NOTES

- I. ALL DIMENSIONS ARE SHOWN IN INCHES.

APPENDIX III
1 1/2 INCH VIDICON CHARACTERISTICS
(G. E. TYPE Z-7815)

<u>Electrical Characteristics</u>		
Heater Voltage	6.3 $\pm 10\%$	Volts
Heater Current	0.6	Amperes
Spectral Response	S18	
Direct Interelectrode Capacities		
Signal Electrode to All Other	6	$\mu\mu\text{F}$
D _x to D _x Horizontal Plates	10	$\mu\mu\text{F}$
D _y to D _y Vertical Plates	10	$\mu\mu\text{F}$
Focusing Method - Electrostatic		
Deflection Method - Electrostatic		
Maximum Useful Image Area		
Diagonal Measurement of 4 by 3 Aspect Ratio	1.000	Inches
<u>Mechanical Characteristics</u>		
Physical Dimensions		
Length	8-1/2 \pm 0.50	Inches
Maximum Diameter	1-5/8 \pm 0.015	Inches
Weight, Approximate	0.5	Pounds
Operating Position	Any	
<u>Typical Operating Conditions</u>		
Scanned Area	0.800 by 0.600	Inch
Faceplate Temperature	30 ^o to 40 ^o	C
Optimum Signal Output Current		
Less 0.02 Dark-Current, With Uniform 2870 ^o K Tungsten Illumination on Faceplate	0.10	$\mu\text{A/FC}$
Resolution (minimum)	800	T. V. Lines
Grid No. 1 Voltage (Collimator)	0 to 20	Volts
Grid No. 2 Voltage (Anode)	300 to 350	Volts
Grid No. 3 Voltage (Gate)	-20 to 0	Volts
Grid No. 4 Voltage (First Lens)	0 to 100	Volts
Grid No. 5 Voltage (Second Lens)	100 to 250	Volts
Grid No. 6 Voltage (Mesh)	1,000-1,100	Volts
Deflection Voltages		
Horizontal D _x to D _x	60	Volts
Vertical D _y to D _y	50	Volts

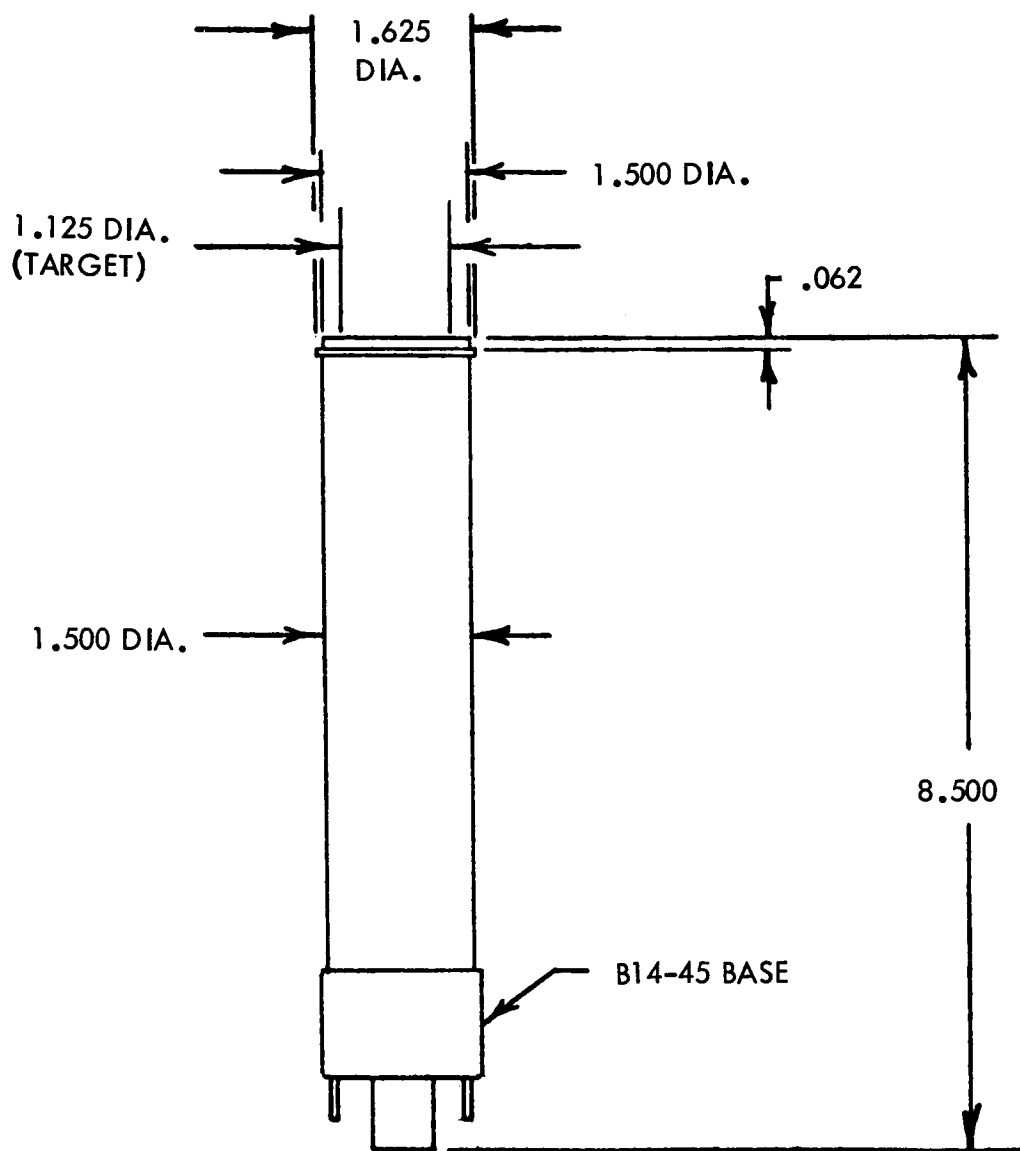
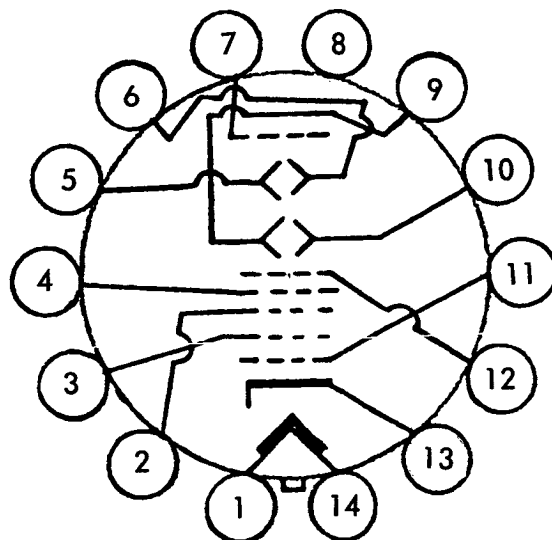


Figure 1. Dimensional Outline 1 1/2 Inch Vidicon



SMALL-SHELL DIHEPIAL 14-PIN BASE

Pin 1: Heater	Pin 8: NC
Pin 2: Grid No. 3 (Gate)	Pin 9: Dy
Pin 3: Grid No. 2 (Anode)	Pin 10: Dy
Pin 4: Grid No. 4 (First Lens)	Pin 11: Grid No. 1 (Collimator)
Pin 5: Dx	Pin 12: Grid No. 5 (Second Lens)
Pin 6: Dx	Pin 13: K Cathode
Pin 7: Grid No. 6 (Mesh)	Pin 14: Heater

Figure 2. Basing Diagram 1 1/2 Inch Vidicon